

NDIPhos as a Platform for Chiral Supramolecular Ligands in Rhodium-Catalyzed Enantioselective Hydrogenation

Supporting Information

Guillaume Force,^a Robert J. Mayer,^b Marie Vayer,^b and David Lebœuf^{b,*}

^a Université Paris-Saclay, CNRS, ICMMO UMR 8182, 91405 Orsay, France.

^b Université de Strasbourg, CNRS, ISIS UMR 7006, 67000 Strasbourg, France.

dleboeuf@unistra.fr

Table of Contents

1. General Remarks	S2
2. Computational Analysis.....	S3
3. Preparation of Chiral Phosphites.....	S19
4. Rh-Catalyzed Enantioselective Hydrogenation	S27
5. NMR Spectra.....	S38
6. References.....	S56

1. General Remarks

Materials: All commercial materials were purchased from Sigma-Aldrich, TCI and FluoroChem, and were used as received, without further purification. (*R*)-BINOL-PCI (CAS: 155613-52-8) was purchased from Strem. The other starting materials were prepared according to known protocols.

L5 was synthesized according to the following procedure: D. J. Frank, A. Franzle, A. Pfaltz, *Chem. Eur. J.* **2013**, *19*, 2405.

Reactions were monitored by thin layer chromatography (TLC) performed on aluminum plates coated with silica gel F₂₅₄ with 0.2 mm thickness. Chromatograms were visualized by fluorescence quenching with UV light at 254 nm and/or by staining using potassium permanganate. Flash column chromatography (FC) was performed using silica gel 60 (230-400 mesh, Merck and co.). Yields refer to chromatographically and spectroscopically pure compounds.

¹H NMR, ¹³C NMR, ¹⁹F NMR, ³¹P NMR spectra were recorded at 298 K on AM250, AV300 or AV360 MHz Bruker spectrometer. ¹H NMR chemical shifts are reported in ppm using residual solvent peak as reference (CDCl₃: δ = 7.26 ppm; DMSO-d₆: 2.50 ppm; MeOD: 3.31 ppm). Data for ¹H NMR are presented as follows: chemical shift δ (ppm), multiplicity (s = singlet, d = doublet, t = triplet, m = multiplet, br = broad), coupling constant J (Hz) and integration; ¹³C NMR spectra were recorded at 75, 91 and 101 MHz using broadband proton decoupling and chemical shifts are reported in ppm using residual solvent peaks as reference (CDCl₃: δ = 77.16 ppm; DMSO-d₆: 39.52 ppm; MeOD: 49.00 ppm). Multiplicity was defined by recorded a ¹³C NMR spectra using the attached proton test (APT). ¹⁹F NMR spectra were recorded at 235 MHz at ambient temperature. ³¹P NMR spectra were recorded at 101 and 121 MHz at ambient temperature. High-resolution mass spectrometry (HRMS) analysis was recorded on MicrOTOFq Bruker spectrometer by electrospray ionization. Melting points were determined using a Reichert melting point apparatus. Infrared spectra were recorded on a FTIR spectrometer (Perkin-Elmer spectrum one, NaCl pellets or Bruker Vertex 70 ATR Pike Germanium) and are reported in cm⁻¹.

2. Computational Analysis

For the computations we adapted a protocol from Grimme and coworkers proposed for the study of noncovalent interactions.¹ This protocol relies on the use of the composite electronic-structure method r²SCAN-3c² which includes the D4-dispersion correction and a geometrical counterpoise correction. In the first step, a conformational search was performed using the CREST program (v. 2.12) at the GFN2-xTB(ALPB=CH₂Cl₂) level.³ For systems with excessive numbers of conformers (>100), single point energies at the r²SCAN-3c(SMD=CH₂Cl₂)//GFN2-xTB(ALPB=CH₂Cl₂) level were used to exclude all conformers with E_{tot} > 30 kJ mol⁻¹. All remaining unique conformers were optimized at the r²SCAN-3c(SMD=CH₂Cl₂) level of theory within ORCA (v. 5.0.3) to give E_{tot} and G_{solv}.^{4,5} Finally, the single-point Hessian (SPH) approach of Grimme was used to calculate G_{mRRHO} at the GFN2-xTB(ALPB) level with the SCAN-3c(SMD=CH₂Cl₂)-optimized structures as input.⁶ In this way, the Gibbs energies G_{high} were obtained as G_{combined} = E_{tot} + G_{solv} + G_{mRRHO}. To verify the applicability of the SPH approach to calculate the thermochemical corrections, a (numerical) frequency analysis was performed in ORCA at the r²SCAN-3c(SMD=CH₂Cl₂) level on the minimum conformers for each species to directly give G_{combined,direct} and to furthermore verify that the minimum conformers are stationary points. Additionally, the minimum conformers for each structure were re-optimized at the M06-L/def2-TZVP(SMD=CH₂Cl₂) level with ORCA, and a frequency analysis was performed at the same theory level. For computations at the M06-L/def2-TZVP(SMD=CH₂Cl₂) level, the defgrid3 was applied with the RIJCOSX approximation and the def2/J auxiliary basis.

To all systems, a free energy change of +7.92 kJ/mol (= R · 298 K · ln(24.47 L mol⁻¹/L mol⁻¹)) was applied for their conversion from gas phase (1 atm) to liquid phase (1 M). Structures were visualized with CYLView.⁷ Non-covalent interaction (NCI) analyses were performed with the Multiwfn (v. 3.8) program.⁸

Tables S1, S2, and S3 feature all raw computational data used to calculate the Gibbs reaction energies in Figures S1 and S2. The geometries of all optimized structures (see the filenames in Tables S1, S2, and S3) are provided as separate multi-xyz files as the supporting information.

Table S1. Results of DFT calculations for the association of $\text{Rh}(\text{COD}_2)^+$ with the model ligand **L** (NDI).

Species	Filename	$E_{\text{tot}} + G_{\text{solv}}^{\text{a}}$ (hartree)	$G_{\text{SPH}}^{\text{b}}$ (hartree)	$G_{\text{combined}}^{\text{c}}$ (hartree)	weighting	$G_{\text{combined,direct}}^{\text{d}}$ (hartree)
COD	cod_1.log	-311.946697	0.145255	-311.801442	0.4767	-311.7984161
	cod_2.log	-311.941853	0.145719	-311.796134	0.0017	
	cod_3.log	-311.939918	0.145948	-311.793970	0.0002	
	cod_4.log	-311.946709	0.145326	-311.801383	0.4478	
	cod_5.log	-311.943641	0.144585	-311.799056	0.0380	
	cod_6.log	-311.943634	0.144637	-311.798997	0.0357	
			weighted	-311.801227		
 cod_1.log						
$\text{Rh}(\text{COD})_2^+$	rh_cod2_1.log	-734.480331	0.312803	-734.167528	0.6758	-734.157718
	rh_cod2_2.log	-734.478330	0.312182	-734.166148	0.1563	
	rh_cod2_3.log	-734.477782	0.311641	-734.166142	0.1554	
	rh_cod2_4.log	-734.476651	0.312889	-734.163762	0.0125	
			weighted	-734.167050		
 rh_cod2_1.log						
L	l_ndi_1.log	-2592.766672	0.484460	-2592.282212	0.0162	
	l_ndi_2.log	-2592.766752	0.483965	-2592.282788	0.0297	

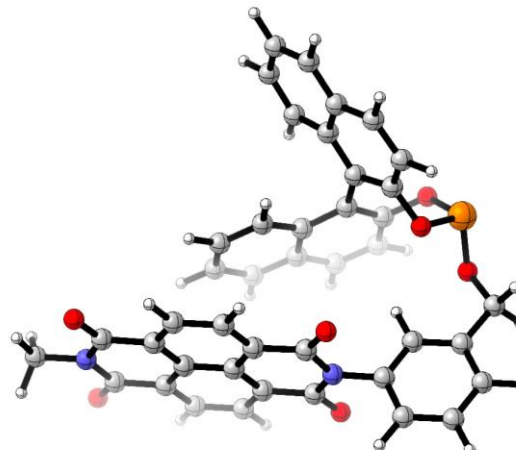
l_ndi_3.log	-2592.766751	0.483899	-2592.282852	0.0318
l_ndi_4.log	-2592.766766	0.483716	-2592.283050	0.0393
l_ndi_5.log	-2592.766756	0.484026	-2592.282730	0.0280
l_ndi_6.log	-2592.766767	0.483918	-2592.282849	0.0317
l_ndi_7.log	-2592.766755	0.483956	-2592.282800	0.0301
l_ndi_8.log	-2592.766769	0.484004	-2592.282765	0.0290
l_ndi_9.log	-2592.766768	0.484007	-2592.282761	0.0289
l_ndi_10.log	-2592.766673	0.484435	-2592.282238	0.0166
l_ndi_11.log	-2592.766769	0.483999	-2592.282770	0.0292
l_ndi_12.log	-2592.766759	0.484145	-2592.282613	0.0247
l_ndi_13.log	-2592.766724	0.484109	-2592.282615	0.0248
l_ndi_14.log	-2592.766733	0.484059	-2592.282674	0.0264
l_ndi_15.log	-2592.766753	0.483928	-2592.282825	0.0309
l_ndi_16.log	-2592.766757	0.483980	-2592.282777	0.0294
l_ndi_17.log	-2592.766771	0.483772	-2592.282999	0.0372
l_ndi_18.log	-2592.766760	0.484014	-2592.282747	0.0285
l_ndi_19.log	-2592.766761	0.483654	-2592.283107	0.0417
l_ndi_20.log	-2592.766760	0.484053	-2592.282708	0.0273
l_ndi_21.log	-2592.768171	0.485171	-2592.283000	0.0373
l_ndi_23.log	-2592.766777	0.483853	-2592.282924	0.0344
l_ndi_24.log	-2592.766745	0.484227	-2592.282518	0.0224
l_ndi_27.log	-2592.766769	0.484044	-2592.282724	0.0278
l_ndi_28.log	-2592.766761	0.484046	-2592.282716	0.0276
l_ndi_29.log	-2592.768180	0.485333	-2592.282846	0.0317
l_ndi_33.log	-2592.768172	0.485317	-2592.282855	0.0320
l_ndi_35.log	-2592.762665	0.483771	-2592.278894	0.0005
l_ndi_37.log	-2592.760563	0.483264	-2592.277299	0.0001
l_ndi_38.log	-2592.760539	0.483053	-2592.277486	0.0001
l_ndi_39.log	-2592.760447	0.483301	-2592.277146	0.0001
l_ndi_40.log	-2592.768166	0.485297	-2592.282870	0.0324
l_ndi_41.log	-2592.760586	0.483164	-2592.277423	0.0001
l_ndi_42.log	-2592.760492	0.483059	-2592.277433	0.0001
l_ndi_43.log	-2592.761974	0.484205	-2592.277769	0.0001
l_ndi_44.log	-2592.761480	0.484176	-2592.277303	0.0001
l_ndi_45.log	-2592.761861	0.483891	-2592.277969	0.0002
l_ndi_46.log	-2592.765917	0.483944	-2592.281973	0.0125
l_ndi_47.log	-2592.765917	0.483969	-2592.281948	0.0122
l_ndi_48.log	-2592.765922	0.483950	-2592.281972	0.0125

-2592.261014

l_ndi_49.log	-2592.761966	0.484247	-2592.277719	0.0001
l_ndi_50.log	-2592.765865	0.483636	-2592.282229	0.0165
l_ndi_51.log	-2592.761604	0.483956	-2592.277648	0.0001
l_ndi_52.log	-2592.765875	0.484739	-2592.281136	0.0052
l_ndi_53.log	-2592.765887	0.484678	-2592.281208	0.0056
l_ndi_54.log	-2592.761926	0.484516	-2592.277410	0.0001
l_ndi_55.log	-2592.761936	0.484459	-2592.277477	0.0001
l_ndi_56.log	-2592.765822	0.484405	-2592.281417	0.0070
l_ndi_57.log	-2592.761424	0.483965	-2592.277460	0.0001
l_ndi_58.log	-2592.761833	0.483932	-2592.277901	0.0002
l_ndi_59.log	-2592.761758	0.483810	-2592.277948	0.0002
l_ndi_60.log	-2592.761786	0.483649	-2592.278138	0.0002
l_ndi_61.log	-2592.761488	0.484153	-2592.277335	0.0001
l_ndi_62.log	-2592.766552	0.484717	-2592.281835	0.0108
l_ndi_63.log	-2592.761492	0.483697	-2592.277795	0.0001
l_ndi_64.log	-2592.760605	0.483186	-2592.277419	0.0001
l_ndi_65.log	-2592.761828	0.483875	-2592.277954	0.0002
l_ndi_66.log	-2592.761880	0.483909	-2592.277971	0.0002
l_ndi_67.log	-2592.761844	0.483671	-2592.278173	0.0002
l_ndi_68.log	-2592.761838	0.483610	-2592.278229	0.0002
l_ndi_69.log	-2592.761861	0.483851	-2592.278009	0.0002
l_ndi_70.log	-2592.761849	0.483798	-2592.278050	0.0002
l_ndi_71.log	-2592.761843	0.483849	-2592.277994	0.0002
l_ndi_72.log	-2592.766745	0.484116	-2592.282629	0.0252
l_ndi_73.log	-2592.761804	0.483473	-2592.278332	0.0003
l_ndi_74.log	-2592.761535	0.484153	-2592.277382	0.0001
l_ndi_75.log	-2592.766772	0.484210	-2592.282562	0.0234
l_ndi_76.log	-2592.761331	0.483930	-2592.277401	0.0001
l_ndi_77.log	-2592.761828	0.483622	-2592.278206	0.0002
l_ndi_78.log	-2592.761802	0.484614	-2592.277188	0.0001
l_ndi_79.log	-2592.761851	0.483478	-2592.278372	0.0003
l_ndi_80.log	-2592.761851	0.483940	-2592.277911	0.0002
l_ndi_81.log	-2592.761827	0.483698	-2592.278130	0.0002
l_ndi_82.log	-2592.766500	0.484366	-2592.282134	0.0149
l_ndi_83.log	-2592.766788	0.484411	-2592.282377	0.0192
l_ndi_84.log	-2592.760621	0.483183	-2592.277438	0.0001
l_ndi_85.log	-2592.761806	0.484047	-2592.277760	0.0001
l_ndi_86.log	-2592.761879	0.483892	-2592.277987	0.0002

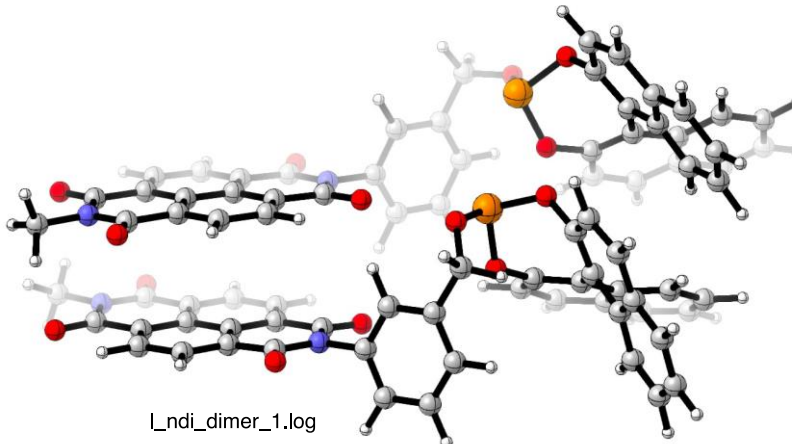
I_ndi_87.log	-2592.761758	0.483674	-2592.278083	0.0002
I_ndi_88.log	-2592.761804	0.484052	-2592.277752	0.0001
I_ndi_89.log	-2592.761805	0.484237	-2592.277568	0.0001
I_ndi_90.log	-2592.761829	0.483656	-2592.278173	0.0002
I_ndi_91.log	-2592.761863	0.483967	-2592.277896	0.0002
I_ndi_92.log	-2592.761811	0.483949	-2592.277863	0.0002
I_ndi_93.log	-2592.761888	0.484018	-2592.277870	0.0002
I_ndi_94.log	-2592.760562	0.483449	-2592.277113	0.0001
I_ndi_95.log	-2592.761354	0.483952	-2592.277402	0.0001
I_ndi_96.log	-2592.761818	0.483848	-2592.277970	0.0002
I_ndi_97.log	-2592.761447	0.483967	-2592.277480	0.0001
I_ndi_98.log	-2592.761809	0.483936	-2592.277874	0.0002
I_ndi_100.log	-2592.761903	0.484092	-2592.277811	0.0002

weighted -2592.282654

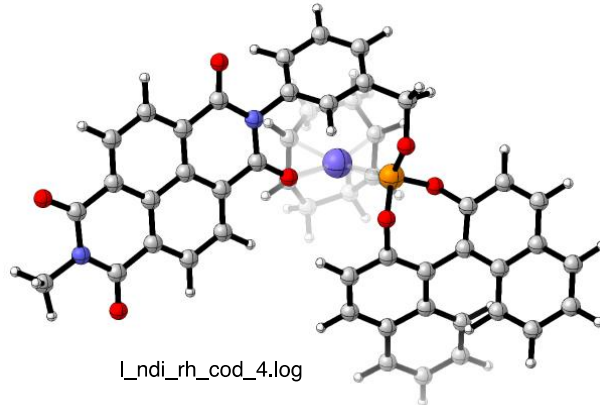


I_ndi_19.log

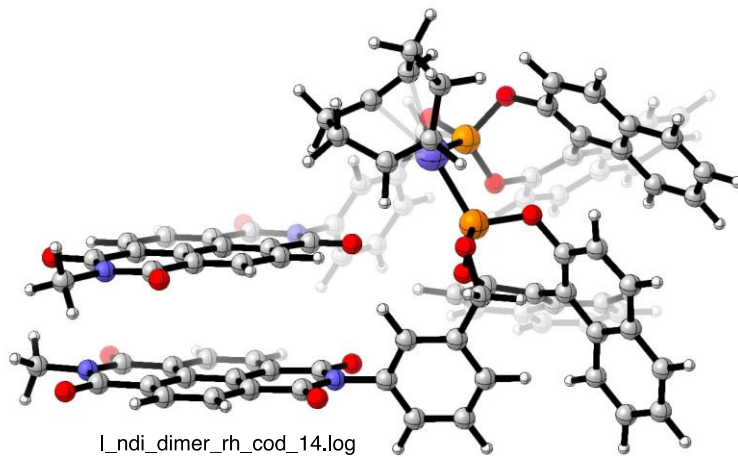
(L) ₂	I_ndi_dimer_1.log	-5185.564539	0.998443	-5184.566096	1.0000	-5184.524944
			weighted	-5184.566096		



(L)(COD)Rh ⁺	<i>l_ndi_rh_cod_1.log</i>	-3015.303781	0.655065	-3014.648716	0.1406
	<i>l_ndi_rh_cod_2.log</i>	-3015.304064	0.656303	-3014.647762	0.0511
	<i>l_ndi_rh_cod_3.log</i>	-3015.304089	0.655164	-3014.648925	0.1754
	<i>l_ndi_rh_cod_4.log</i>	-3015.304076	0.654823	-3014.649254	0.2486
	<i>l_ndi_rh_cod_5.log</i>	-3015.303258	0.654793	-3014.648466	0.1078
	<i>l_ndi_rh_cod_6.log</i>	-3015.302378	0.655415	-3014.646963	0.0219
	<i>l_ndi_rh_cod_7.log</i>	-3015.303156	0.655278	-3014.647878	0.0578
	<i>l_ndi_rh_cod_8.log</i>	-3015.303201	0.655307	-3014.647894	0.0588
	<i>l_ndi_rh_cod_9.log</i>	-3015.302135	0.655290	-3014.646845	0.0193
	<i>l_ndi_rh_cod_10.log</i>	-3015.302071	0.655364	-3014.646707	0.0167
	<i>l_ndi_rh_cod_11.log</i>	-3015.302141	0.655376	-3014.646765	0.0178
	<i>l_ndi_rh_cod_12.log</i>	-3015.302065	0.655408	-3014.646657	0.0158
	<i>l_ndi_rh_cod_13.log</i>	-3015.302126	0.655285	-3014.646841	0.0193
	<i>l_ndi_rh_cod_14.log</i>	-3015.302019	0.655255	-3014.646764	0.0178
	<i>l_ndi_rh_cod_15.log</i>	-3015.302081	0.655526	-3014.646555	0.0142
	<i>l_ndi_rh_cod_16.log</i>	-3015.301974	0.655616	-3014.646358	0.0115
	<i>l_ndi_rh_cod_17.log</i>	-3015.299090	0.654727	-3014.644363	0.0014
	<i>l_ndi_rh_cod_18.log</i>	-3015.299079	0.654846	-3014.644234	0.0012
	<i>l_ndi_rh_cod_19.log</i>	-3015.299096	0.654643	-3014.644454	0.0015
	<i>l_ndi_rh_cod_20.log</i>	-3015.298993	0.654637	-3014.644355	0.0014
	weighted		-3014.648386		



$(\text{L})_2(\text{COD})\text{Rh}^+$	l_ndi_dimer_rh_cod_4.log	-5608.128732	1.169774	-5606.958958	0.0002	
	l_ndi_dimer_rh_cod_10.log	-5608.131885	1.170653	-5606.961233	0.0021	
	l_ndi_dimer_rh_cod_12.log	-5608.129099	1.170635	-5606.958465	0.0001	
	l_ndi_dimer_rh_cod_13.log	-5608.128935	1.171969	-5606.956966	0.0000	
	l_ndi_dimer_rh_cod_14.log	-5608.135650	1.168884	-5606.966765	0.7261	-5606.915406
	l_ndi_dimer_rh_cod_16.log	-5608.131874	1.172002	-5606.959872	0.0005	
	l_ndi_dimer_rh_cod_17.log	-5608.136754	1.170969	-5606.965786	0.2570	
	l_ndi_dimer_rh_cod_19.log	-5608.136555	1.173542	-5606.963013	0.0136	
	l_ndi_dimer_rh_cod_24.log	-5608.134732	1.174831	-5606.959900	0.0005	
	l_ndi_dimer_rh_cod_71.log	-5608.125516	1.170546	-5606.954969	0.0000	
	weighted			-5606.966442		



^a at the r²SCAN-3c(SMD=CH₂Cl₂) level. ^b Free energy corrections at the GFN2-xTB(ALPB=CH₂Cl₂)-SPH level. ^c Gibbs energy at the (SMD=CH₂Cl₂)/r²SCAN-3c+ GFN2-xTB(ALPB=CH₂Cl₂)-SPH level. ^d Gibbs energy at the (SMD=CH₂Cl₂)/r²SCAN-3c with free energy corrections from numerical frequency analysis.

Table S2. Results of DFT calculations for the association of Rh(COD)₂⁺ with the model ligand L (NDI) at the (SMD=CH₂Cl₂)/M06-L/def2-TZVP level.

Species	Filename	E _{tot} + G _{solv} ^a (hartree)	G _{combined,direct} ^a (hartree)
COD	cod_m06l_1	-312.103925	-311.953562
Rh(COD) ₂ ⁺	rh_cod2_m06l_1	-734.803264	-734.479603
L	I_ndi_m06l_19	-2593.733214	-2593.220104
(L) ₂	I_ndi_dimer_m06l_1	-5187.490620	-5186.433611
(L)(COD)Rh ⁺	I_ndi_rh_cod_m06l_4	-3016.445639	-3015.754833
(L) ₂ (COD)Rh ⁺	I_ndi_dimer_rh_cod_m06l_14	-5610.233657	-5608.997255

^a at the (SMD=CH₂Cl₂)/M06-L/def2-TZVP level.

Calculations at the (SMD=CH₂Cl₂)/r²SCAN-3c level (single conformer)

Calculations at the (SMD=CH₂Cl₂)/r²SCAN-3c+GFN2-xTB[ALPB=CH₂Cl₂]-SPH (Boltzmann-weighted)

Calculations at the (SMD=CH₂Cl₂)/M06-L/def2-TZVP level (single conformer)

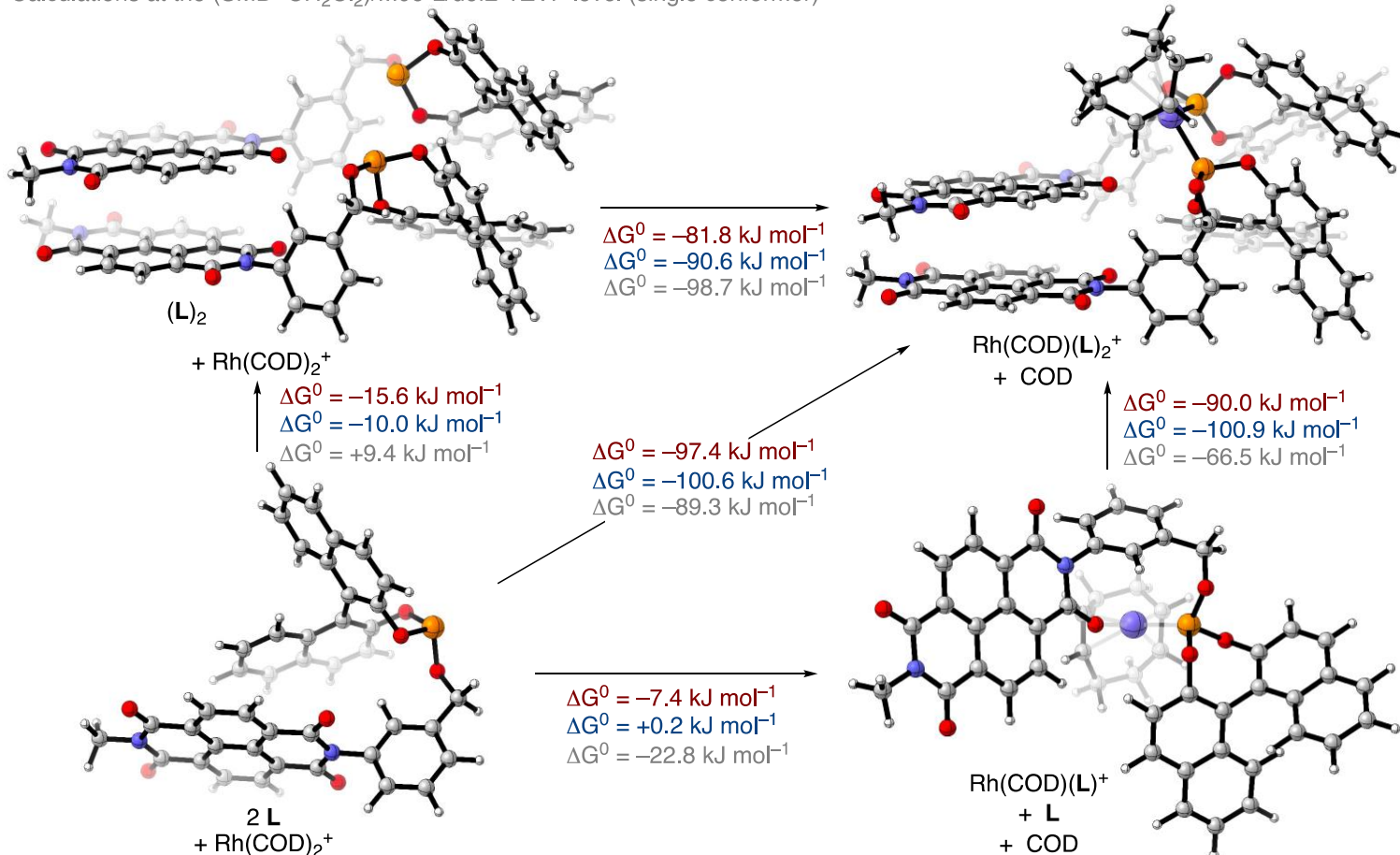
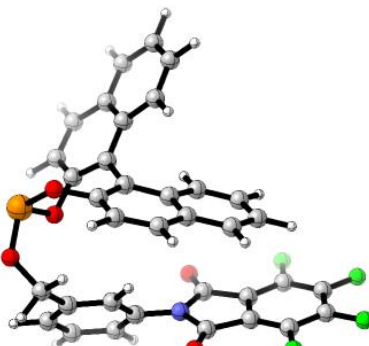


Figure S1. Geometries of the most favorable conformers for each species optimized at the (SMD=CH₂Cl₂)/r²SCAN-3c level and associated Gibbs free energies for complex formation calculated from Boltzmann-weighted Gibbs energies at the (SMD=CH₂Cl₂)/r²SCAN-3c+GFN2-xTB[ALPB=CH₂Cl₂]-SPH level (shown in blue; G_{combined} in Table S1), from Gibbs energies of the lowest conformers calculated from numerical frequency analysis at the (SMD=CH₂Cl₂)/r²SCAN-3c level (shown in red; $G_{\text{combined,direct}}$ in Table S1), or from Gibbs energies of the lowest conformers calculated from numerical frequency analysis at the (SMD=CH₂Cl₂)/M06-L/def2-TZVP level (shown in grey; from Table S2).

Table S3. Results of DFT calculations for the association of Rh(COD₂)⁺ with the ligand **L3**.

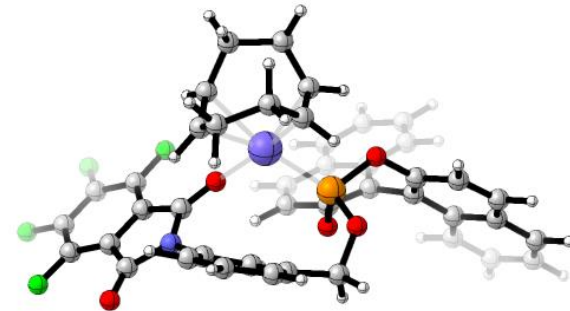
Species	Filename	E _{tot} + G _{solv} ^a (hartree)	G _{SPH} ^b (hartree)	G _{combined} ^c (hartree)	weighting	G _{combined,direct} ^d (hartree)
L3	I_tfpi_1.log	-2515.953101	0.369214	-2515.583887	0.0309	
	I_tfpi_2.log	-2515.953125	0.369241	-2515.583884	0.0308	
	I_tfpi_3.log	-2515.953102	0.369326	-2515.583776	0.0275	
	I_tfpi_4.log	-2515.953134	0.369213	-2515.583922	0.0321	
	I_tfpi_6.log	-2515.953107	0.369289	-2515.583818	0.0288	
	I_tfpi_7.log	-2515.953146	0.369224	-2515.583922	0.0321	
	I_tfpi_9.log	-2515.952981	0.369694	-2515.583287	0.0164	
	I_tfpi_10.log	-2515.953162	0.369306	-2515.583857	0.0300	
	I_tfpi_11.log	-2515.953168	0.369205	-2515.583963	0.0335	
	I_tfpi_12.log	-2515.954553	0.369557	-2515.584996	0.1002	
	I_tfpi_13.log	-2515.954542	0.369492	-2515.585050	0.1062	-2515.568315
	I_tfpi_14.log	-2515.952744	0.369089	-2515.583655	0.0242	
	I_tfpi_15.log	-2515.952723	0.369162	-2515.583561	0.0219	
	I_tfpi_16.log	-2515.952534	0.368832	-2515.583702	0.0254	
	I_tfpi_17.log	-2515.954529	0.369554	-2515.584975	0.0980	
	I_tfpi_18.log	-2515.952658	0.368894	-2515.583765	0.0272	
	I_tfpi_19.log	-2515.952708	0.369065	-2515.583643	0.0239	
	I_tfpi_20.log	-2515.952700	0.369099	-2515.583601	0.0228	
	I_tfpi_21.log	-2515.952670	0.369107	-2515.583564	0.0220	
	I_tfpi_22.log	-2515.952694	0.369137	-2515.583556	0.0218	
	I_tfpi_23.log	-2515.952788	0.368900	-2515.583888	0.0310	
	I_tfpi_24.log	-2515.952795	0.368889	-2515.583906	0.0316	
	I_tfpi_25.log	-2515.951820	0.369600	-2515.582220	0.0053	
	I_tfpi_26.log	-2515.949527	0.368793	-2515.580733	0.0011	
	I_tfpi_27.log	-2515.949677	0.368595	-2515.581081	0.0016	
	I_tfpi_28.log	-2515.948977	0.369838	-2515.579139	0.0002	
	I_tfpi_29.log	-2515.948901	0.369764	-2515.579137	0.0002	
	I_tfpi_30.log	-2515.952656	0.368811	-2515.583845	0.0296	
	I_tfpi_31.log	-2515.952564	0.368655	-2515.583909	0.0317	
	I_tfpi_32.log	-2515.952516	0.368814	-2515.583702	0.0254	
	I_tfpi_33.log	-2515.949688	0.368775	-2515.580913	0.0013	
	I_tfpi_34.log	-2515.952641	0.369036	-2515.583606	0.0230	
	I_tfpi_35.log	-2515.952560	0.368577	-2515.583982	0.0342	
	I_tfpi_36.log	-2515.952521	0.368922	-2515.583599	0.0228	

I_tfpi_37.log	-2515.949624	0.368710	-2515.580913	0.0013
I_tfpi_38.log	-2515.949626	0.368683	-2515.580943	0.0014
I_tfpi_39.log	-2515.949639	0.368876	-2515.580764	0.0011
I_tfpi_40.log	-2515.947319	0.368523	-2515.578796	0.0001
I_tfpi_41.log	-2515.947871	0.368628	-2515.579243	0.0002
I_tfpi_42.log	-2515.947861	0.368996	-2515.578865	0.0002
I_tfpi_43.log	-2515.947746	0.369117	-2515.578629	0.0001
I_tfpi_44.log	-2515.947765	0.369014	-2515.578751	0.0001
I_tfpi_45.log	-2515.947905	0.369086	-2515.578818	0.0001
I_tfpi_46.log	-2515.947756	0.369018	-2515.578738	0.0001
I_tfpi_47.log	-2515.946910	0.368720	-2515.578190	0.0001
I_tfpi_48.log	-2515.946919	0.368468	-2515.578451	0.0001
I_tfpi_49.log	-2515.947288	0.368825	-2515.578463	0.0001
I_tfpi_50.log	-2515.946919	0.368531	-2515.578388	0.0001
I_tfpi_51.log	-2515.946906	0.368572	-2515.578334	0.0001
I_tfpi_52.log	-2515.946865	0.368595	-2515.578270	0.0001
I_tfpi_54.log	-2515.947908	0.368813	-2515.579095	0.0002
		weighted	-2515.584112	



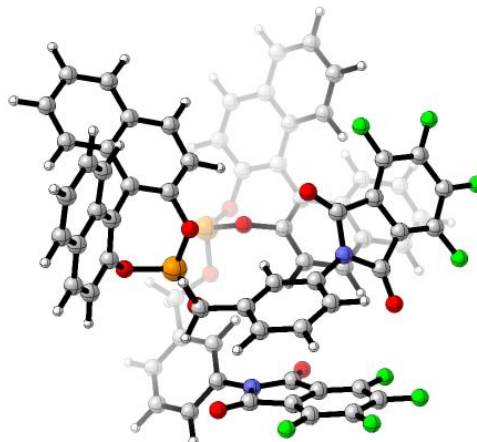
I_tfpi_13.log

(L3)(COD)Rh ⁺	I_tfpi_rh_cod_1.log	-2938.486570	0.539497	-2937.947073	0.9918	-2937.923048
	I_tfpi_rh_cod_2.log	-2938.466992	0.537680	-2937.929311	0.0000	
	I_tfpi_rh_cod_3.log	-2938.465759	0.537051	-2937.928707	0.0000	
	I_tfpi_rh_cod_4.log	-2938.466476	0.538723	-2937.927753	0.0000	
	I_tfpi_rh_cod_5.log	-2938.481338	0.538794	-2937.942545	0.0082	
		weighted	-2937.947036			



I_tfpi_rh_cod_1.log

(L3)₂	I_tfpi_dimer_2.log I_tfpi_dimer_3.log I_tfpi_dimer_5.log I_tfpi_dimer_8.log I_tfpi_dimer_12.log I_tfpi_dimer_14.log I_tfpi_dimer_15.log	-5031.929796 -5031.930780 -5031.924287 -5031.922171 -5031.925560 -5031.925483 -5031.925182	0.766219 0.765934 0.766487 0.766417 0.766819 0.766669 0.766235	-5031.163577 -5031.164846 -5031.157800 -5031.155754 -5031.158741 -5031.158814 -5031.158946	0.2057 0.7898 0.0005 0.0001 0.0012 0.0013 0.0015	
			weighted	-5031.164557		

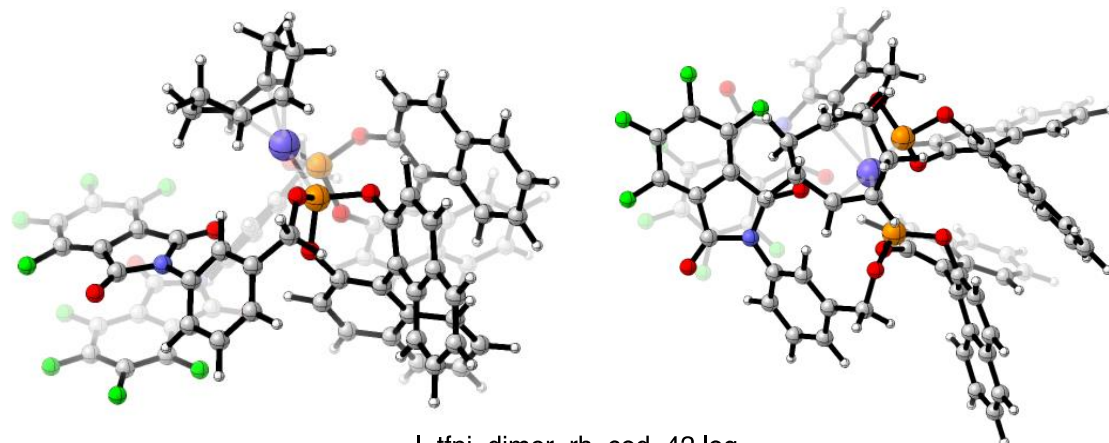


I_tfpi_dimer_3.log

(L3)₂(COD)Rh⁺	I_tfpi_dimer_rh_cod_1.log I_tfpi_dimer_rh_cod_2.log	-5454.498893 -5454.492758	0.939128 0.939331	-5453.559765 -5453.553427	0.0010 0.0000	
--	--	------------------------------	----------------------	------------------------------	------------------	--

_tfpi_dimer_rh_cod_3.log	-5454.502366	0.940232	-5453.562134	0.0128
_tfpi_dimer_rh_cod_4.log	-5454.497817	0.937752	-5453.560065	0.0014
_tfpi_dimer_rh_cod_5.log	-5454.497765	0.937892	-5453.559874	0.0012
_tfpi_dimer_rh_cod_6.log	-5454.494951	0.939505	-5453.555447	0.0000
_tfpi_dimer_rh_cod_7.log	-5454.493894	0.938843	-5453.555051	0.0000
_tfpi_dimer_rh_cod_8.log	-5454.502287	0.938090	-5453.564197	0.1143
_tfpi_dimer_rh_cod_9.log	-5454.488806	0.939315	-5453.549490	0.0000
_tfpi_dimer_rh_cod_10.log	-5454.492727	0.939709	-5453.553018	0.0000
_tfpi_dimer_rh_cod_11.log	-5454.498809	0.940075	-5453.558734	0.0003
_tfpi_dimer_rh_cod_12.log	-5454.502056	0.940173	-5453.561883	0.0098
_tfpi_dimer_rh_cod_13.log	-5454.502196	0.940295	-5453.561901	0.0100
_tfpi_dimer_rh_cod_14.log	-5454.498261	0.939879	-5453.558382	0.0002
_tfpi_dimer_rh_cod_15.log	-5454.501988	0.939333	-5453.562656	0.0223
_tfpi_dimer_rh_cod_16.log	-5454.497563	0.938804	-5453.558759	0.0004
_tfpi_dimer_rh_cod_17.log	-5454.493960	0.939322	-5453.554638	0.0000
_tfpi_dimer_rh_cod_18.log	-5454.502157	0.937945	-5453.564213	0.1162
_tfpi_dimer_rh_cod_20.log	-5454.491762	0.939231	-5453.552531	0.0000
_tfpi_dimer_rh_cod_22.log	-5454.498962	0.938938	-5453.560024	0.0014
_tfpi_dimer_rh_cod_23.log	-5454.491892	0.939707	-5453.552185	0.0000
_tfpi_dimer_rh_cod_24.log	-5454.493795	0.937653	-5453.556142	0.0000
_tfpi_dimer_rh_cod_25.log	-5454.502122	0.937939	-5453.564183	0.1126
_tfpi_dimer_rh_cod_26.log	-5454.495790	0.939685	-5453.556105	0.0000
_tfpi_dimer_rh_cod_27.log	-5454.502231	0.938087	-5453.564144	0.1081
_tfpi_dimer_rh_cod_28.log	-5454.491395	0.939922	-5453.551473	0.0000
_tfpi_dimer_rh_cod_29.log	-5454.494131	0.939122	-5453.555009	0.0000
_tfpi_dimer_rh_cod_31.log	-5454.497257	0.939373	-5453.557884	0.0001
_tfpi_dimer_rh_cod_32.log	-5454.494662	0.936911	-5453.557750	0.0001
_tfpi_dimer_rh_cod_33.log	-5454.491387	0.942343	-5453.549044	0.0000
_tfpi_dimer_rh_cod_34.log	-5454.501818	0.938934	-5453.562883	0.0284
_tfpi_dimer_rh_cod_35.log	-5454.495374	0.938073	-5453.557301	0.0001
_tfpi_dimer_rh_cod_36.log	-5454.501991	0.937841	-5453.564151	0.1088
_tfpi_dimer_rh_cod_37.log	-5454.495032	0.939216	-5453.555816	0.0000
_tfpi_dimer_rh_cod_38.log	-5454.498368	0.939264	-5453.559104	0.0005
_tfpi_dimer_rh_cod_39.log	-5454.490446	0.939398	-5453.551048	0.0000
_tfpi_dimer_rh_cod_40.log	-5454.498912	0.939069	-5453.559843	0.0011
_tfpi_dimer_rh_cod_41.log	-5454.497377	0.938848	-5453.558529	0.0003
_tfpi_dimer_rh_cod_42.log	-5454.501992	0.937631	-5453.564361	0.1361
_tfpi_dimer_rh_cod_45.log	-5454.494624	0.940143	-5453.554481	0.0000

_tfpi_dimer_rh_cod_46.log	-5454.492377	0.938043	-5453.554334	0.0000
_tfpi_dimer_rh_cod_47.log	-5454.488758	0.938177	-5453.550581	0.0000
_tfpi_dimer_rh_cod_48.log	-5454.498179	0.937894	-5453.560284	0.0018
_tfpi_dimer_rh_cod_49.log	-5454.488808	0.938162	-5453.550646	0.0000
_tfpi_dimer_rh_cod_50.log	-5454.492749	0.938354	-5453.554395	0.0000
_tfpi_dimer_rh_cod_51.log	-5454.493191	0.938002	-5453.555189	0.0000
_tfpi_dimer_rh_cod_52.log	-5454.497171	0.938365	-5453.558806	0.0004
_tfpi_dimer_rh_cod_53.log	-5454.495203	0.937629	-5453.557574	0.0001
_tfpi_dimer_rh_cod_54.log	-5454.494647	0.938641	-5453.556006	0.0000
_tfpi_dimer_rh_cod_55.log	-5454.493386	0.939028	-5453.554358	0.0000
_tfpi_dimer_rh_cod_56.log	-5454.492170	0.939609	-5453.552561	0.0000
_tfpi_dimer_rh_cod_57.log	-5454.493538	0.938464	-5453.555075	0.0000
_tfpi_dimer_rh_cod_58.log	-5454.501954	0.937932	-5453.564023	0.0950
_tfpi_dimer_rh_cod_59.log	-5454.497882	0.938415	-5453.559468	0.0008
_tfpi_dimer_rh_cod_60.log	-5454.491149	0.938435	-5453.552715	0.0000
_tfpi_dimer_rh_cod_61.log	-5454.492921	0.939191	-5453.553730	0.0000
_tfpi_dimer_rh_cod_63.log	-5454.492103	0.938025	-5453.554079	0.0000
_tfpi_dimer_rh_cod_64.log	-5454.492735	0.938724	-5453.554012	0.0000
_tfpi_dimer_rh_cod_65.log	-5454.492527	0.937985	-5453.554542	0.0000
_tfpi_dimer_rh_cod_66.log	-5454.502016	0.937996	-5453.564020	0.0947
_tfpi_dimer_rh_cod_68.log	-5454.499423	0.938088	-5453.561335	0.0055
_tfpi_dimer_rh_cod_69.log	-5454.491553	0.939503	-5453.552049	0.0000
_tfpi_dimer_rh_cod_71.log	-5454.489332	0.937566	-5453.551766	0.0000
_tfpi_dimer_rh_cod_72.log	-5454.490113	0.938271	-5453.551842	0.0000
_tfpi_dimer_rh_cod_74.log	-5454.492104	0.937817	-5453.554287	0.0000
_tfpi_dimer_rh_cod_75.log	-5454.492245	0.938392	-5453.553853	0.0000
_tfpi_dimer_rh_cod_76.log	-5454.491514	0.938340	-5453.553173	0.0000
_tfpi_dimer_rh_cod_78.log	-5454.491984	0.939141	-5453.552844	0.0000
_tfpi_dimer_rh_cod_80.log	-5454.499489	0.938524	-5453.560966	0.0037
_tfpi_dimer_rh_cod_81.log	-5454.495321	0.936819	-5453.558502	0.0003
_tfpi_dimer_rh_cod_82.log	-5454.495353	0.939089	-5453.556264	0.0000
_tfpi_dimer_rh_cod_83.log	-5454.499485	0.938168	-5453.561316	0.0054
_tfpi_dimer_rh_cod_84.log	-5454.492370	0.938958	-5453.553412	0.0000
_tfpi_dimer_rh_cod_85.log	-5454.495476	0.939683	-5453.555793	0.0000
_tfpi_dimer_rh_cod_86.log	-5454.499435	0.938297	-5453.561138	0.0045
		weighted	-5453.563920	



I_tfpI_dimer_rh_cod_42.log

^a at the r²SCAN-3c(SMD=CH₂Cl₂) level. ^b Free energy corrections at the GFN2-xTB(ALPB=CH₂Cl₂)-SPH level. ^c Gibbs energy at the (SMD=CH₂Cl₂)/r²SCAN-3c+ GFN2-xTB(ALPB=CH₂Cl₂)-SPH level. ^d Gibbs energy at the (SMD=CH₂Cl₂)/r²SCAN-3c level from free energy corrections from numerical frequency analysis.

Calculations at the (SMD=CH₂Cl₂)/r²SCAN-3c level (single conformer)
 Calculations at the (SMD=CH₂Cl₂)/r²SCAN-3c+GFN2-xTB[ALPB=CH₂Cl₂]-SPH (Boltzmann-weighted)

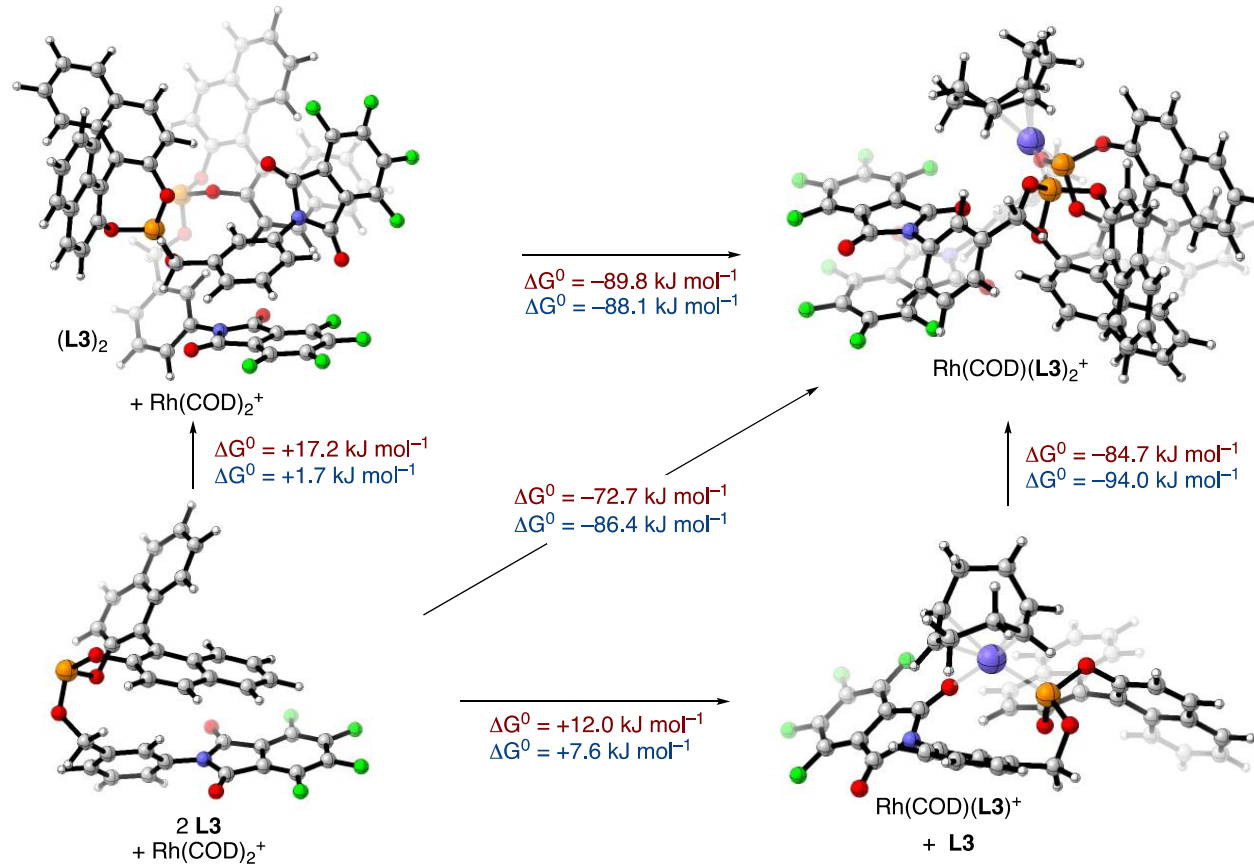
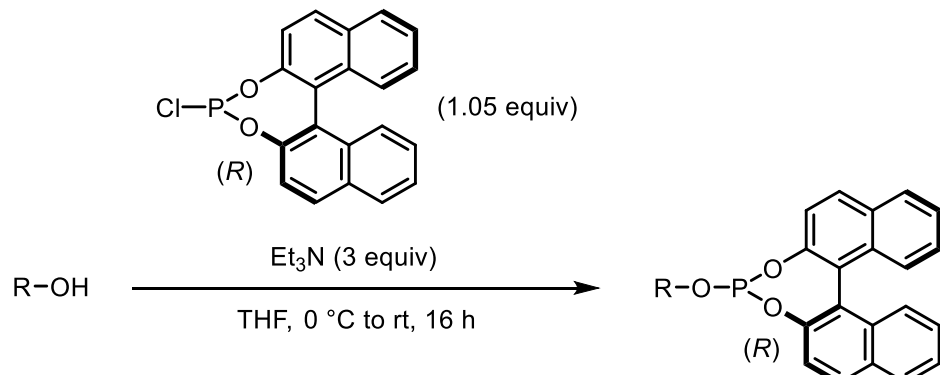


Figure S2. Geometries of the most favorable conformers for each species optimized at the (SMD=CH₂Cl₂)/r²SCAN-3c level and associated Gibbs free energies for complex formation calculated from Boltzmann-weighted Gibbs energies at the (SMD=CH₂Cl₂)/r²SCAN-3c+GFN2-xTB[ALPB=CH₂Cl₂]-SPH level (shown in blue; G_{combined} in Table S3) or from Gibbs energies of the lowest conformers calculated from numerical frequency analysis at the (SMD=CH₂Cl₂)/r²SCAN-3c level (shown in red; $G_{\text{combined,direct}}$ in Table S3). Note that π - π stacking in (L3)₂ occurs not between the two tetrafluorophthalimide groups but rather between a tetrafluorophthalimide and the aryl ring of the linker. For the fully assembled species Rh(COD)(L3)₂⁺, however, the most stable conformer shows stacking between the two tetrafluorophthalimide groups.

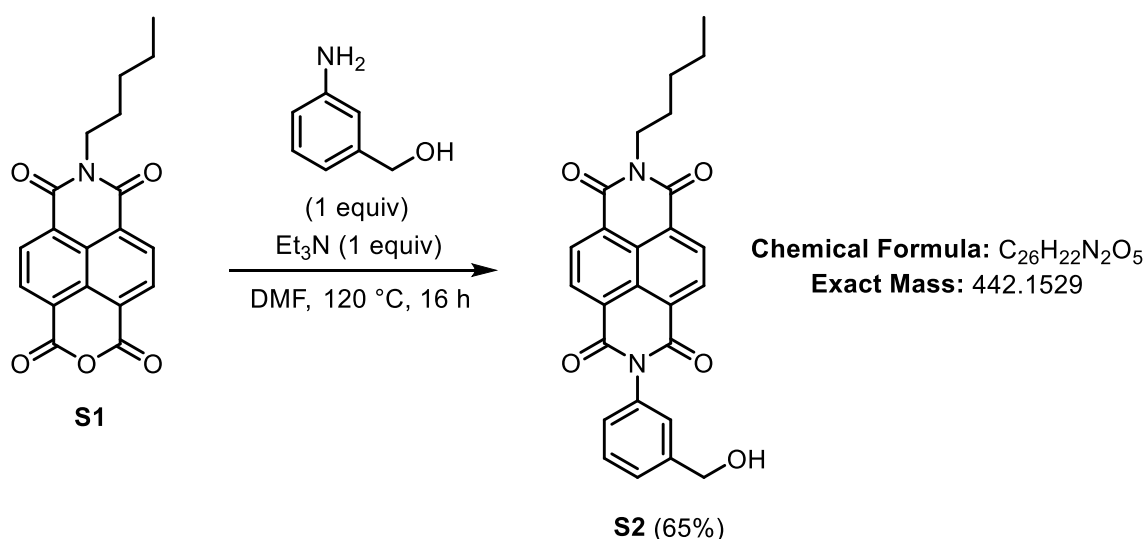
3. Preparation of Chiral Phosphites

General procedure for the synthesis of chiral phosphites (A)



(*R*)-BINOL-PCI (1.05 equiv) was added to a stirred solution of the selected alcohol (1 equiv) and triethylamine (3 equiv) in THF (0.1M). The reaction mixture was stirred at room temperature for 18 h and filtered. The solvent was removed by rotary evaporation and the crude product was purified by flash column chromatography over a short gel of silica using DCM as eluent. In some cases, ¹H NMR analysis of the collected fraction revealed the presence of some BINOL (derived from partial degradation of the ligand during the column), which could be removed with an alkaline workup: the collected fraction was dissolved in DCM, and rapidly washed three times with aqueous NaOH solution (1M) and twice with water. The organic layer was dried over anhydrous MgSO₄ and filtered. The solvent was removed by rotary evaporation to afford the desired phosphite. Phosphites prepared were kept in a glove box.

2-(3-(hydroxymethyl)phenyl)-7-pentylbenzo[1m] [3,8]phenanthroline-1,3,6,8(2H,7H)-tetraone (S2)



To a solution of **S1**⁹ (1.11 g, 3.31 mmol, 1 equiv) in DMF (20 mL) were added 3-aminobenzyl alcohol (407 mg, 3.31 mmol, 1 equiv) and triethylamine (0.46 mL, 3.31 mmol, 1 equiv). The reaction mixture was heated to 120 °C for 16 h. Then, it was cooled to room temperature, diluted with water, and

extracted with DCM (3 x 20 mL). The combined organic layers were washed with water (twice), brine, dried over anhydrous MgSO₄ and filtered. The solvent was removed by rotary evaporation. The crude product was purified by flash column chromatography (97:3 DCM/MeOH) to afford **S2** as a light brown solid (953 mg, 2.15 mmol, 65%).

Mp = 305–307 °C.

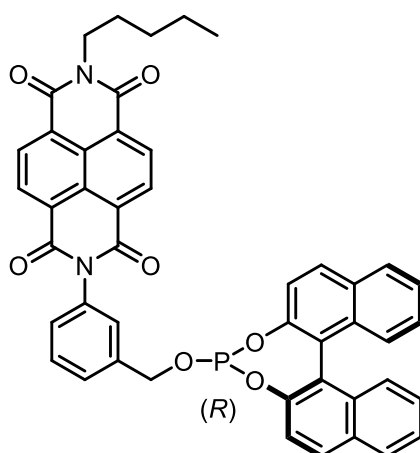
¹H NMR (300 MHz, DMSO-*d*₆) δ = 8.66 (s, 4H), 7.51 (t, *J* = 7.7 Hz, 1H), 7.43 (d, *J* = 7.7 Hz, 1H), 7.38 (s, 1H), 7.30 (d, *J* = 7.7 Hz, 1H), 5.35 (t, *J* = 5.6 Hz, 1H), 4.58 (d, *J* = 5.6 Hz, 2H), 4.12–3.99 (m, 2H), 1.76–1.62 (m, 2H), 1.44–1.33 (m, 4H), 0.89 (t, *J* = 6.9 Hz, 3H).

¹³C NMR (91 MHz, DMSO-*d*₆) δ = 162.8, 162.5, 143.8, 135.4, 130.44, 130.37, 128.7, 127.2, 126.8, 126.5, 126.4, 126.1, 126.0, 62.5, 40.1, 28.7, 27.0, 21.9, 13.9, one carbon hidden.

IR (film, cm⁻¹): ν_{max} = 3378, 296, 2865, 1708, 1655, 1581, 1548, 1402, 1345, 1250, 1197, 1086, 968, 768.

HRMS (ESI⁺): *m/z* calcd for C₂₆H₂₂N₂NaO₅ [M+Na]⁺: 465.1421, found: 465.1403.

2-(3-(((11*b*R)-dinaphtho[2,1-*d*:1',2'-*f*][1,3,2]dioxaphosphhepin-4-yloxy)methyl)phenyl)-7-pentylbenzo[*lmn*][3,8]phenanthroline-1,3,6,8(2*H*,7*H*)-tetraone (L1**)**



Chemical Formula: C₄₆H₃₃N₂O₇P
Exact Mass: 756.2025

Following the general procedure A, starting from **S2** (100 mg, 0.226 mmol, 1 equiv), (*R*)-BINOL-PCl (83 mg, 0.237 mmol, 1.05 equiv), triethylamine (94 μL, 0.678 mmol, 3 equiv) and THF (3 mL). After purification the product **L1** was obtained as an orange solid (103 mg, 0.136 mmol, 60%).

Mp = 195–197 °C.

¹H NMR (360 MHz, CDCl₃) δ = 8.77 (s, 4H), 7.97 (d, *J* = 8.8 Hz, 1H), 7.92–7.83 (m, 3H), 7.53 (t, *J* = 8.0 Hz, 2H), 7.45–7.38 (m, 3H), 7.36–7.31 (m, 3H), 7.29–7.21 (m, 4H), 5.09 (dd, *J* = 12.9, 7.8 Hz, 1H), 4.85 (dd, *J* = 12.9, 7.8 Hz, 1H), 4.23–4.17 (m, 2H), 1.81–1.73 (m, 2H), 1.49–1.36 (m, 4H), 0.94 (t, *J* = 6.9 Hz, 3H).

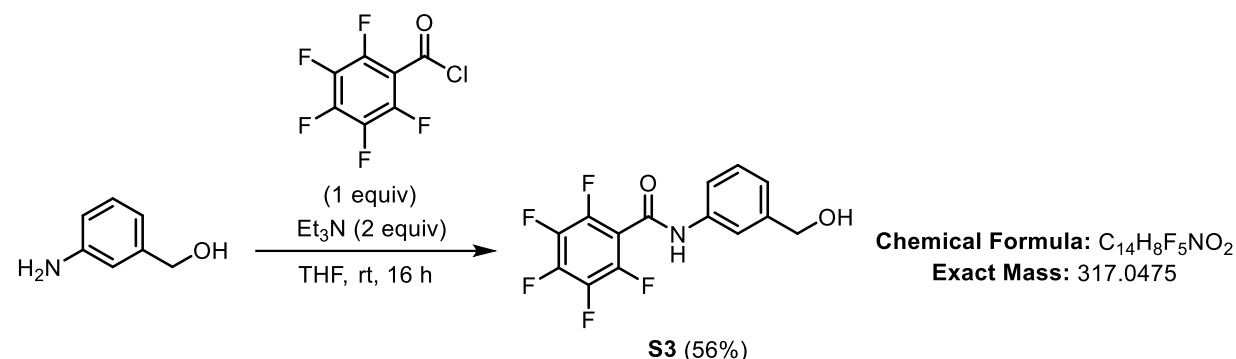
¹³C NMR (101 MHz, CDCl₃) δ = 163.1, 162.9, 152.9, 148.8 (2C), 147.5, 139.3 (2C), 134.9, 133.5, 132.9, 132.7, 131.6, 131.5, 131.2, 130.6, 130.4, 129.8, 129.6, 128.5 (2C), 128.1, 128.0, 127.6, 127.3, 127.1, 126.8, 126.5, 126.4, 125.3, 125.1, 124.4, 124.2, 122.7, 122.0, 121.7, 117.9, 111.0, 65.8 (d, *J* = 4.0 Hz), 41.2, 29.3, 27.9, 22.5, 14.1.

^{31}P NMR (121 MHz, CDCl_3) δ = 138.2.

IR (film, cm^{-1}): ν_{max} = 2958, 2870, 1705, 1660, 1581, 1454, 1373, 1344, 1248, 1193, 1086, 816.

HRMS (ESI $^+$): m/z calcd for $\text{C}_{46}\text{H}_{33}\text{N}_2\text{NaO}_7\text{P}$ [M+Na] $^+$: 779.7018, found: 779.7010.

2,3,4,5,6-pentafluoro-N-(3-(hydroxymethyl)phenyl)benzamide (S3)



To a solution of pentafluorobenzoyl chloride (1 g, 4.34 mmol, 1 equiv) in THF (30 mL) was added 3-aminobenzyl alcohol (534 mg, 4.34 mmol, 1 equiv) and triethylamine (1.2 mL, 8.68 mmol, 2 equiv) at 0 °C. The reaction mixture was stirred at room temperature for 16 h. Then, the reaction mixture was quenched with a solution of sat. NH_4Cl and extracted with ethyl acetate (10 mL \times 3). The combined organics layers were washed with brine, dried over anhydrous MgSO_4 , and filtered. The solvent was removed by rotary evaporation and the crude product was purified by flash column chromatography (7/3 to 1/1 pentane/EtOAc) to afford product **S3** as a white solid (776 mg, 56%).

Mp = 191–193 °C.

^1H NMR (300 MHz, MeOD) δ = 7.69–7.65 (m, 1H), 7.59–7.53 (m, 1H), 7.36 (t, J = 7.8 Hz, 1H), 7.19 (d, J = 7.6 Hz, 1H), 4.63 (s, 2H), NH and OH unobserved.

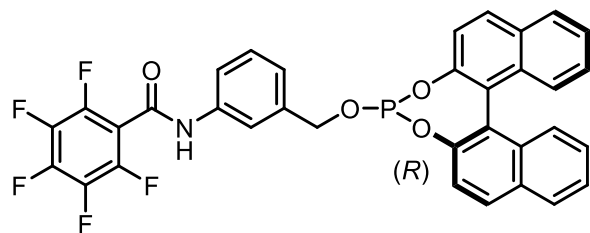
^{13}C NMR (91 MHz, MeOD) δ = 157.3, 145.2 (dm, J = 246.2 Hz), 144.0, 143.5 (dm, J = 259.8 Hz), 139.1, 138.9 (dm, J = 254.4 Hz), 130.1, 124.7, 120.0, 119.6, 113.8 (m), 64.9.

^{19}F NMR (235 MHz, MeOD) δ = -141.5 (ddd, J = 20.5, 6.5, 2.3 Hz), -152.6 (tt, J = 19.9, 2.0 Hz), -161.1–161.5 (m).

IR (film, cm^{-1}): ν_{max} = 3358, 1670, 1618, 1494, 1431, 1271, 1108, 994.

HRMS (ESI $^+$): m/z calcd for $\text{C}_{14}\text{H}_8\text{F}_5\text{NNaO}_2$ [M+Na] $^+$: 340.0367, found: 340.0355.

N-(3-((11*b*R)-dinaphtho[2,1-*d*:1',2'-*f*][1,3,2]dioxaphosphhepin-4-yloxy)methyl)phenyl)-2,3,4,5,6-pentafluorobenzamide (L2)



Chemical Formula: C₃₄H₁₉F₅NO₄P

Exact Mass: 631.0972

Following the general procedure A, starting from **S3** (200 mg, 0.632 mmol, 1 equiv), (*R*)-BINOL-PCl (232 mg, 0.663 mmol, 1.05 equiv), triethylamine (0.26 mL, 1.89 mmol, 3 equiv) and THF (7 mL). After purification the product **L2** was obtained as a white foam (160 mg, 40%).

Mp = 164–166 °C.

¹H NMR (300 MHz, CDCl₃) δ = 8.11 (brs, 1H), 8.01 (d, *J* = 8.8 Hz, 1H), 7.96 (d, *J* = 8.2 Hz, 1H), 7.92 (d, *J* = 8.7 Hz, 2H), 7.54 (d, *J* = 8.7 Hz, 1H), 7.54 (d, *J* = 8.2 Hz, 1H), 7.50–7.41 (m, 4H), 7.41–7.34 (m, 3H), 7.32–7.27 (m, 2H), 7.11 (d, *J* = 7.7 Hz, 1H), 4.98 (dd, *J* = 12.5, 7.6 Hz, 1H), 4.75 (dd, *J* = 12.5, 7.6 Hz, 1H).

¹³C NMR (75 MHz, CDCl₃) δ = 155.6, 148.7 (2C), 147.5, 144.2 (dm, *J* = 254.0 Hz), 142.6 (dm, *J* = 253.9 Hz), 138.7, 138.6, 137.6 (dm, *J* = 246.5 Hz), 136.9, 132.9, 132.7, 131.7, 131.1, 130.7, 130.3, 129.4, 128.5 (2C), 127.1, 126.5 (2C), 125.3, 125.1, 124.6, 122.7 (2C), 121.8, 121.5, 120.0, 119.2, 111.6 (m), 66.1 (d, *J* = 4.5 Hz).

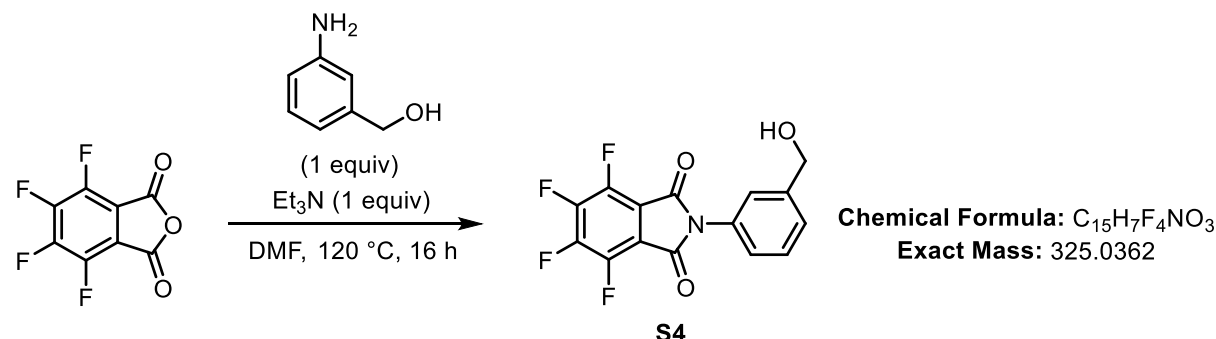
¹⁹F NMR (235 MHz, CDCl₃) δ = -139.7–140.3 (m), -149.5–150.1 (m), -159.3–159.9 (m).

³¹P NMR (101 MHz, CDCl₃) δ = 138.7.

IR (film, cm⁻¹): ν_{max} = 3431, 1704, 1656, 1618, 1519, 1500, 1343, 1248, 1189, 994, 767.

HRMS (ESI⁺): *m/z* calcd for C₃₄H₁₉F₅NNaO₄P [M+Na]⁺: 654.0864, found: 654.0847.

4,5,6,7-tetrafluoro-2-(3-(hydroxymethyl)phenyl)isoindoline-1,3-dione (S4)



Chemical Formula: C₁₅H₇F₄NO₃
Exact Mass: 325.0362

To a solution of tetrafluorophthalic anhydride (500 mg, 2.27 mmol, 1 equiv) in DMF (10 mL) were added aminobenzyl alcohol (279 mg, 2.27 mmol, 1 equiv) and triethylamine (0.31 mL, 2.27 mmol, 1 equiv.)

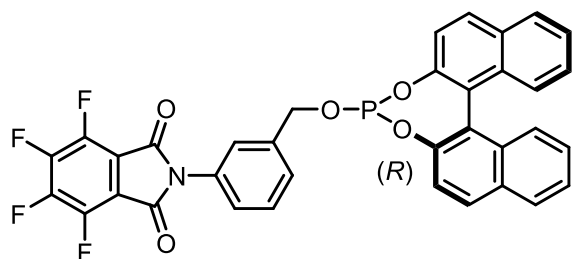
The reaction mixture was heated to 120 °C for 16 h. Then, it was cooled to room temperature, diluted with water, and extracted with DCM (3 x 20 mL). The combined organic layers were washed with water (twice), brine, dried over anhydrous MgSO₄ and filtered. The solvent was removed by rotary evaporation. The crude product was engaged in the next step without further purification.

¹H NMR (250 MHz, MeOD) δ = 7.68 (s, 1H), 7.63–7.54 (m, 1H), 7.34 (t, J = 7.8 Hz, 1H), 7.17 (d, J = 7.8 Hz, 1H), 4.62 (s, 2H), OH unobserved.

¹⁹F NMR (235 MHz, MeOD) δ = -140.6 (dtt, J = 13.8, 6.4, 3.1 Hz), -141.6 (ddt, J = 20.8, 13.2, 5.8 Hz), -154.7–154.9 (m), -157.4 (ddt, J = 21.3, 18.7, 2.7 Hz).

HRMS (ESI⁺): m/z calcd for C₁₅H₇F₄NNaO₃ [M+Na]⁺: 348.0260, found: 348.0314.

2-(3-((11b*R*)-dinaphtho[2,1-d:1',2'-f][1,3,2]dioxaphosphhepin-4-yloxy)methyl)phenyl)-4,5,6,7-tetrafluoroisoindoline-1,3-dione (L3**)**



Chemical Formula: C₃₅H₁₈F₄NO₅P
Exact Mass: 639.0859

Following the general procedure D, starting from **S4** (200 mg, 0.614 mmol, 1 equiv.), (*R*)-BINOL-PCI (226 mg, 0.645 mmol, 1.05 equiv.), triethylamine (0.25 mL, 1.84 mmol, 3 equiv.) and THF (7 mL). After purification the product **L3** was obtained as a white foam (179 mg, 0.280 mmol, 45%).

Mp = 172–174 °C.

¹H NMR (300 MHz, CDCl₃) δ = 8.21 (d, J = 13.3 Hz, 1H), 8.00 (d, J = 8.8 Hz, 1H), 7.92 (t, J = 8.5 Hz, 2H), 7.87–7.77 (m, 1H), 7.62 (d, J = 8.1 Hz, 1H), 7.54 (d, J = 9.1 Hz, 1H), 7.51–7.47 (m, 1H), 7.47–7.42 (m, 2H), 7.39–7.34 (m, 3H), 7.30–7.24 (m, 2H), 7.12 (d, J = 7.7 Hz, 1H), 5.01 (dd, J = 12.5, 7.7 Hz, 1H), 4.77 (dd, J = 12.5, 7.7 Hz, 1H).

¹³C NMR (101 MHz, CDCl₃) δ = 158.5, 148.8 (2C), 147.6, 147.2–144.1 (m), 142.5–139.4 (m), 138.8 (2C), 137.3, 133.0, 132.7, 131.7, 131.2, 130.7, 130.3, 129.5, 128.5 (2C), 127.1, 126.5, 126.4, 125.3, 125.1, 124.5, 121.9, 121.6, 120.4, 119.6, 113.4, 113.1, 66.2 (d, J = 4.0 Hz).

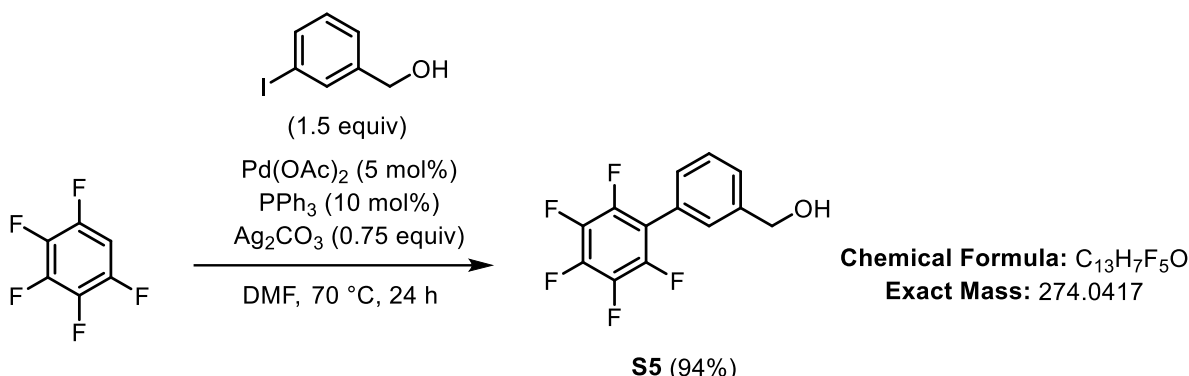
¹⁹F NMR (235 MHz, CDCl₃) δ = -135.8–136.1 (m), -138.6–139.0 (m), -147.8–148.1 (m), -153.2–153.5 (m).

³¹P NMR (121 MHz, CDCl₃) δ = 138.7.

IR (film, cm⁻¹): ν_{max} = 1704, 1657, 1617, 1596, 1517, 1373, 1345, 1248, 1188, 1149, 994, 749.

HRMS (ESI⁺): m/z calcd for C₃₅H₁₈F₄NNaO₅P [M+Na]⁺: 662.0756, found: 662.0795.

(2',3',4',5',6'-pentafluoro-[1,1'-biphenyl]-3-yl)methanol (S5)



To a septum-capped 50 mL Schlenk tube were added Pd(OAc)₂ (88 mg, 0.395 mmol, 0.05 equiv), PPh₃ (207 mg, 0.790 mmol, 0.1 equiv), Ag₂CO₃ (1.63 g, 5.92 mmol, 0.75 equiv) and 3-iodobenzyl alcohol (1 mL, 7.90 mmol, 1 equiv) under argon, followed by pentafluorobenzene (1.31 mL, 11.90 mmol, 1.5 equiv) and DMF (20 mL). The reaction mixture was heated at 70 °C for 24 h. Then, the reaction mixture was cooled to room temperature, and ethyl acetate (200 mL) and water (80 mL) were added to it. The organic layer was separated, and the aqueous phase was extracted with ethyl acetate (2 x 80 mL). The combined organic layers were dried over anhydrous MgSO₄ and filtered. The solvent was removed by rotary evaporation. The crude product was purified by flash column chromatography (8/2 pentane/EtOAc) to afford product **S5** as white solid (2.04 g, 94%).

Mp = 71–73 °C.

¹H NMR (400 MHz, MeOD) δ = 7.49–7.36 (m, 3H), 7.33–7.23 (m, 1H), 4.92 (brs, 1H), 4.65 (s, 2H).

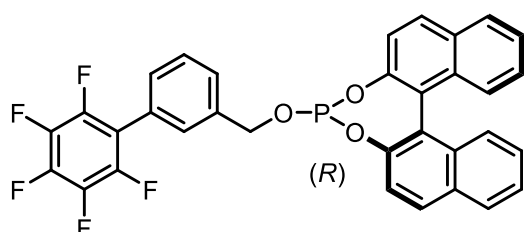
¹³C NMR (101 MHz, MeOD) δ = 145.5 (dm, *J* = 246.4 Hz), 143.7, 141.6 (dm, *J* = 252.9 Hz), 149.1 (dm, *J* = 251.3 Hz), 129.9, 129.7, 129.5, 128.9, 127.5, 117.4 (td, *J* = 17.4, 2.3 Hz), 64.7.

¹⁹F NMR (235 MHz, MeOD) δ = -143.19 (dd, *J* = 22.1, 8.2 Hz), -155.45 (t, *J* = 22.1 Hz), -162.1–-162.3 (m).

IR (film, cm⁻¹): ν_{max} = 3292, 1585, 1523, 1497, 1254, 1071, 1043, 984.

HRMS (ESI⁺): *m/z* calcd for C₁₃H₇F₅NaO [M+Na]⁺: 297.0309 found: 297.0301.

(11*bR*)-4-((2',3',4',5',6'-pentafluoro-[1,1'-biphenyl]-3-yl)methoxy)dinaphtho[2,1-*d*:1',2'-*f*][1,3,2]dioxaphosphepine (L4)



Chemical Formula: C₃₃H₁₈F₅O₃P
Exact Mass: 588.0914

Following the general procedure D, starting from **S5** (200 mg, 0.729 mmol, 1 equiv), (*R*)-BINOL-PCI (268 mg, 0.765 mmol, 1.05 equiv), triethylamine (0.3 mL, 2.18 mmol, 3 equiv) and THF (8 mL). After purification the product **L4** was obtained as a white foam (124 mg, 0.211 mmol, 29%).

Mp = 79–81 °C.

¹H NMR (300 MHz, CDCl₃) δ = 8.03 (d, *J* = 8.8 Hz, 1H), 7.98–7.89 (m, 3H), 7.59 (d, *J* = 8.7 Hz, 1H), 7.51–7.37 (m, 9H), 7.34–7.28 (m, 2H), 5.11 (dd, *J* = 12.6, 7.8 Hz, 1H), 4.87 (dd, *J* = 12.6, 7.8 Hz, 1H).

¹³C NMR (91 MHz, CDCl₃) δ = 148.8, 148.7, 147.5, 144.2 (dm, *J* = 247.3 Hz), 140.6 (dm, *J* = 236.4 Hz), 138.2, 138.1, 137.9 (dm, *J* = 236.3 Hz), 132.9, 132.7, 131.7, 131.1, 130.7, 130.3, 129.8, 129.1, 129.0, 128.5, 128.4, 127.1, 126.7, 126.5, 125.3, 125.1, 124.2, 124.1, 122.8, 121.9, 121.5, 115.8 (t, *J* = 15.6 Hz), 66.1 (d, *J* = 4.1 Hz).

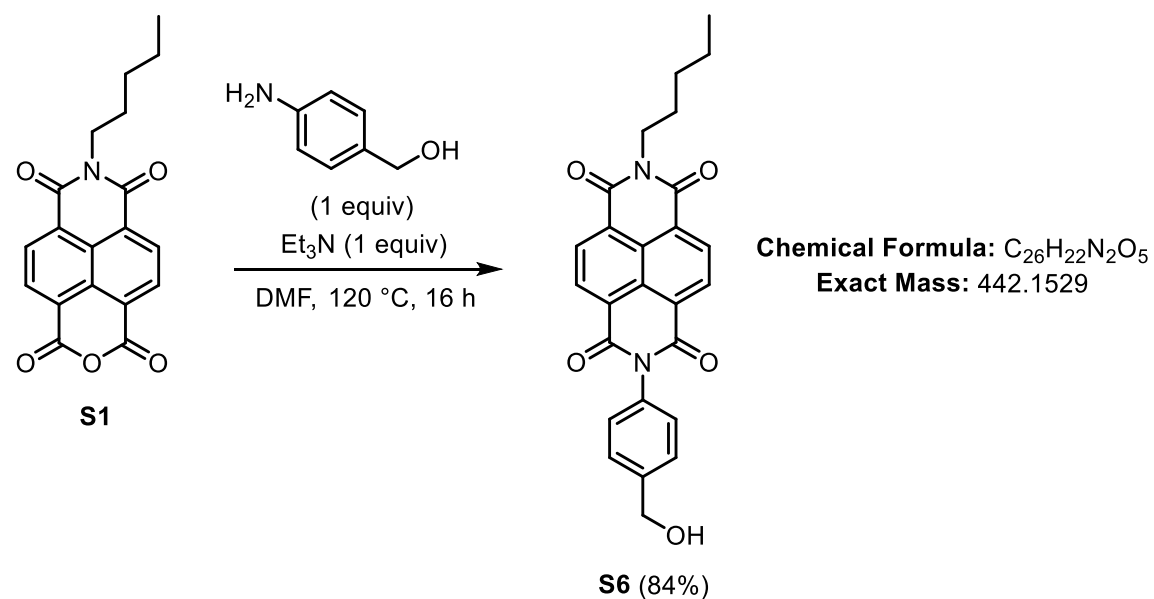
¹⁹F NMR (235 MHz, CDCl₃) δ = -142.8 (dd, *J* = 22.3, 8.2 Hz), -155.1 (t, *J* = 22.3 Hz), -161.7–162.0 (m).

³¹P NMR (121 MHz, CDCl₃) δ = 138.5.

IR (film, cm⁻¹): ν_{max} = 1660, 1638, 1520, 1489, 1452, 1278, 1196, 1084, 996, 764.

HRMS (APCI): *m/z* calcd for C₃₃H₁₉F₅O₃P [M+H]⁺: 589.0986, found: 589.0939.

2-(4-(hydroxymethyl)phenyl)-7-pentylbenzo[*lmn*][3,8]phenanthroline-1,3,6,8(2*H*,7*H*)-tetraone (**S6**)



To a solution of **XX⁹** (687 mg, 2.04 mmol, 1 equiv) in DMF (15 mL) were added 4-aminobenzyl alcohol (251 mg, 2.04 mmol, 1 equiv) and triethylamine (0.28 mL, 2.04 mmol, 1 equiv.). The reaction mixture was heated to 120 °C for 16 h. Then, it was cooled to room temperature, diluted with water, and extracted with DCM (3 x 15 mL). The combined organic layers were washed with water (twice), brine, dried over anhydrous MgSO₄ and filtered. The solvent was removed by rotary evaporation. The crude product was purified by flash column chromatography (97:3 DCM/MeOH) to afford **X** as a light brown solid (758 mg, 1.71 mmol, 84%).

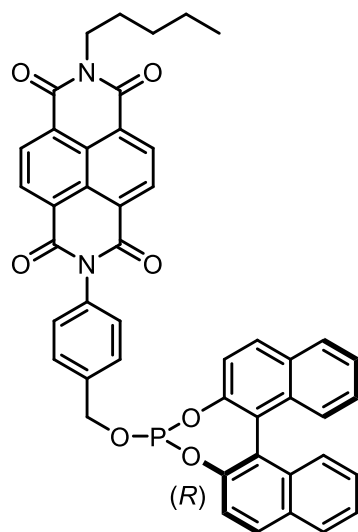
Mp = 309–311 °C.

¹H NMR (300 MHz, CDCl₃) δ = 8.79 (s, 4H), 7.58 (d, J = 7.5 Hz, 2H), 7.31 (d, J = 7.5 Hz, 2H), 4.81 (s, 2H), 4.22–4.18 (m, 2H), 1.78–1.72 (m, 2H), 1.44–1.35 (m, 4H), 0.92 (t, J = 6.9 Hz, 3H), OH unobserved.

IR (film, cm⁻¹): ν_{max} = 3387, 2958, 2871, 1704, 1655, 1581, 1453, 1345, 1248, 1192, 1086, 768.

HRMS (ESI⁺): *m/z* calcd for C₂₆H₂₂N₂NaO₅ [M+Na]⁺: 465.1421, found: 465.1394.

2-((4-(((11*b*R)-dinaphtho[2,1-d:1',2'-f][1,3,2]dioxaphosphhepin-4-yloxy)methyl)phenyl)-7-pentylbenzo[1*m*n][3,8]phenanthroline-1,3,6,8(2*H*,7*H*)-tetraone (L6**)**



Chemical Formula: C₄₆H₃₃N₂O₇P
Exact Mass: 756.2025

Following the general procedure A, starting from **S1** (250 mg, 0.565 mmol, 1 equiv), (*R*)-BINOL-PCl (207 mg, 0.593 mmol, 1.05 equiv), triethylamine (0.23 mL, 1.69 mmol, 3 equiv) and THF (6 mL). After purification the product **L6** was obtained as an orange solid (204 mg, 48%). The product was contaminated by an unidentified impurity.

Mp = 188–190 °C.

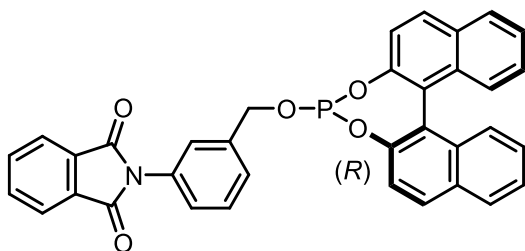
¹H NMR (360 MHz, CDCl₃) δ = 8.76 (s, 4H), 7.98 (d, J = 8.8 Hz, 1H), 7.95–7.90 (m, 3H), 7.54 (d, J = 8.8 Hz, 1H), 7.49 (d, J = 7.9 Hz, 2H), 7.45–7.38 (m, 2H), 7.36–7.24 (m, 7H), 5.09 (dd, J = 12.3, 8.4 Hz, 1H), 4.86 (dd, J = 12.3, 8.4 Hz, 1H), 4.24–4.15 (m, 2H), 1.84–1.66 (m, 2H), 1.49–1.35 (m, 4H), 0.94 (t, J = 6.9 Hz, 3H).

³¹P NMR (101 MHz, CDCl₃) δ = 138.3.

IR (film, cm⁻¹): ν_{max} = 2958, 2869, 1705, 1663, 1581, 1454, 1343, 1249, 1195, 1016, 970, 882.

HRMS (ESI⁺): *m/z* calcd for C₄₆H₃₃N₂NaO₇P [M+Na]⁺: 779.7018, found: 779.7005.

2-(3-((11*b*R)-dinaphtho[2,1-d:1',2'-f][1,3,2]dioxaphosphhepin-4-yloxy)methyl)phenyl)isoindoline-1,3-dione (L7**)**



Chemical Formula: C₃₅H₂₂NO₅P

Exact Mass: 567.1236

Following the general procedure A, starting from **S7**¹⁰ (200 mg, 0.790 mmol, 1 equiv), (*R*)-BINOL-PCI (290 mg, 0.829 mmol, 1.05 equiv), triethylamine (0.33 mL, 2.37 mmol, 3 equiv) and THF (8 mL). After purification the product **L7** was obtained as a white foam (273 mg, 61%).

Mp = 106–108 °C.

¹H NMR (360 MHz, CDCl₃) δ = 8.02–7.89 (m, 6H), 7.81–7.76 (m, 2H), 7.57 (d, *J* = 8.7 Hz, 1H), 7.51–7.33 (m, 9H), 7.31–7.24 (m, 2H), 5.09 (dd, *J* = 12.6, 7.7 Hz, 1H), 4.84 (dd, *J* = 12.6, 7.7 Hz, 1H).

¹³C NMR (75 MHz, CDCl₃) δ = 167.2, 148.8, 148.7, 147.6, 138.7, 138.6, 134.5, 132.9, 132.7, 132.0, 131.8, 131.7, 131.1, 130.6, 130.4, 129.3, 128.5, 127.1, 126.4, 126.3, 126.2, 125.5, 125.2, 125.0, 124.2, 124.1, 123.8, 122.7, 121.9, 121.6, 66.0 (d, *J* = 4.1 Hz).

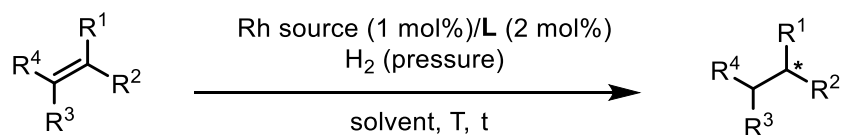
³¹P NMR (75 MHz, CDCl₃) δ = 138.2.

IR (film, cm⁻¹): ν_{max} = 1704, 1696, 1620, 1589, 1432, 1373, 1350, 1190, 1150, 994.

HRMS (ESI⁺): *m/z* calcd for C₃₅H₁₈F₄NNaO₅P [M+Na]⁺: 590.1133, found: 590.1124.

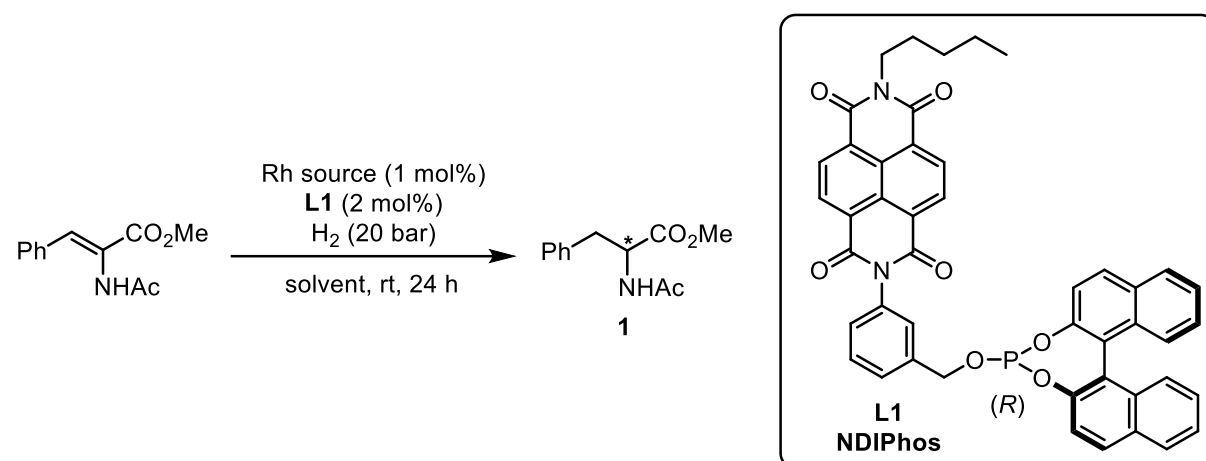
4. Rh-Catalyzed Enantioselective Hydrogenation

General procedure for enantioselective hydrogenation



In an autoclave was placed a vial with olefin substrate (0.4 mmol, 1 equiv.), Rh source (0.004 mmol, 1 mol%), **LX** (0.008 mmol, 2 mol%) and solvent (3 mL). The reaction mixture was purged three times with H₂ (10 bar) and stirred at the indicated temperature for the indicated time under H₂ at the indicated pressure. Then, the mixture was passed through a short pad of silica and rinsed with ethyl acetate. The solvent was removed by rotary evaporation and the crude product was purified by flash column chromatography using gradients of pentane and ethyl acetate, to afford the target product.

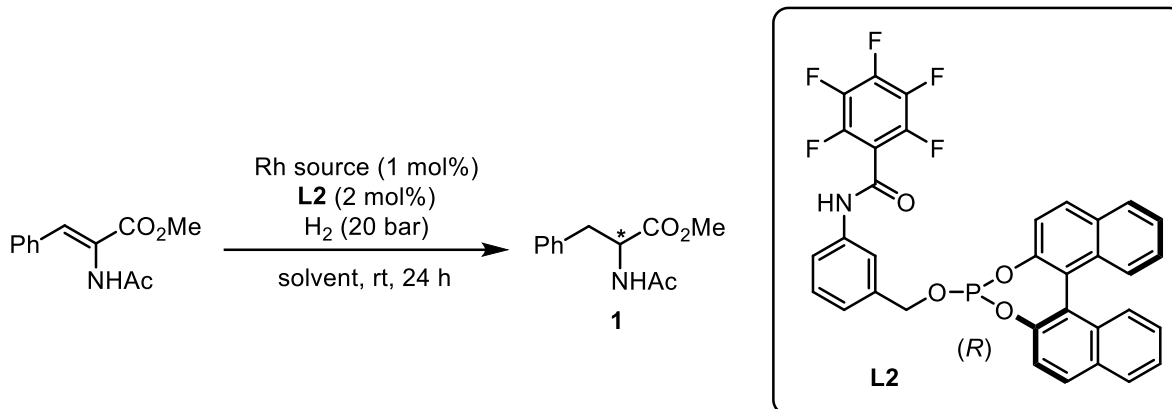
Optimization with ligand L1.^[a]



Entry	Rh source	Solvent	Conversion ^[b]	ee ^[c]
1		DCM	>99%	87%
2		Toluene	>99%	71%
3		MeOH	>99%	9%
4		1,4-Dioxane	>99%	35%
5		PhNO ₂	>99%	93%
6		PhBr	>99%	92%
7	[Rh(COD)(MeCN) ₂]BF ₄	Benzene	>99%	80%
8		1,3-Dimethoxybenzene	>99%	70%
9		MeNO ₂	>99%	NR
10		HFIP	>99%	55%
11		Toluene/PhNO ₂ (10:1)	>99%	94%
12		DCM/C ₆ F ₆ (10:1)	>99%	95%
13		DCM/PhNO ₂ (10:1)	>99%	95%
14		DCM/PhNO ₂ (10:1)	>99%	90% ^[d]
15	[Rh(COD) ₂]OTf	DCM/PhNO ₂ (10:1)	>99%	96%
16	[Rh(COD) ₂]SbF ₆	DCM/PhNO ₂ (10:1)	>99%	96%
17	[Rh(COD) ₂]SbF ₆	DCM/PhNO ₂ (10:1)	>99%	98% ^[e]
18	[Rh(COD) ₂]BARF	DCM/PhNO ₂ (10:1)	>99%	96%

[a] Reaction conditions: substrate/ligand/catalyst=100:2:1, solvent c = 0.13 M, T = 25 °C. [b] Determined by ¹H NMR. [c] Determined by HPLC equipped with a chiral column Daicel Chiraldapak IA. [d] [Rh(COD)(MeCN)₂]BF₄ (2 mol%). [e] Reaction at 0 °C.

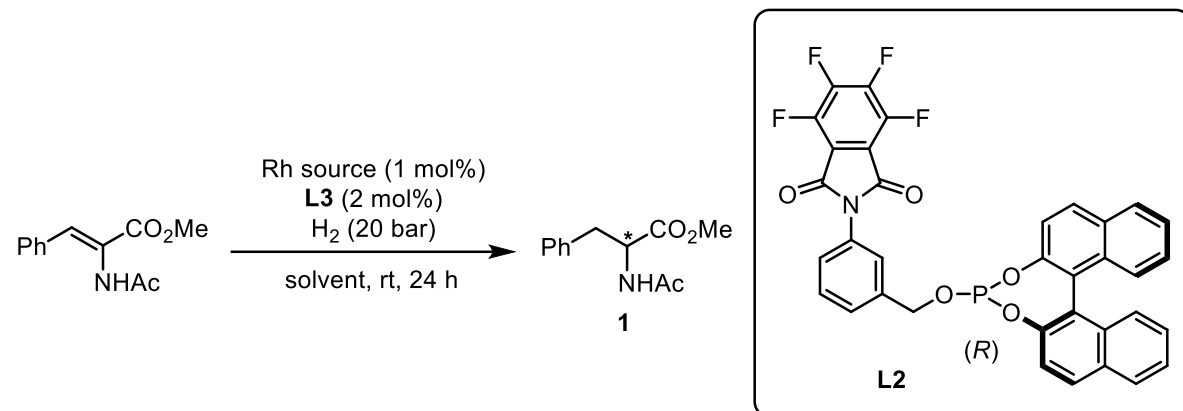
Optimization with ligand L2.^[a]



Entry	Rh source	Solvent	Conversion ^[b]	ee ^[c]
1		DCM	>99%	93%
2		Toluene	>99%	97%
3		MeOH	>99%	45%
4	$[\text{Rh}(\text{COD})(\text{MeCN})_2]\text{BF}_4$	Dioxane	>99%	89%
6		Isopropanol	>99%	50%
7		HFIP	>99%	60%
8		DCM/PhNO ₂ (10:1)	>99%	93%
9	$[\text{Rh}(\text{COD})_2]\text{OTf}$	Toluene	>99%	98%
10	$[\text{Rh}(\text{COD})_2]\text{SbF}_6$	Toluene	>99%	95%
11	$[\text{Rh}(\text{COD})_2]\text{BARF}$	Toluene	>99%	94%
12	$[\text{Rh}(\text{COD})(\text{acac})]$	Toluene	>99%	NR
13	$[\text{Rh}(\text{COD})_2\text{Cl}_2]$	Toluene	>99%	NR

[a] Reaction conditions: substrate/ligand/catalyst=100:2:1, solvent c = 0.13 M, T = 25 °C. [b] Determined by ¹H NMR. [c] Determined by HPLC equipped with a chiral column Daicel Chiralpak IA.

Optimization with ligand L3.^[a]

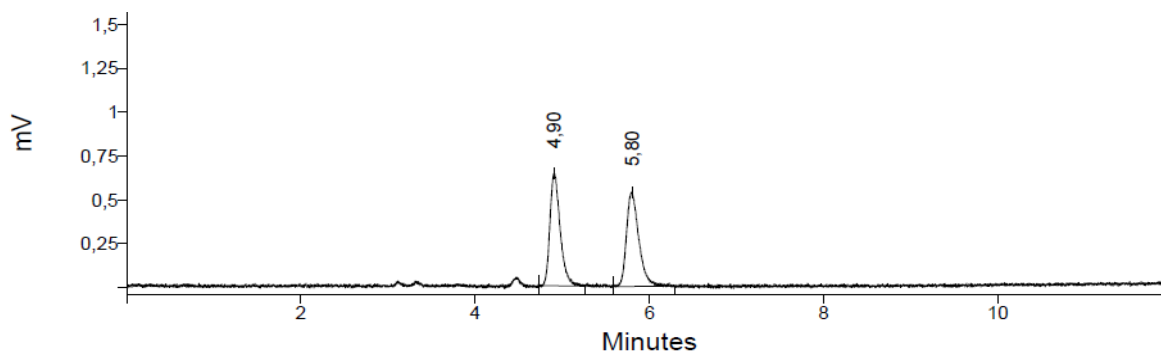


Entry	Rh source	Solvent	Conversion ^[b]	ee ^[c]
1		DCM	>99%	92%
2		Toluene	>99%	96%
3		MeOH	>99%	45%
4	$[\text{Rh}(\text{COD})(\text{MeCN})_2]\text{BF}_4$	Dioxane	>99%	56%
6		Isopropanol	>99%	55%
7		HFIP	>99%	59%
8		DCM/PhNO ₂ (10:1)	>99%	93%
9	$[\text{Rh}(\text{COD})_2]\text{OTf}$	Toluene	>99%	91%
10	$[\text{Rh}(\text{COD})_2]\text{SbF}_6$	Toluene	>99%	95%
11	$[\text{Rh}(\text{COD})_2]\text{BARF}$	Toluene	>99%	91%

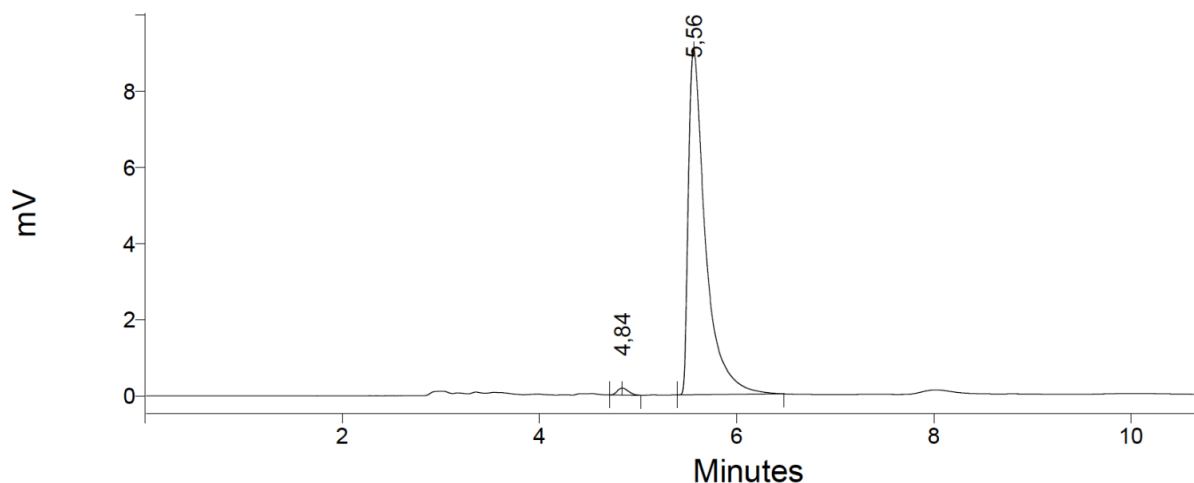
[a] Reaction conditions: substrate/ligand/catalyst=100:2:1, solvent c = 0.13 M, T = 25 °C. [b] Determined by ¹H NMR. [c] Determined by HPLC equipped with a chiral column Daicel Chiralpak IA.

Methyl 2-acetamido-3-phenylpropanoate (1)

HPLC conditions: column: Daicel Chiralpak IA; eluent: 75:25 hex/i-PrOH; flow: 1 mL/min; $\lambda = 254$ nm; 20 °C; $t_{\text{minor}} = 4.9$ min; $t_{\text{major}} = 5.8$ min.



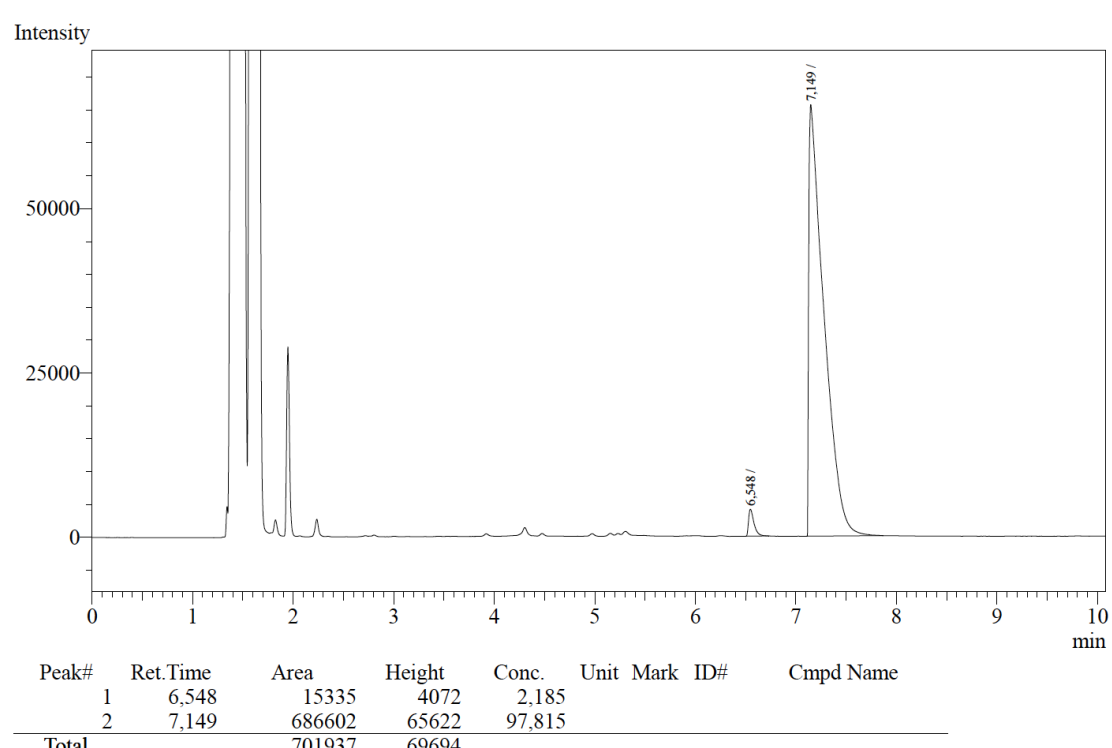
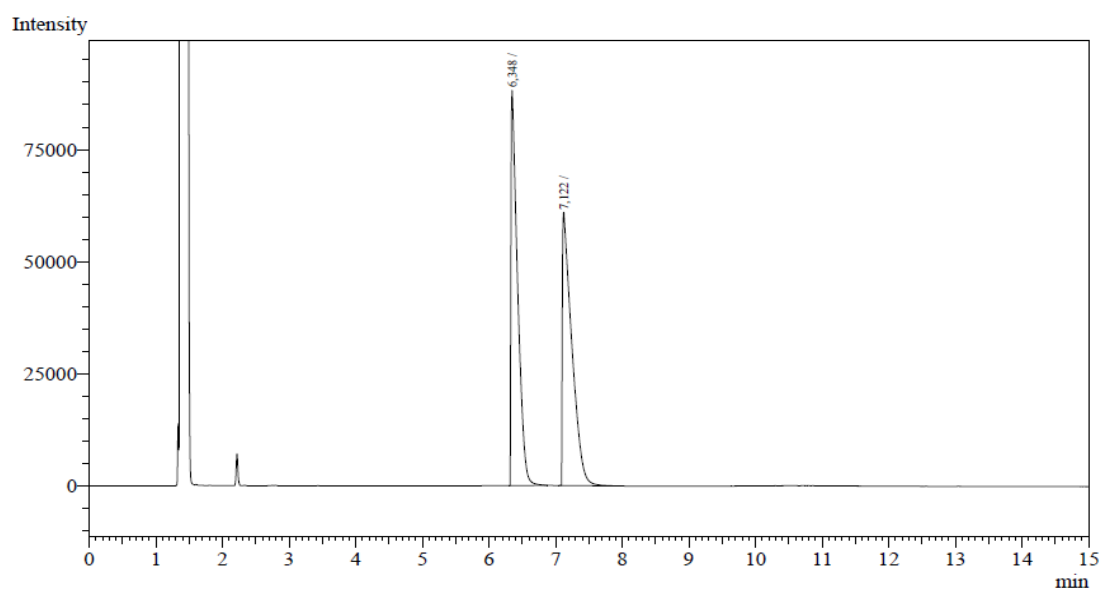
#	Nom du pic	Tr.	Aire	% Aire	Asymétrie (USP, EP)	Plateaux (EP)
1		4,90	5,24	49,74		1,45 9017,39
2		5,80	5,29	50,26		1,35 8738,11
SOMME		10,53			100,00	



#	Nom du pic	Tr.	Aire	% Aire	Asymétrie (USP, EP)	Plateaux (EP)
1		4,84	1,44	1,30		1,15 8624,39
2		5,56	109,32	98,70		2,53 6180,67
SOMME		110,76			100,00	

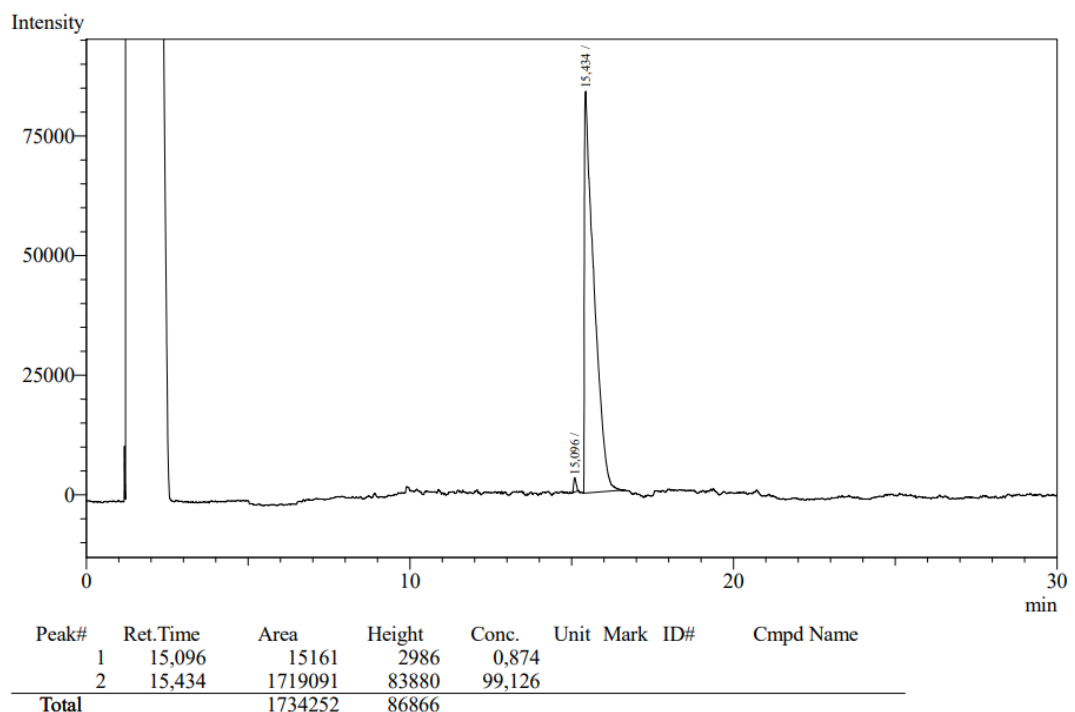
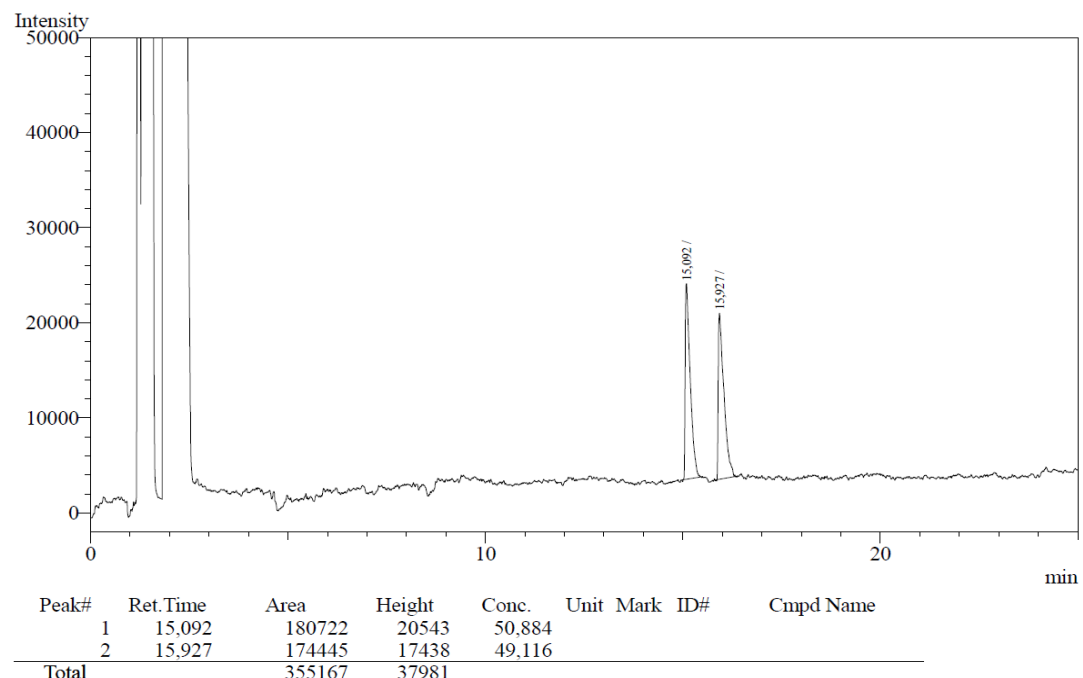
Methyl 2-acetamidopropanoate (2)

GC conditions: capillary column: β -DEX 225, 0.25 μm ; diameter = 0.25 mm; length = 30 m; isothermal: 130 °C; $t_{\text{minor}} = 6.3 \text{ min}$; $t_{\text{major}} = 7.1 \text{ min}$.



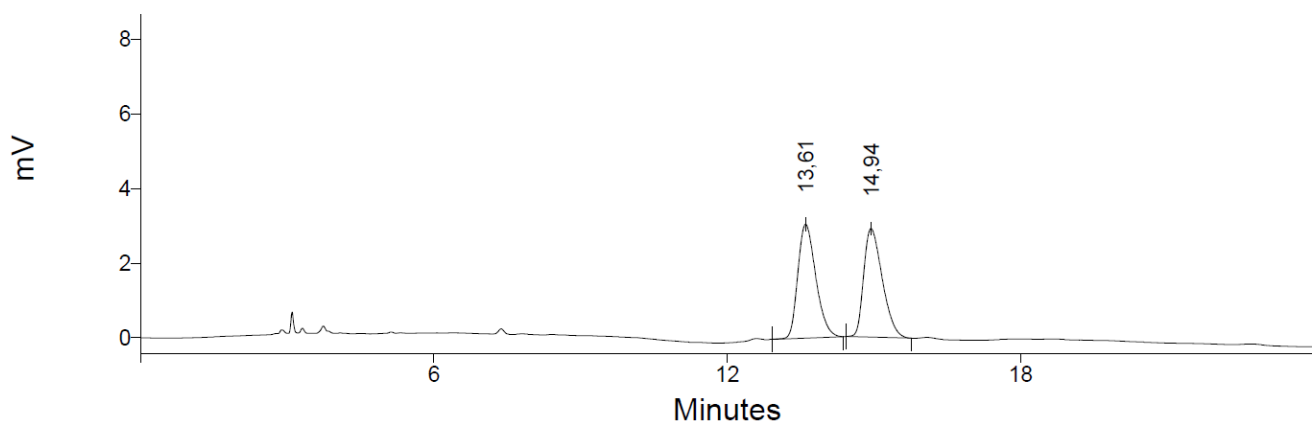
Dimethyl 2-methylsuccinate (3)

GC conditions: capillary column: β -DEX 225, 0.25 μm ; diameter = 0.25 mm; length = 30 m; isothermal: 80 °C; $t_{\text{minor}} = 15.1$ min; $t_{\text{major}} = 15.9$ min.

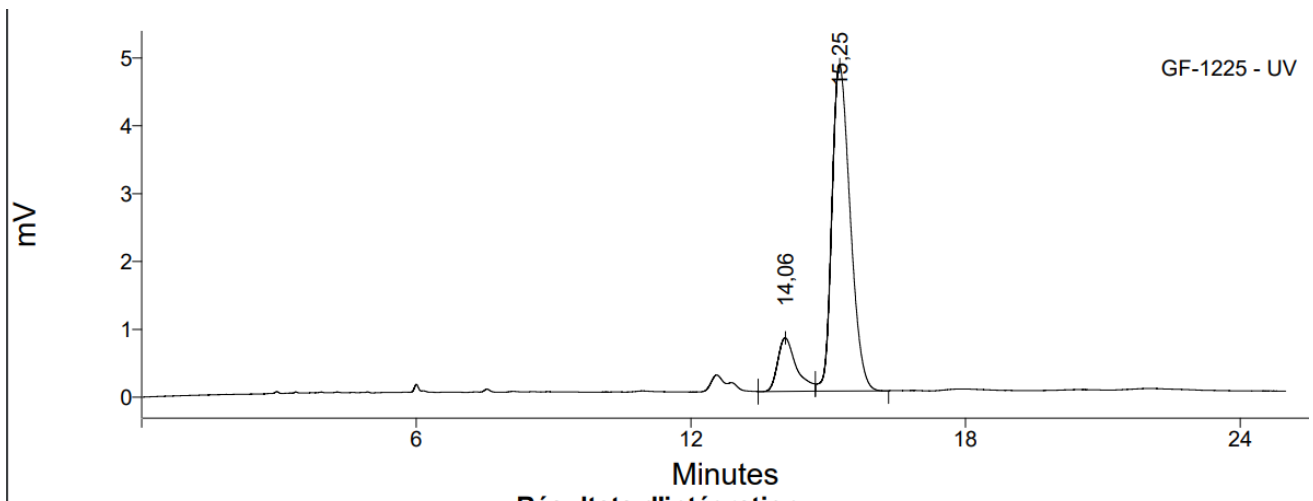


N-(1,2,3,4-tetrahydronaphthalen-1-yl)acetamide (4)

HPLC conditions: column: Phenomenex Lux-Cellulose-2; eluent: 90:10 hex/i-PrOH; flow: 1 mL/min; $\lambda = 254$ nm; 20 °C; $t_{\text{minor}} = 13.6$ min; $t_{\text{major}} = 14.9$ min.



#	Nom du pic	Tr.	Aire	% Aire	Asymétrie (USP, EP)	Plateaux (EP)
1		13,61	77,95	50,35	1,34	6528,48
2		14,94	76,86	49,65	1,39	7334,88
SOMME			154,81	100,00		

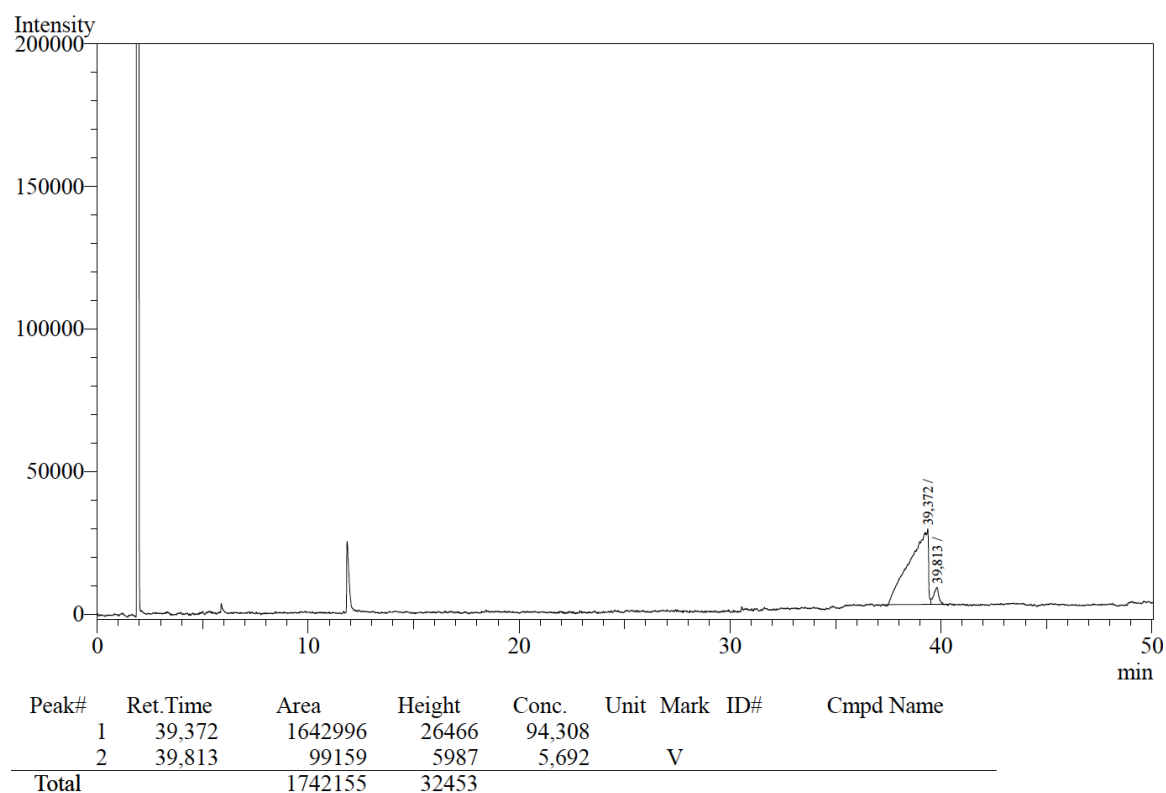
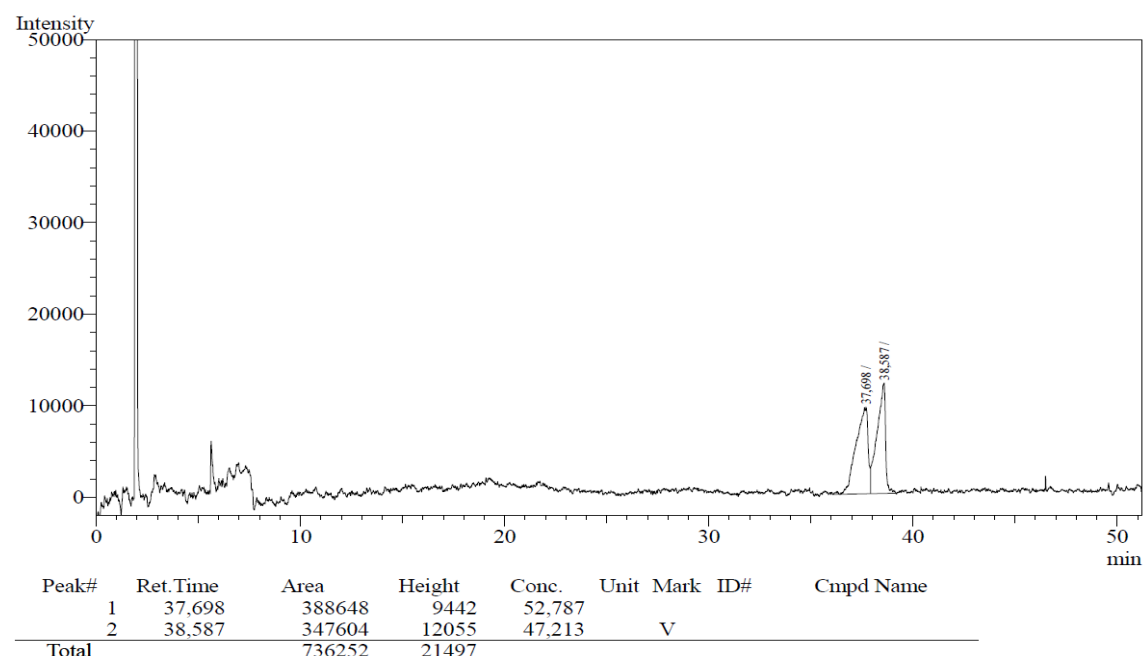


Résultats d'intégration

#	Nom du pic	Tr.	Aire	% Aire	Asymétrie (USP, EP)	Plateaux (EP)
1		14,06	22,23	14,25	#	6826,39
2		15,25	133,73	85,75	1,32	6967,12
SOMME			155,96	100,00		

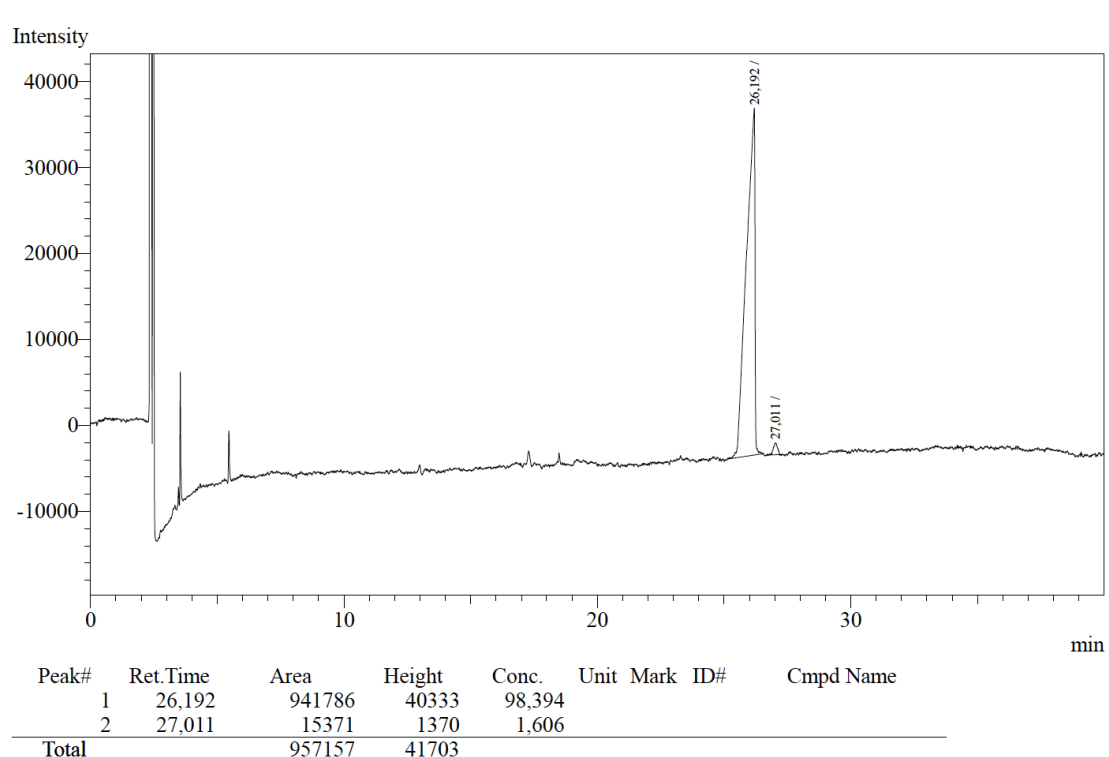
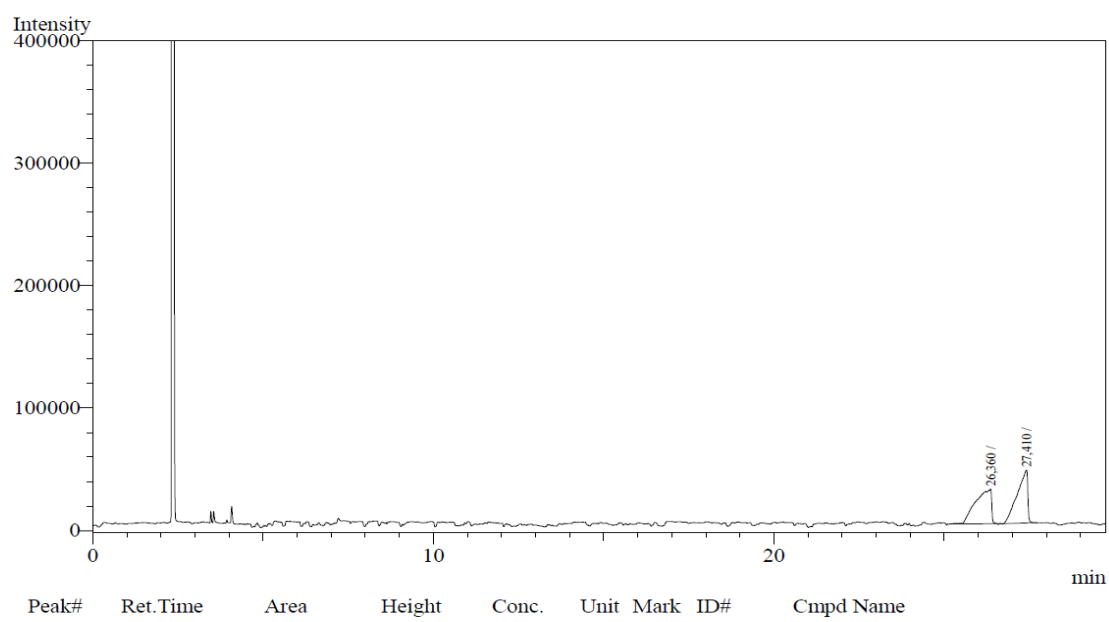
2-Acetamidopropanoic acid (5)

GC conditions: capillary column: CHIRALDEX- β -PM, 0.12 μm ; diameter = 0.25 mm; length = 50 m; isothermal: 130 °C; $t_{\text{major}} = 37.7 \text{ min}$; $t_{\text{minor}} = 38.6 \text{ min}$)



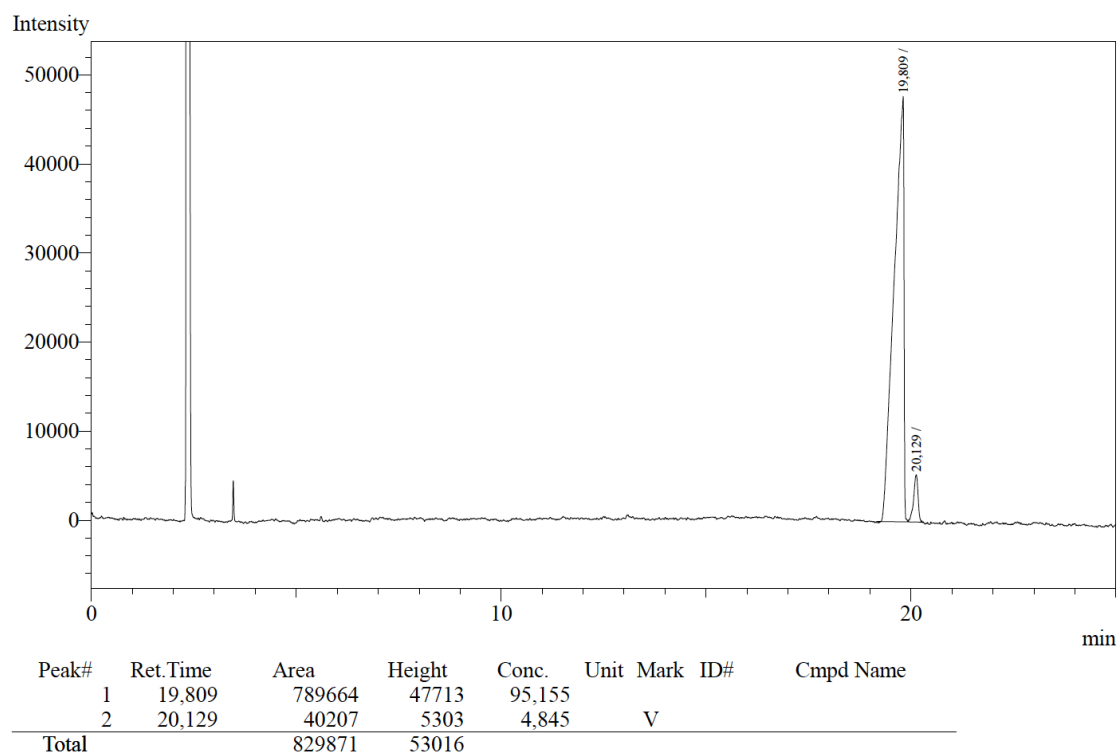
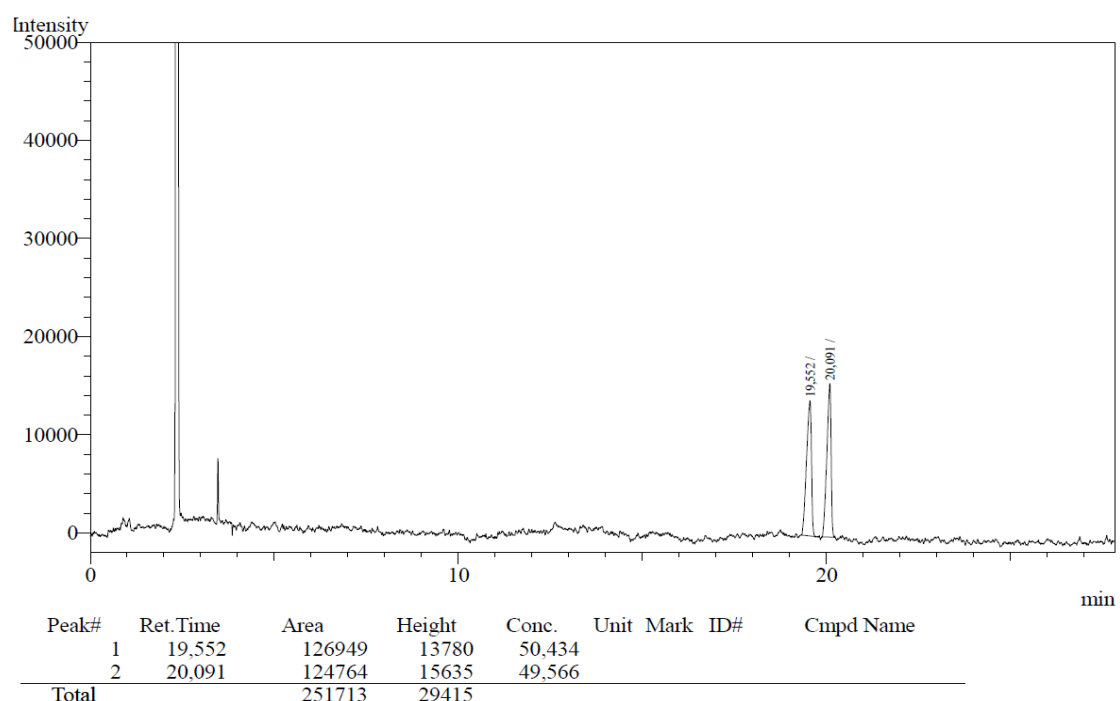
Methyl 3-acetamido-2-methylpropanoate (6)

GC conditions: capillary column: CHIRALDEX- β -PM, 0.12 μm ; diameter = 0.25 mm; length = 50 m; isothermal: 110 °C; $t_{\text{major}} = 26.4 \text{ min}$; $t_{\text{minor}} = 27.4 \text{ min}$)

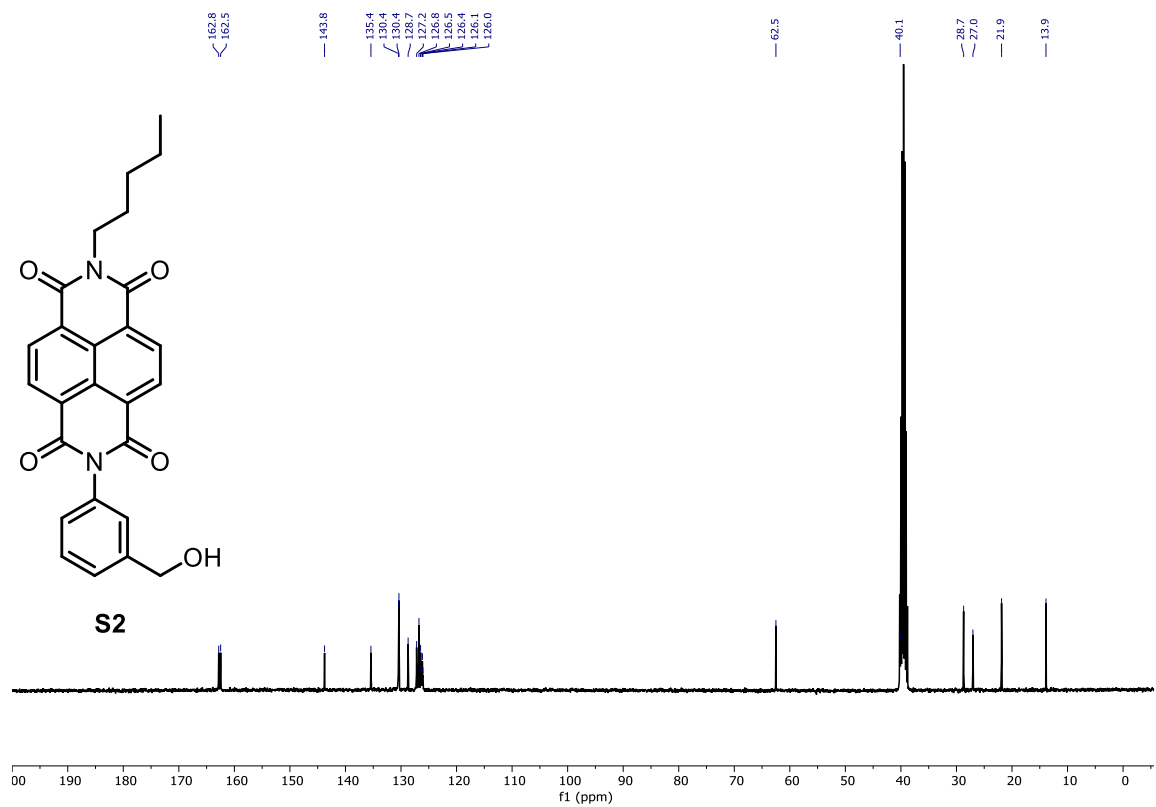
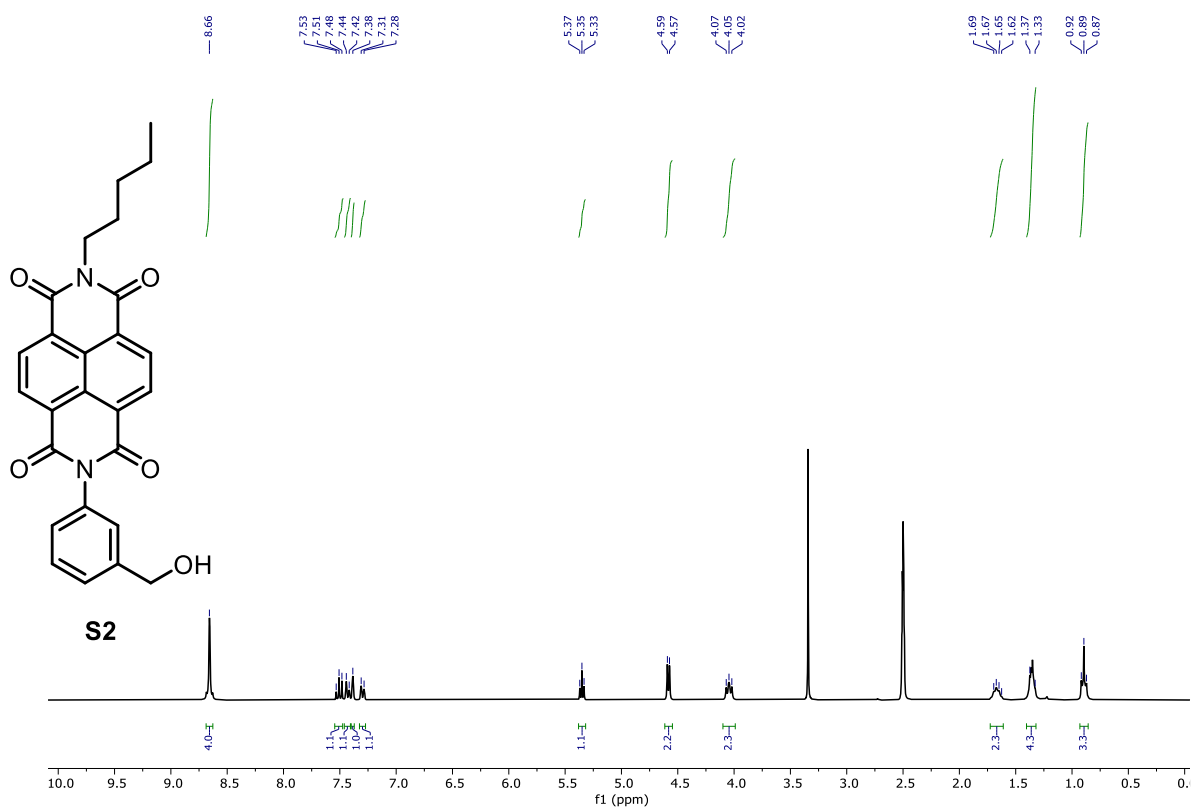


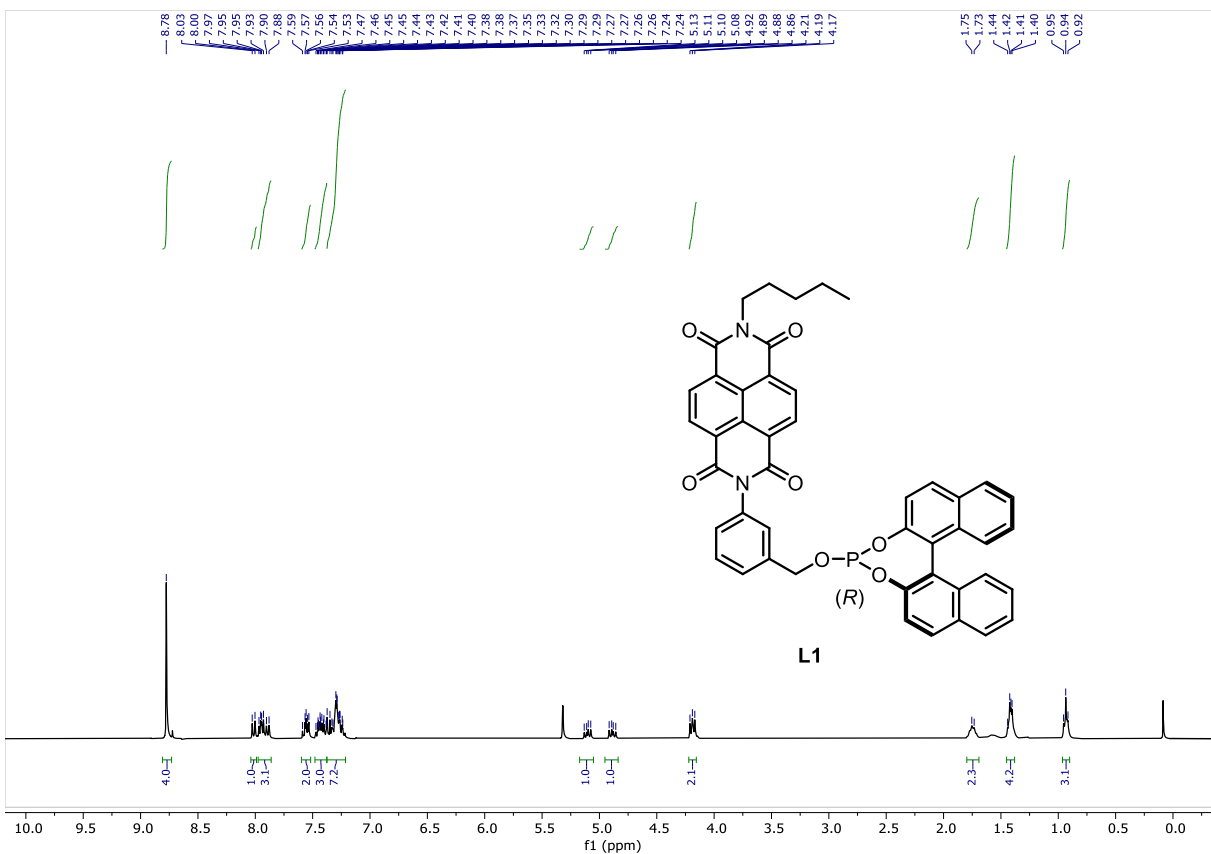
Methyl 2-acetamido-3-methylbutanoate (7)

GC conditions: capillary column: CHIRALDEX- β -PM, 0.12 μ m; diameter = 0.25 mm; length = 50 m; isothermal: 110 °C; $t_{\text{major}} = 19.5 \text{ min}$; $t_{\text{minor}} = 20.1 \text{ min}$.

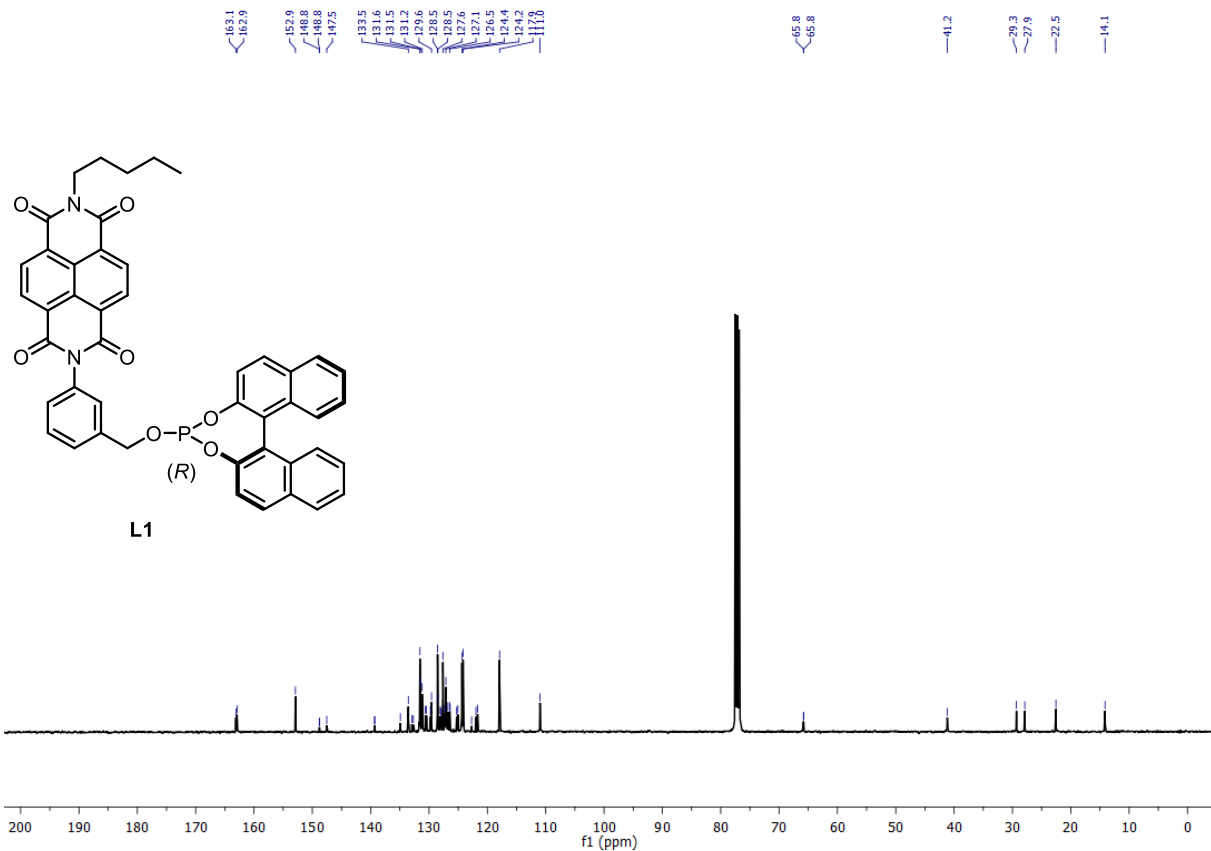


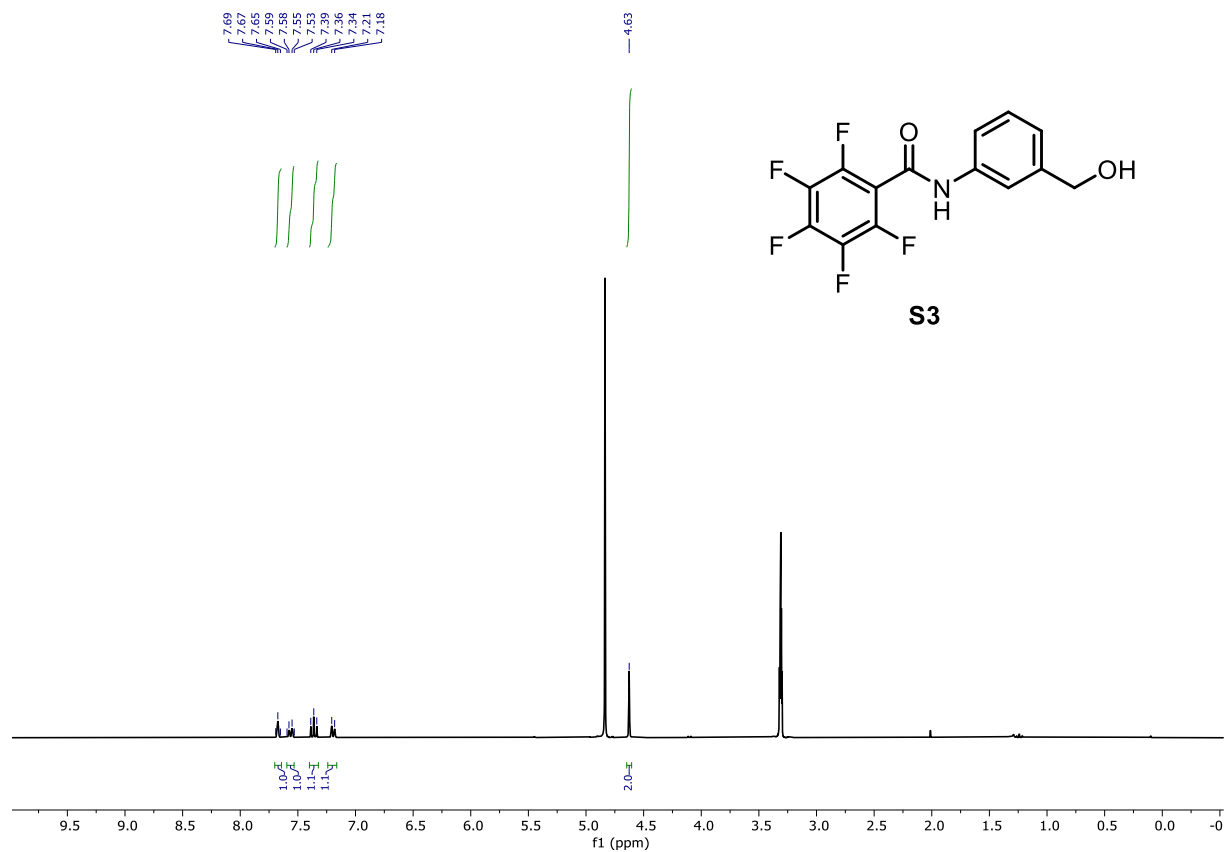
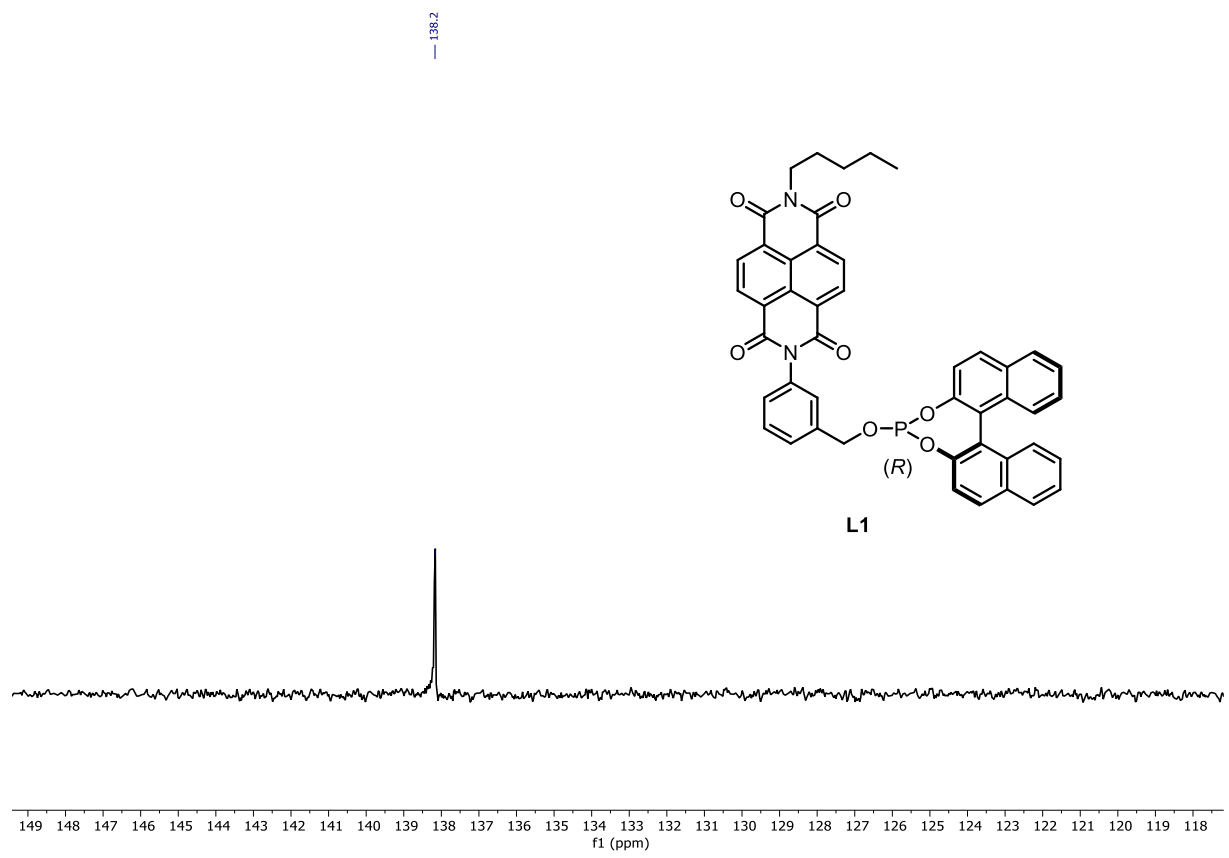
5. NMR Spectra

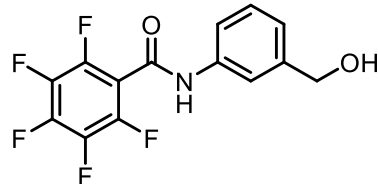




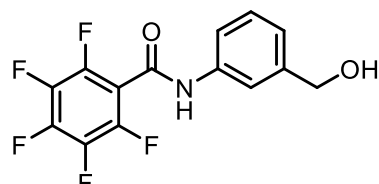
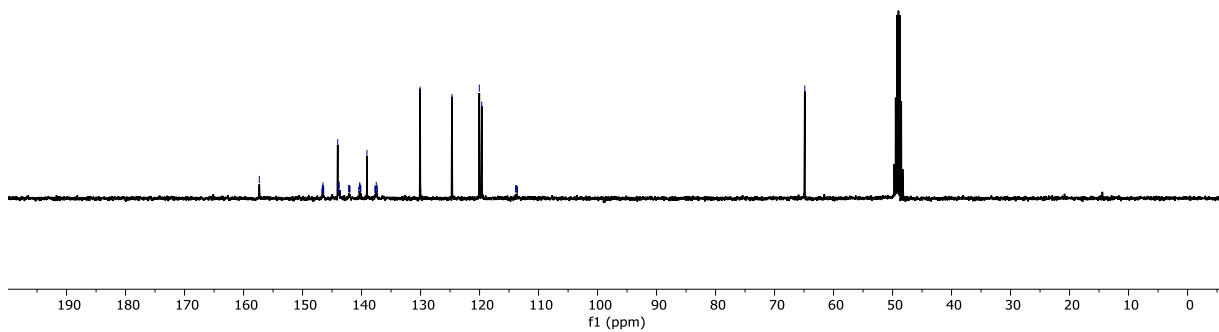
iii



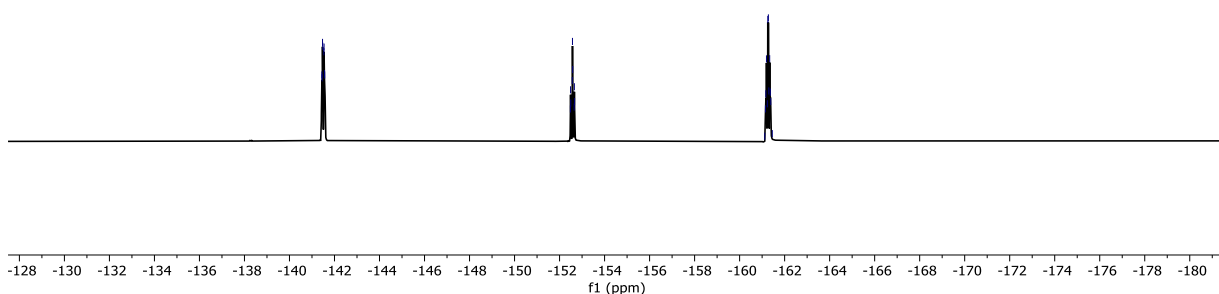


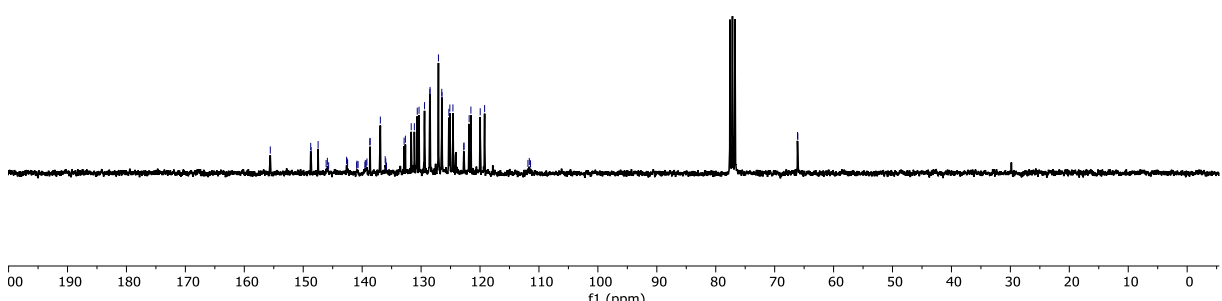
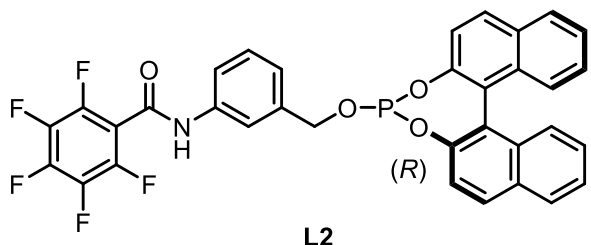
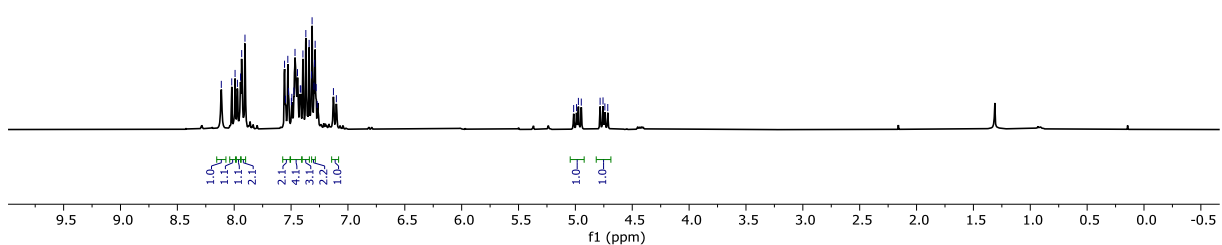
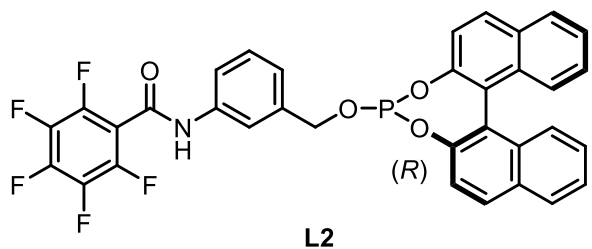
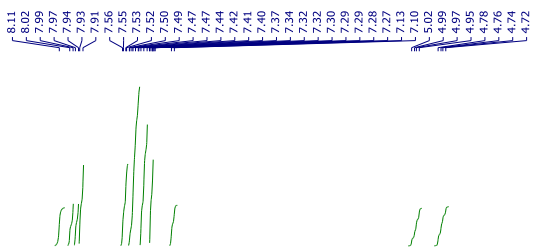


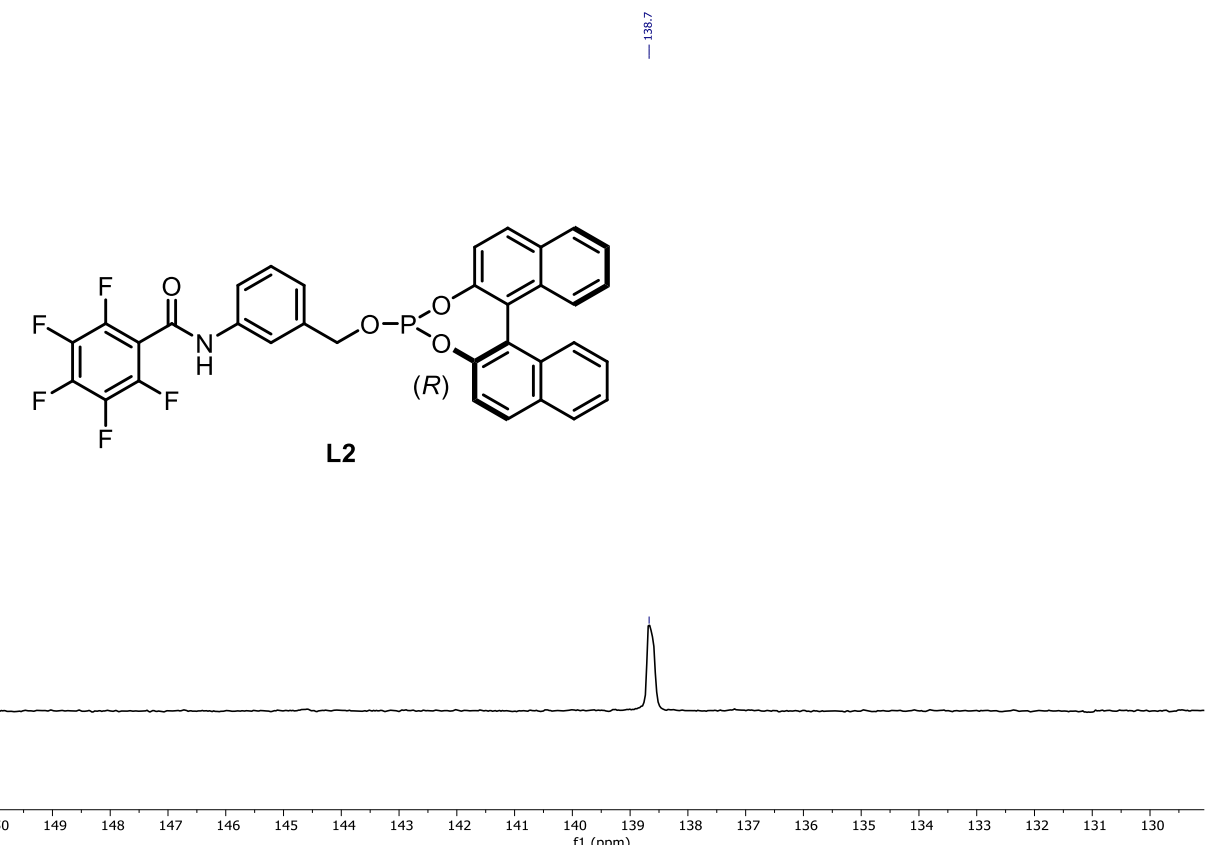
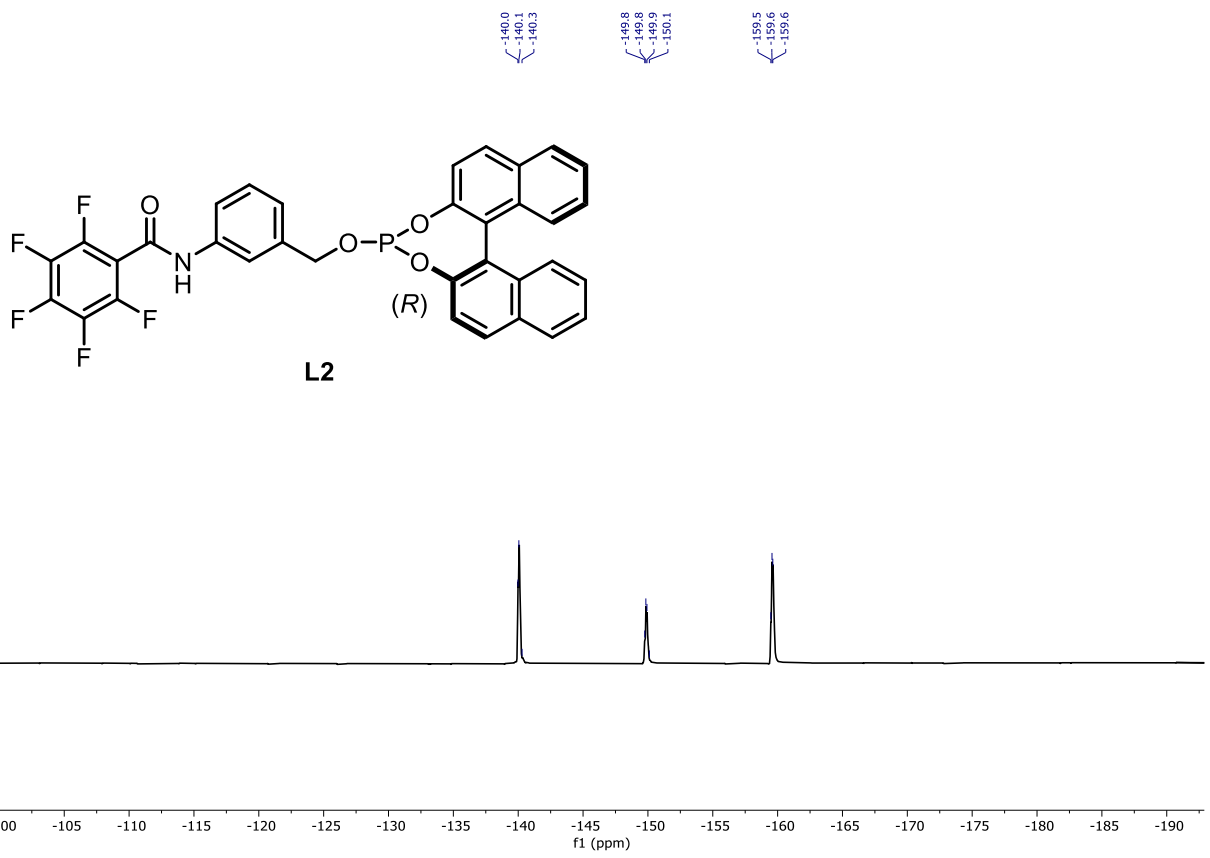
S3

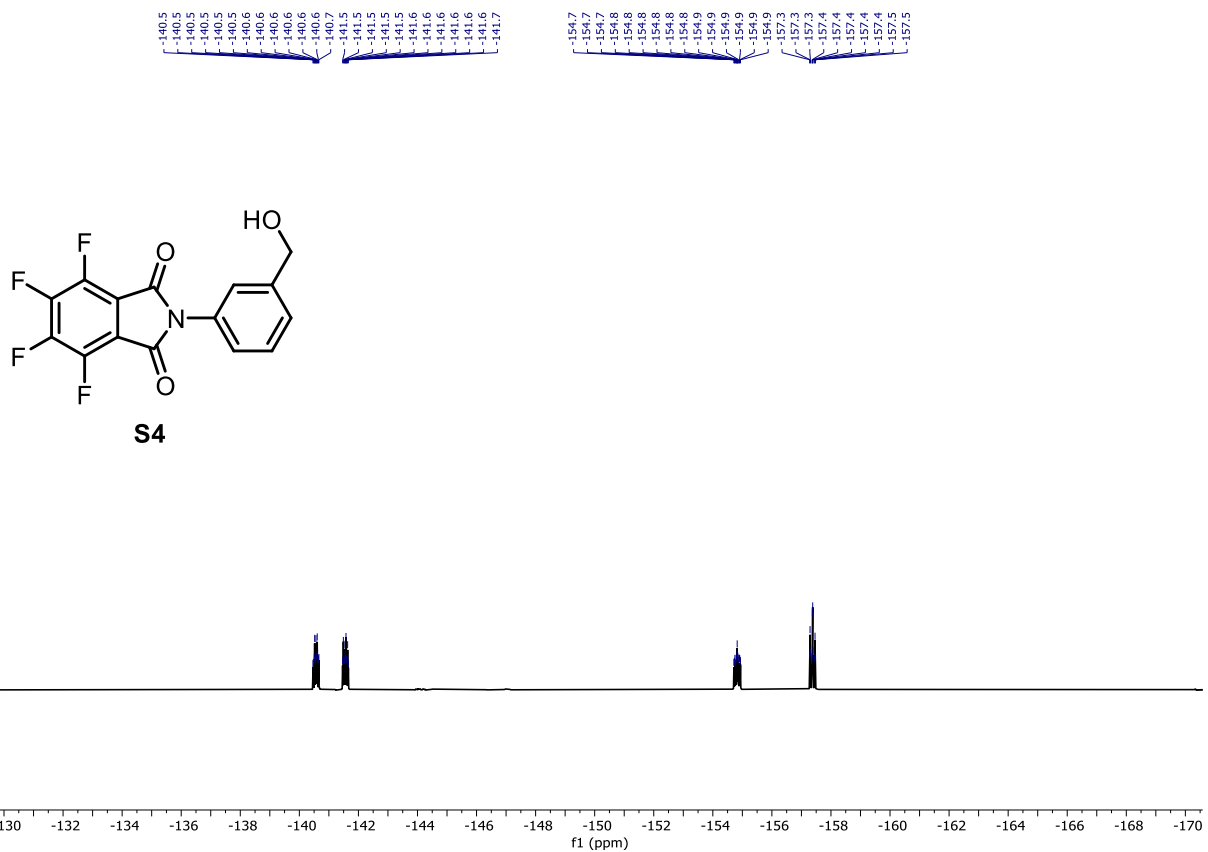
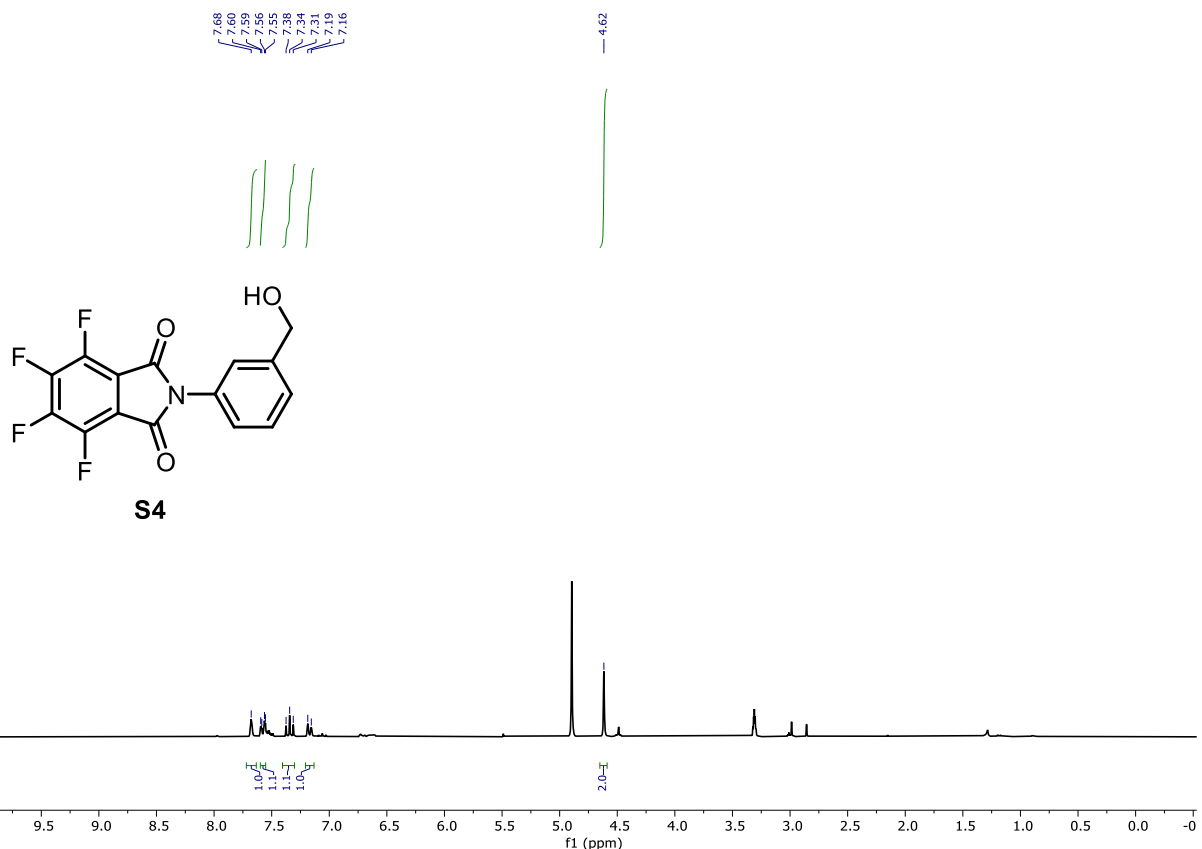


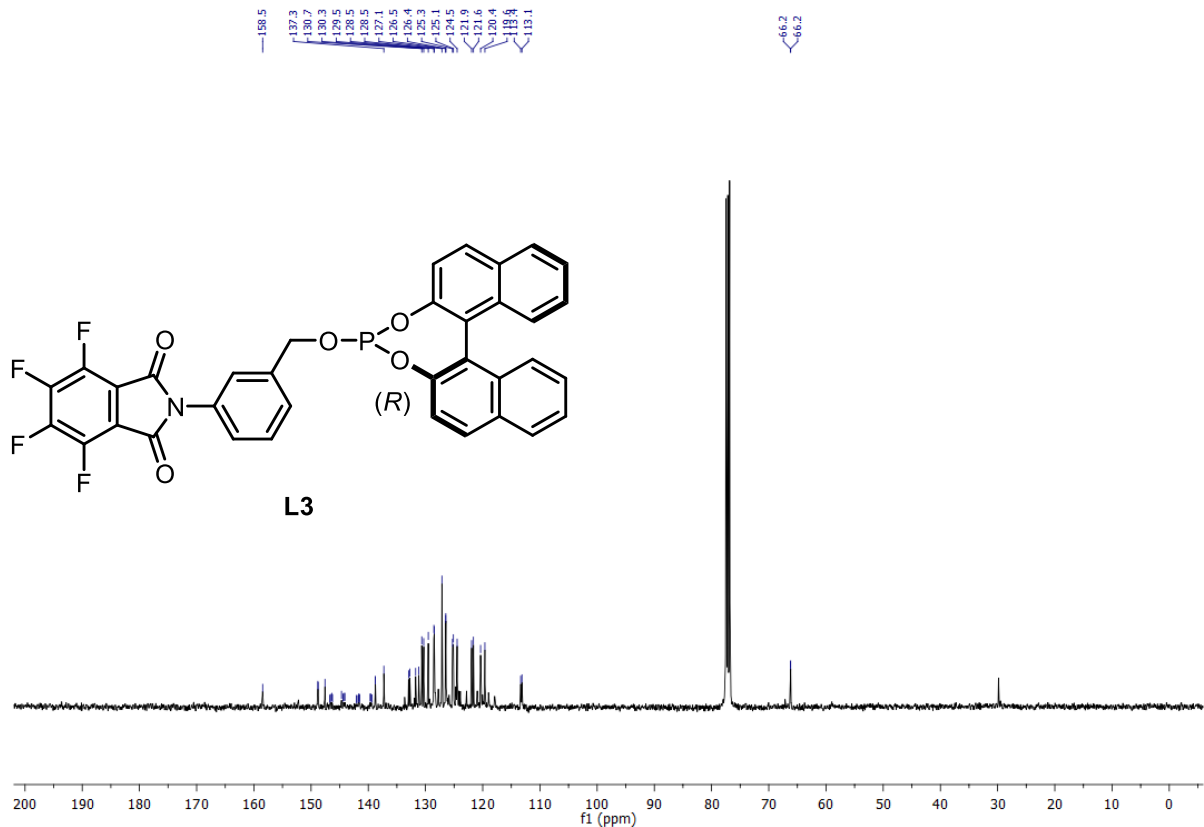
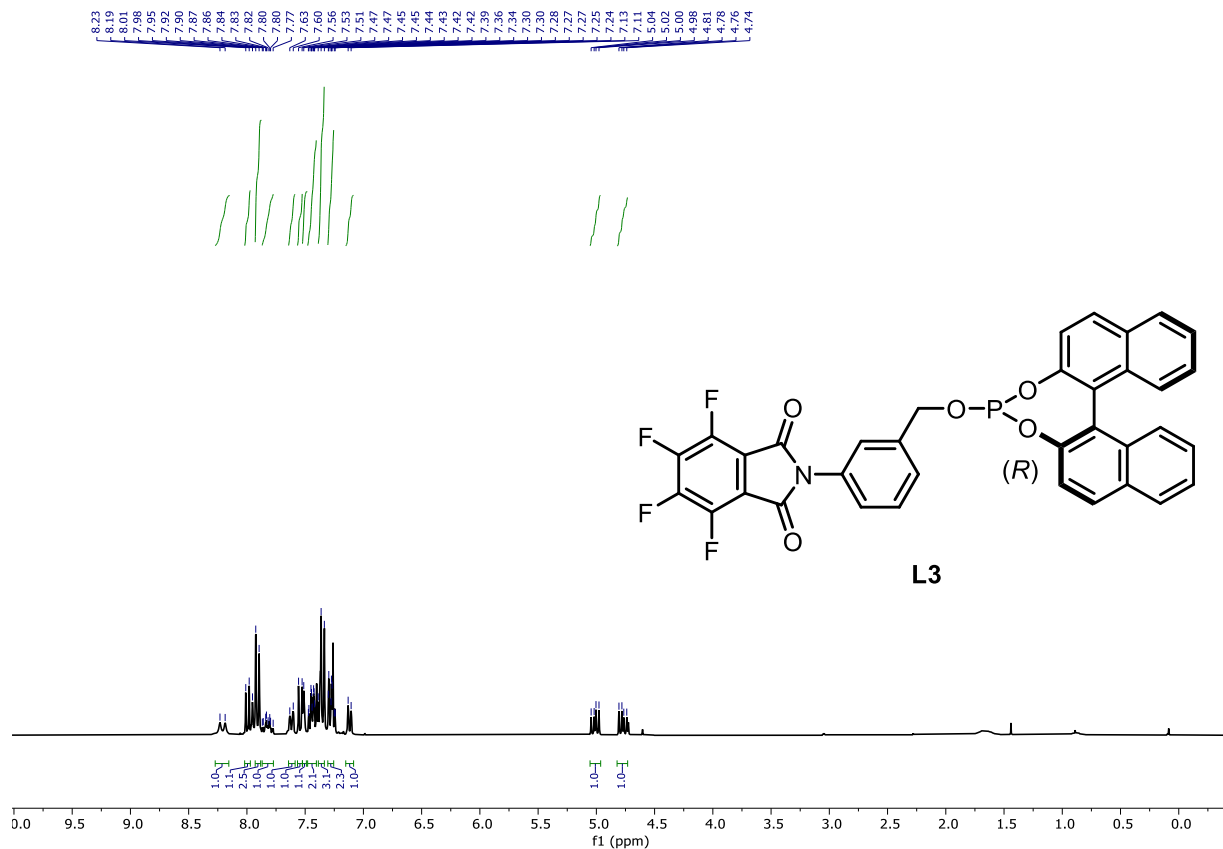
S3

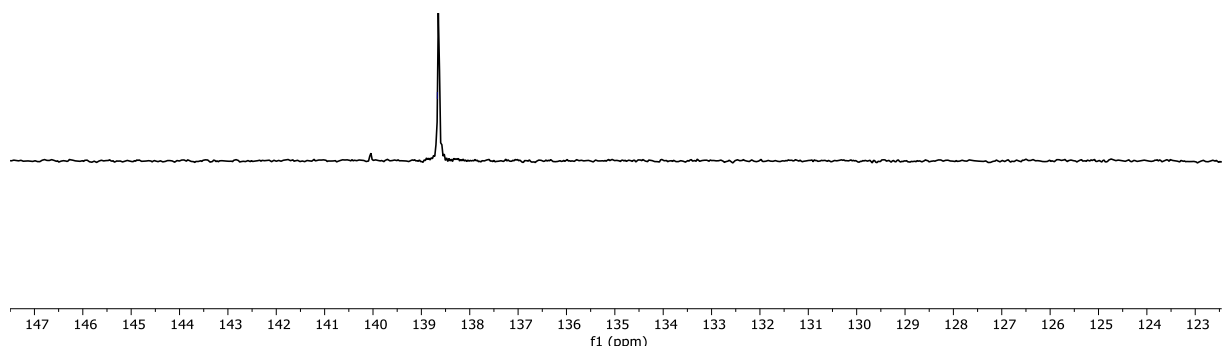
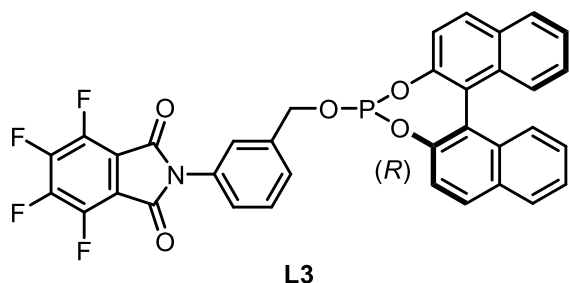
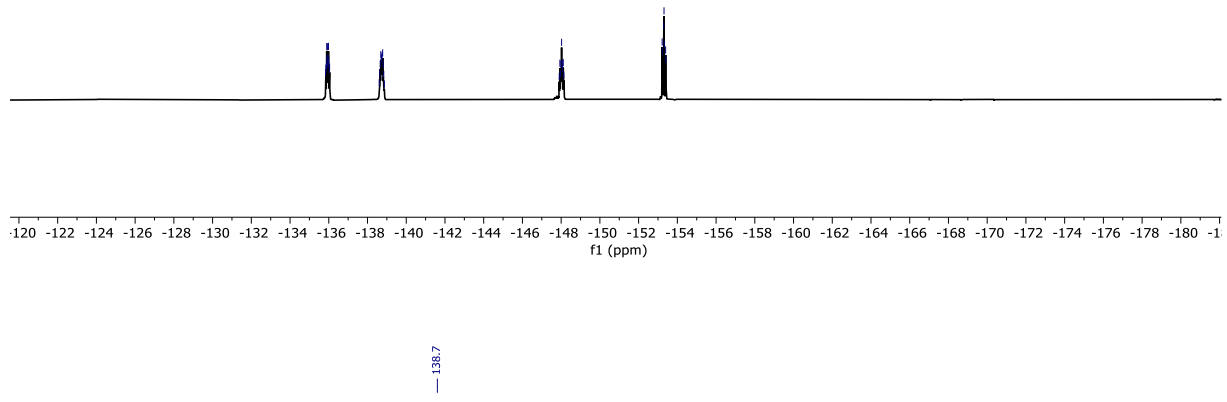
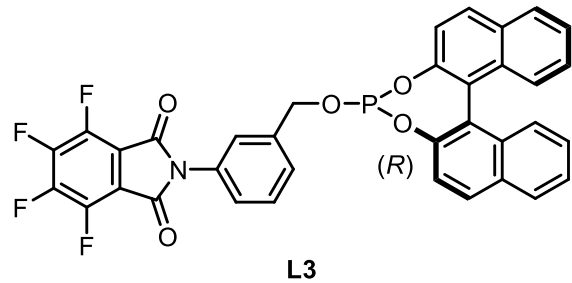


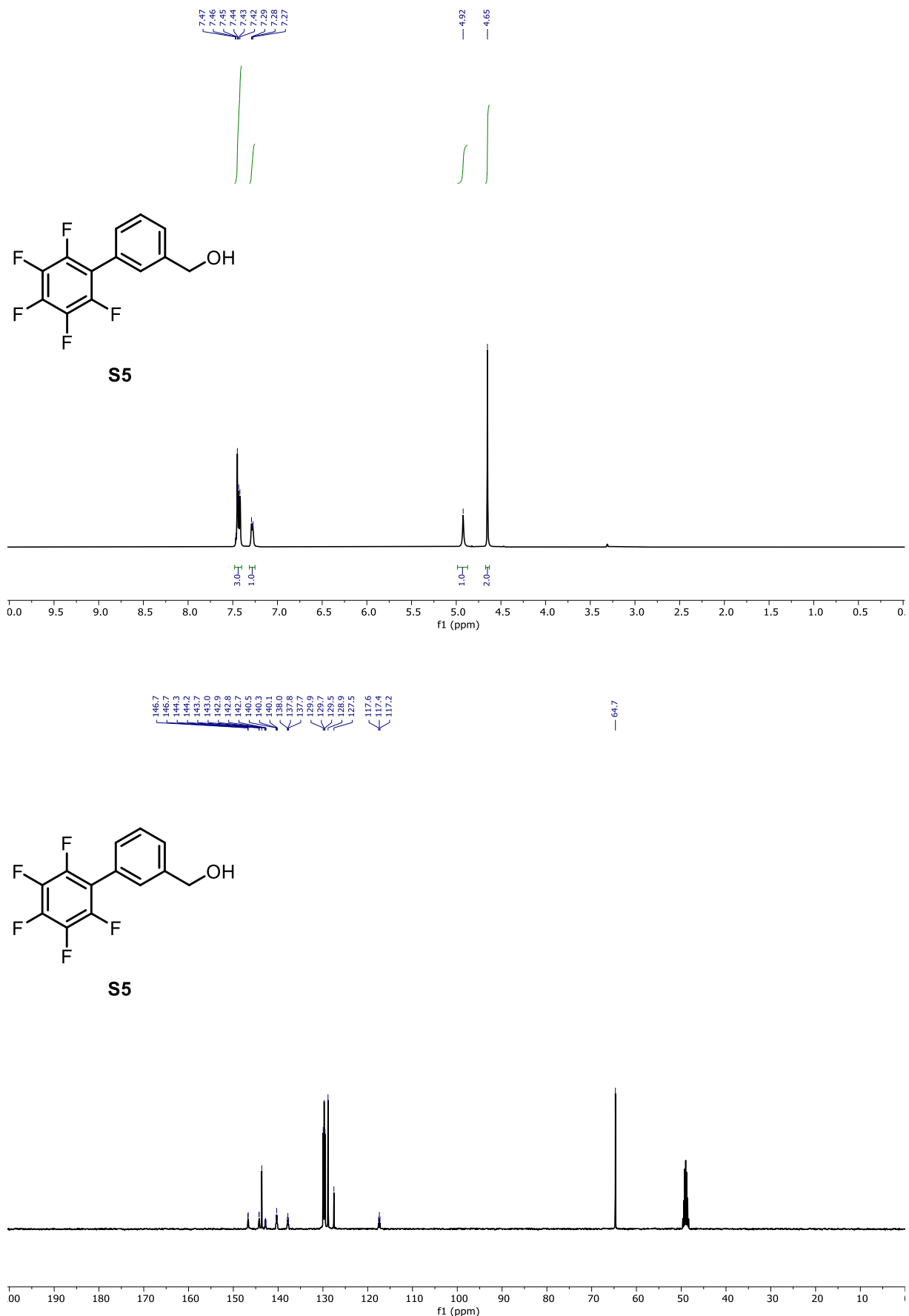


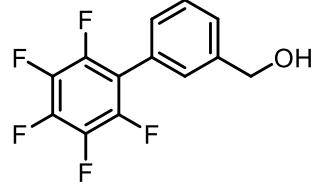




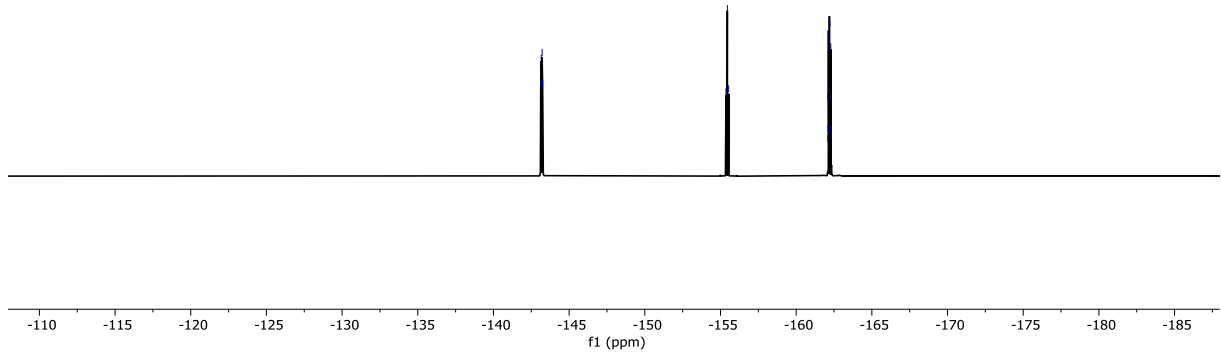




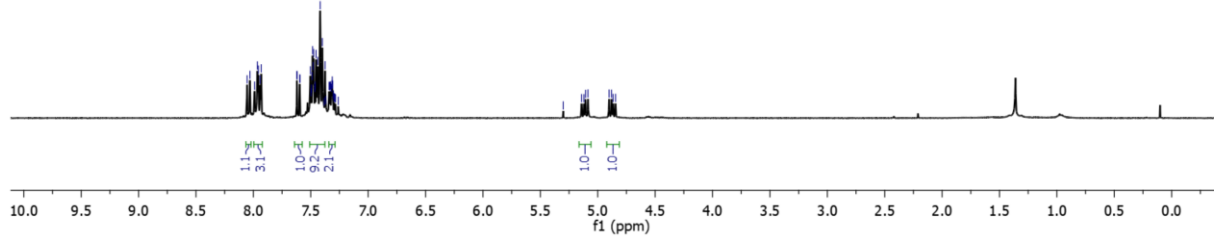


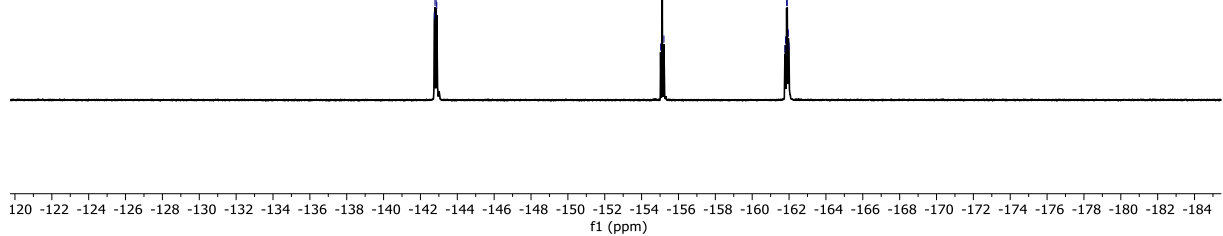
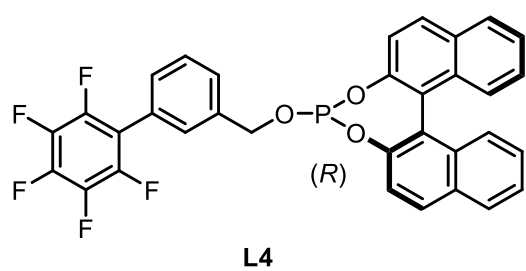
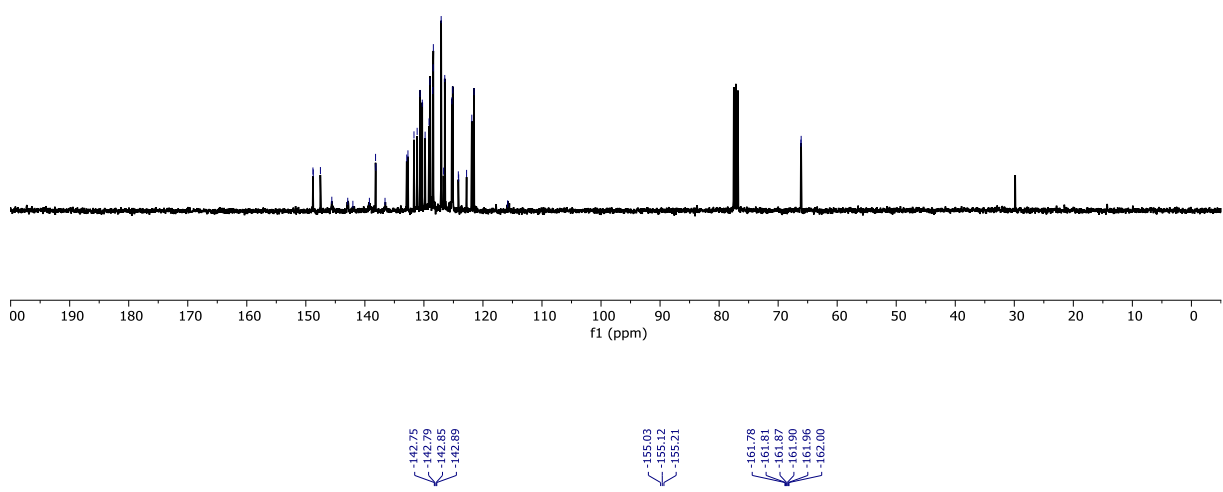
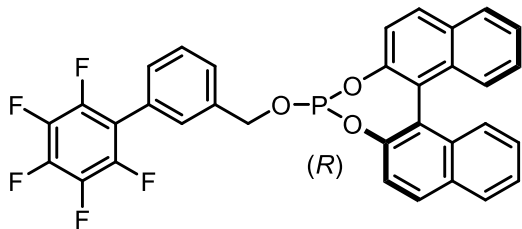


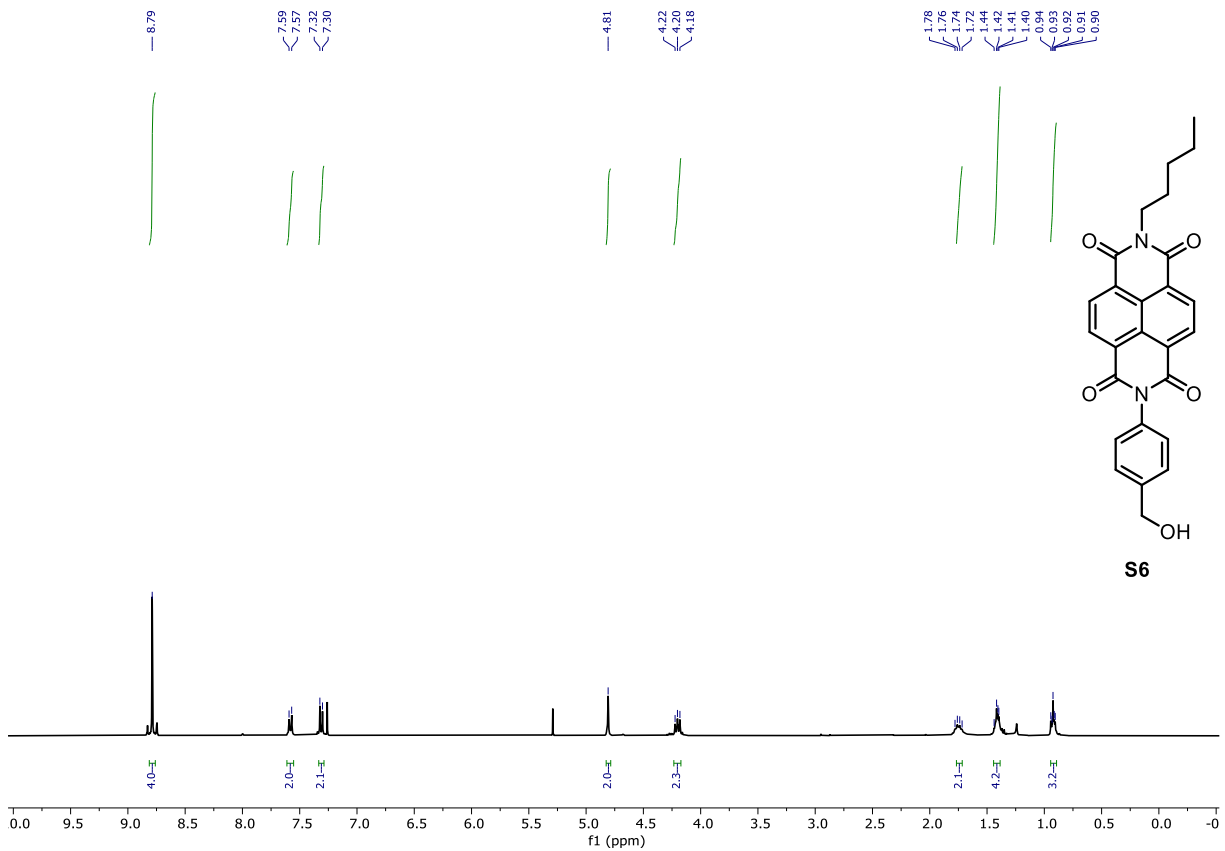
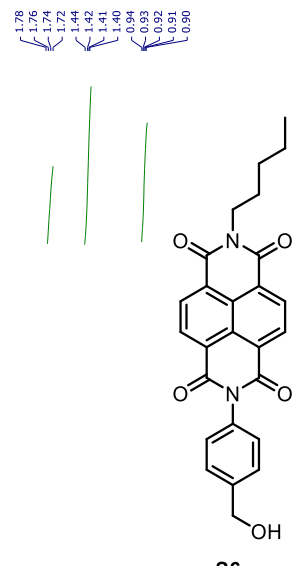
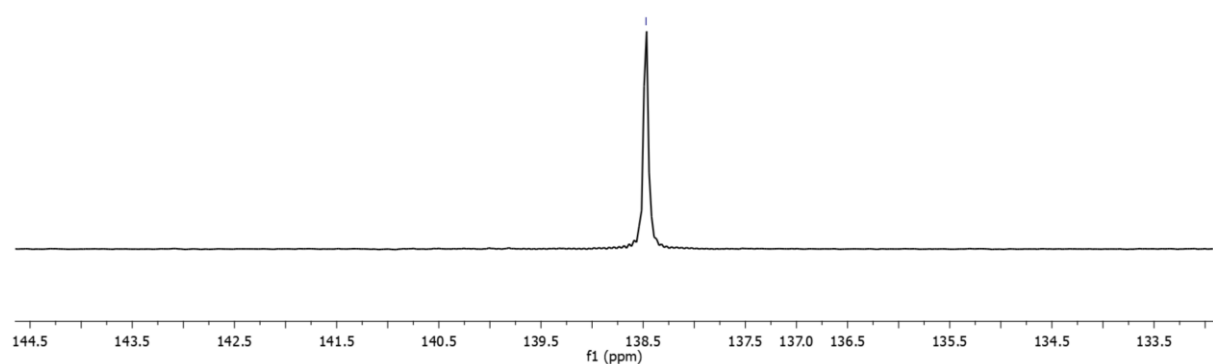
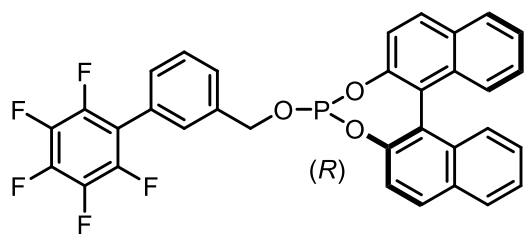
S5

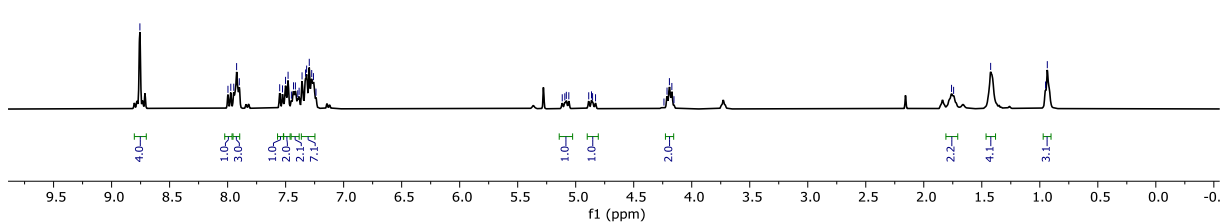
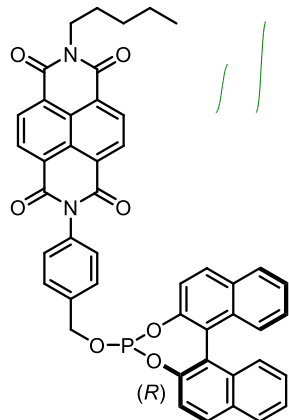


L4

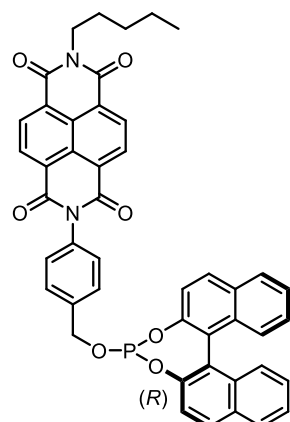




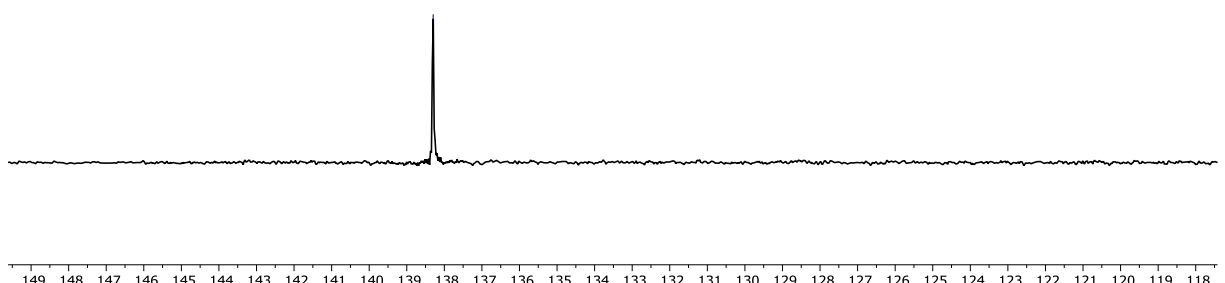


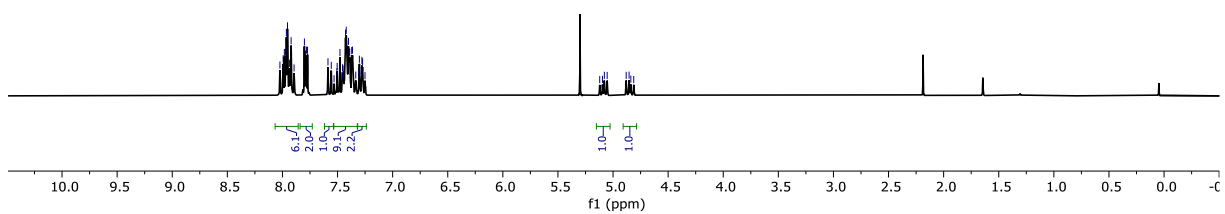
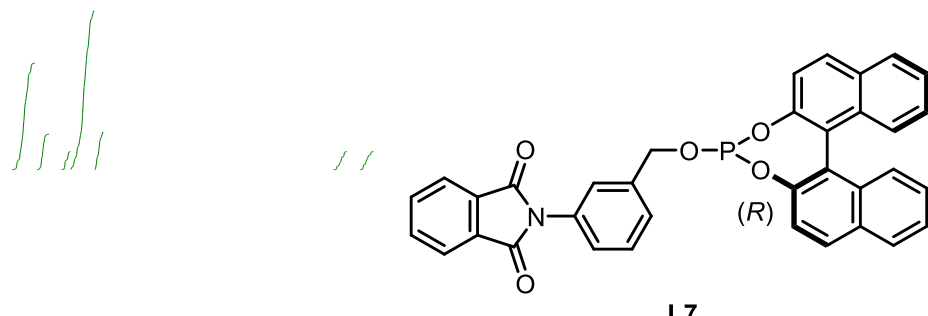


— 138.3



L6

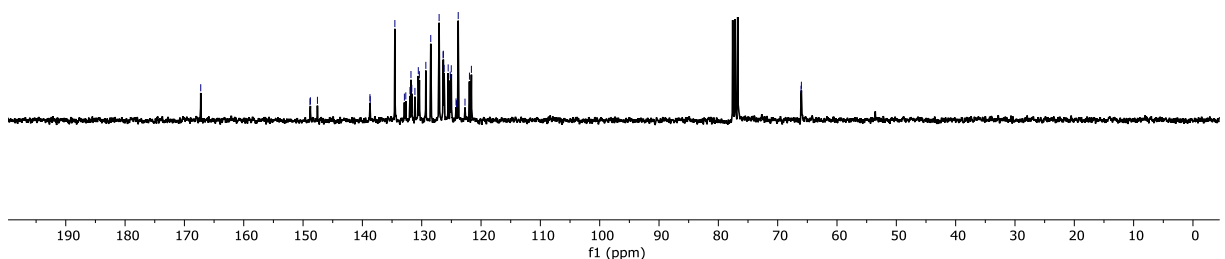
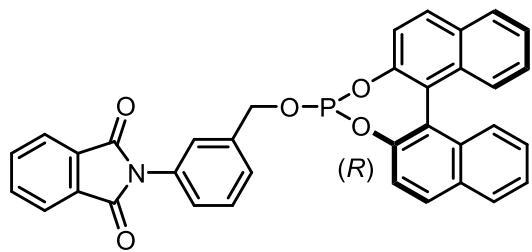


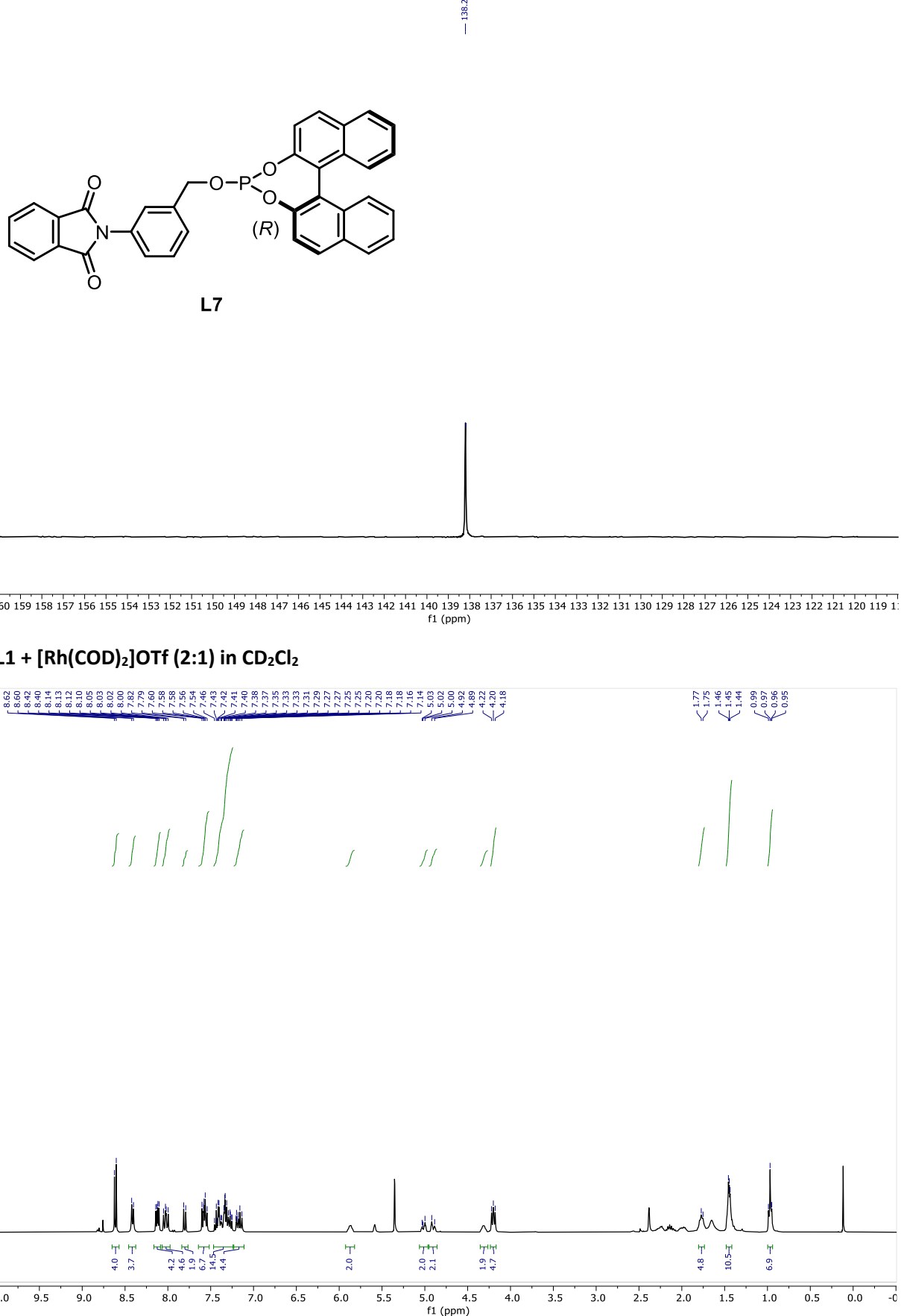


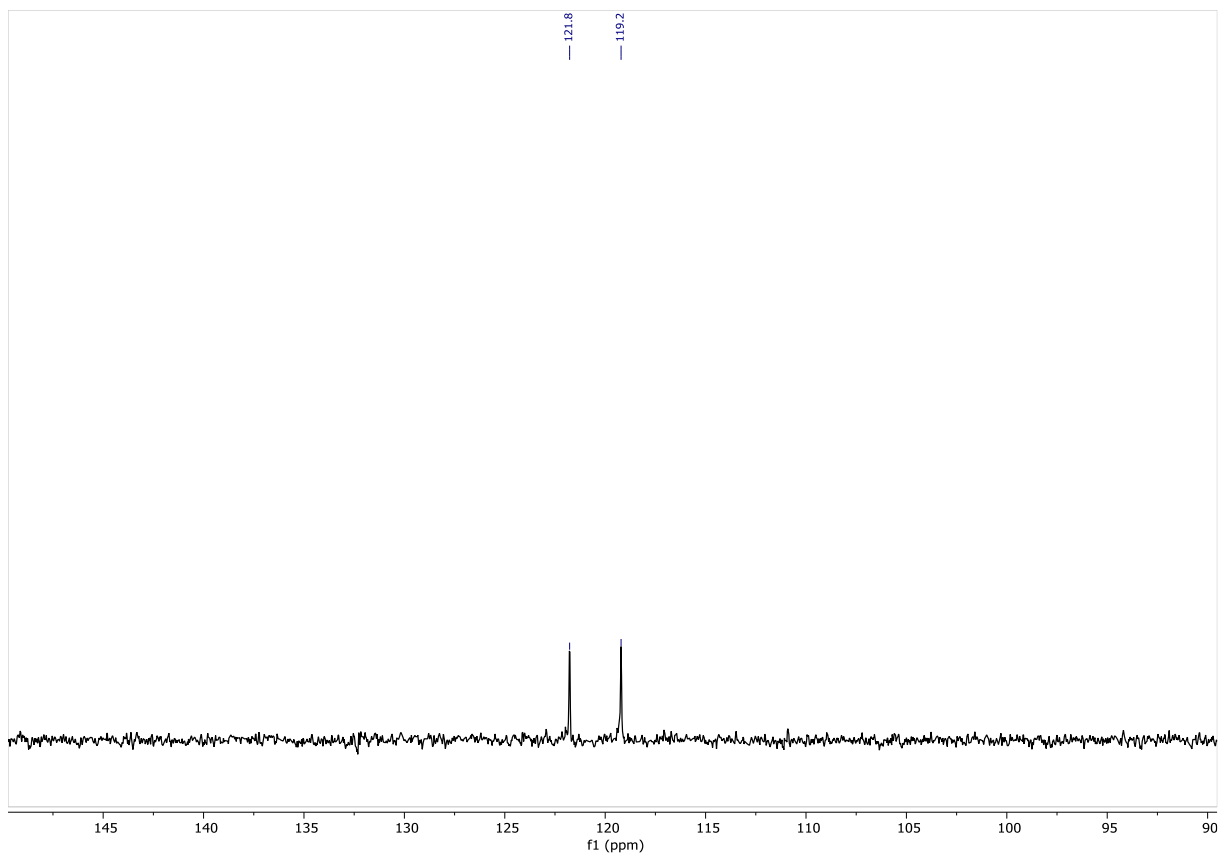
— 167.2

148.8
 148.8
 147.6
 147.6
 138.7
 138.7
 134.5
 134.5
 132.9
 132.7
 132.0
 131.8
 131.7
 131.7
 131.1
 131.1
 130.6
 130.6
 130.4
 130.4
 129.3
 128.5
 127.1
 127.1
 126.4
 126.4
 126.2
 126.2
 125.5
 125.5
 125.2
 125.0
 124.2
 124.1
 123.8
 123.8
 122.7
 122.7
 122.0
 122.0
 121.6
 121.6

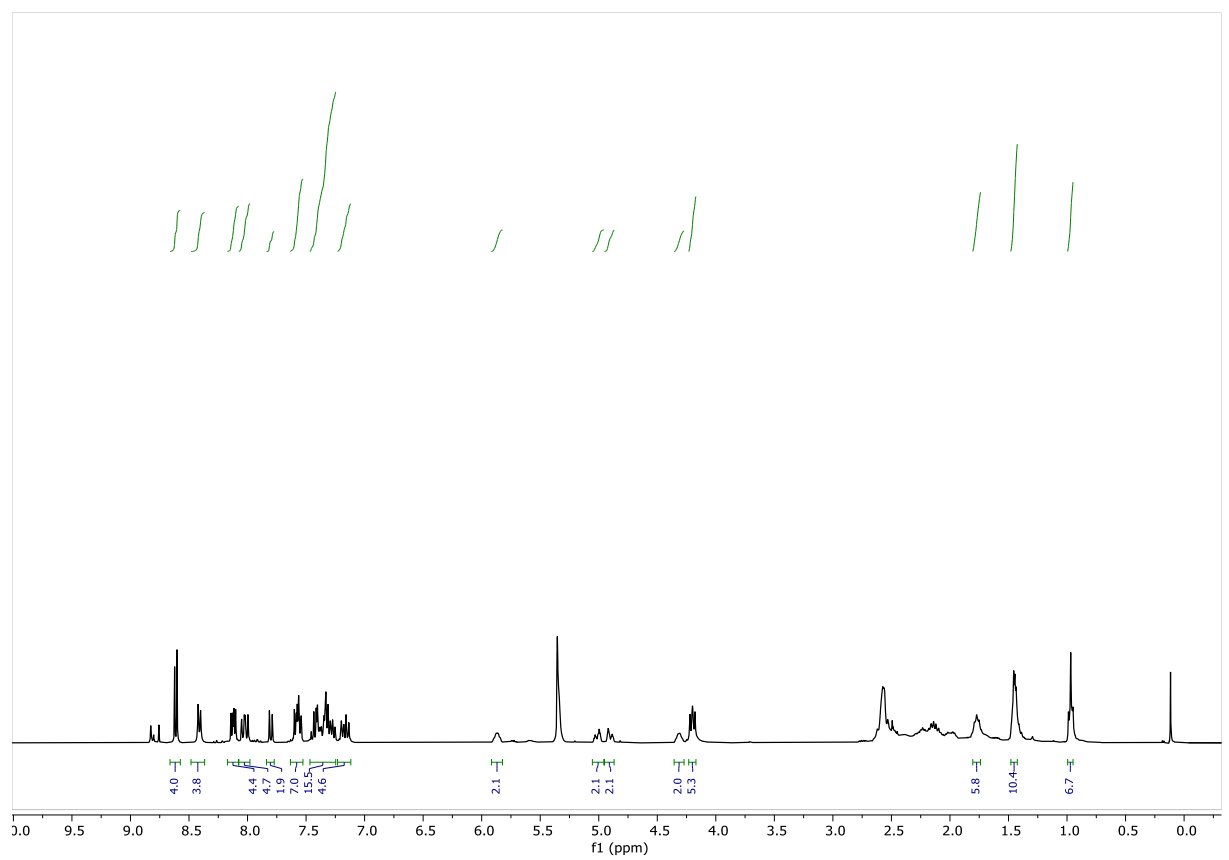
66.1
 66.0

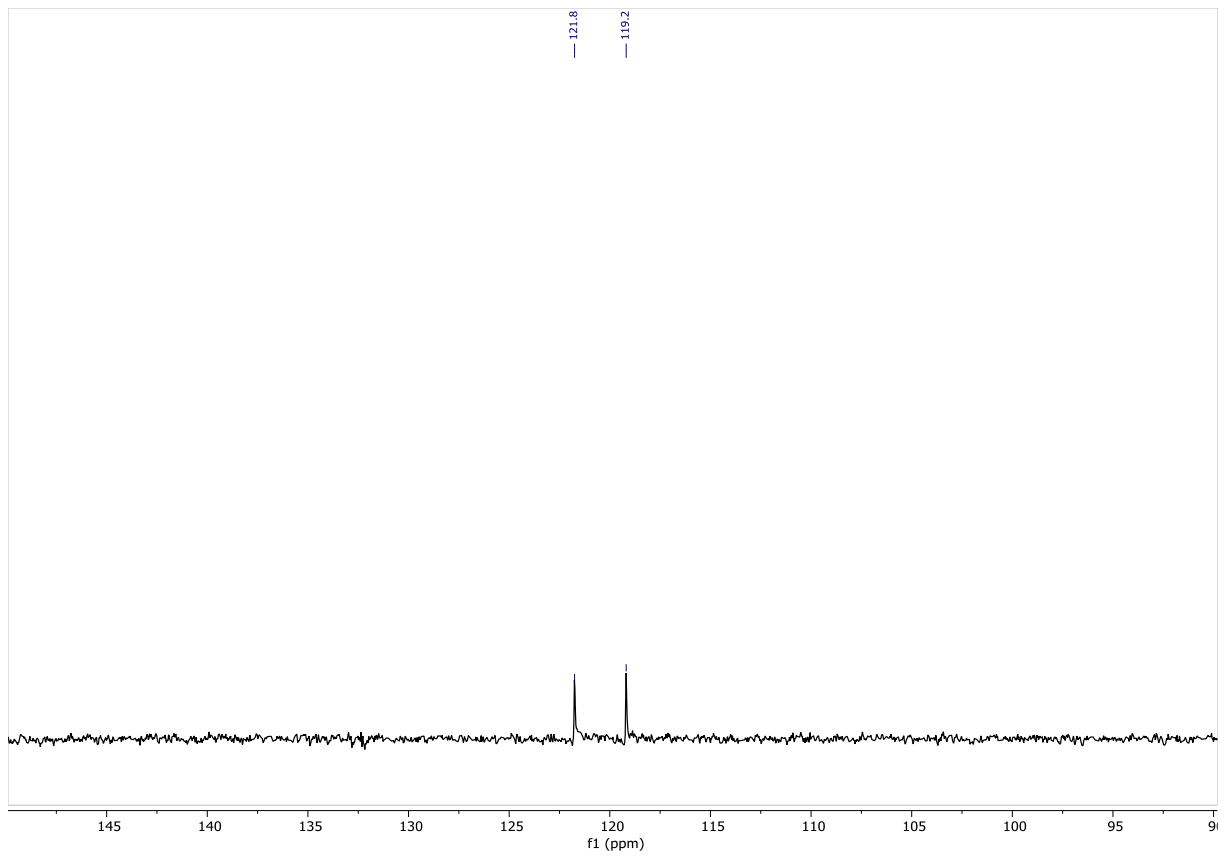






L1 + $[\text{Rh}(\text{COD})_2]\text{OTf}$ (1:1) in CD_2Cl_2





6. References

- [1] (a) M. Bursch, J.-M. Mewes, A. Hansen and S. Grimme, *Angew. Chem. Int. Ed.*, 2022, **61**, e202205735; (b) J. Gorges, S. Grimme and A. Hansen, *Phys. Chem. Chem. Phys.*, 2022, **24**, 28831-28843.
- [2] S. Grimme, A. Hansen, S. Ehlert and J.-M. Mewes, *J. Chem. Phys.*, 2021, **154**, 064103.
- [3] (a) P. Pracht, F. Bohle and S. Grimme, *Phys. Chem. Chem. Phys.*, 2020, **22**, 7169; (b) C. Bannwarth, S. Ehlert and S. Grimme, *J. Chem. Theory Comput.*, 2019, **15**, 1652; (c) S. Ehlert, M. Stahn, S. Spicher and S. Grimme, *J. Chem. Theory Comput.*, 2021, **17**.
- [4] F. Neese, *Wiley Interdiscip. Rev.: Comput. Mol. Sci.*, 2022, e1606.
- [5] A. V. Marenich, C. J. Cramer and D. G. Truhlar, *J. Chem. Theory Comput.*, 2013, **9**, 609.
- [6] S. Spicher and S. Grimme, *J. Chem. Theory Comput.*, 2021, **17**, 1701.
- [7] Visualisation was performed with CYLview20; Legault, C. Y., Université de Sherbrooke, 2020 (<http://www.cylview.org>).
- [8] (a) E. R. Johnson, S. Keinan, P. Mori-Sánchez, J. Contreras-García, A. J. Cohen and W. Yang, *J. Am. Chem. Soc.*, 2010, **132**, 6498; (b) T. Lu and F. Chen, *J. Comput. Chem.*, 2012, **33**, 580.
- [9] T. Wen, J.-Y. Lee, M.-C. Li, J.-C. Tsai and R.-M. Ho, *Chem. Mater.*, 2017, **29**, 4493.
- [10] J. Grabowski, J. M. Granda and J. Jurczak, *Org. Biomol. Chem.*, 2018, **16**, 3114.